WRPS-66072
Revision 0

FY2019 Long-Term PCT of ILAW Glasses

Prepared for the U.S. Department of Energy
Assistant Secretary for Environmental Management

Contractor for the U.S. Department of Energy
Office of River Protection under Contract DE-AC27-08RV14800

P.O. Box 850
Richland, Washington 99352

WRPS-66072
Revision 0

FY2019 Long-Term PCT of ILAW Glasses

I. L. Pegg
The Catholic University of America

I. S. Muller
The Catholic University of America

R. S. Skeen
Washington River Protection Solutions

Date Published
February 2021

Department of Energy

Prepared for the U.S. Department of Energy
Assistant Secretary for Environmental Management

Contractor for the U.S. Department of Energy
Office of River Protection under Contract DE-AC27-08RV14800

P.O. Box 850
Richland, Washington 99352

APPROVED
By Sarah Harrison at 11:31 am, May 25, 2021

Release Approval Date

VSL-19R4620-1

Final Report

FY2019 Long-Term PCT of ILAW Glasses

prepared by

Isabelle S. Muller and Ian L. Pegg

Vitreous State Laboratory
The Catholic University of America
Washington, DC 20064

for

Atkins Energy Federal EPC, Inc.
Columbia, MD 21046

and

Washington River Protection *Solutions*, LLC
Richland, WA

September 3, 2019

Rev. 0, 9/30/19

Completeness of Testing:

This report describes the results of work and testing specified by WRPS. The work and any associated testing followed established quality assurance requirements. The descriptions provided in this test report are an accurate account of both the conduct of the work and the data collected. Results required by the test program are reported. Also reported are any unusual or anomalous occurrences that are different from the starting hypotheses. The test results and this report have been reviewed and verified.

I. L. Pegg: _____ **Date:** 9/30/19
VSL Program Director/Principal Investigator

I. Joseph: Innocent Joseph **Date:** 9/30/19
Atkins Sub-Contract Manager

TABLE OF CONTENTS

List of Tables

List of Figures

List of Abbreviations

ANL-LRM	Argonne National Laboratory – Low-Activity Waste Reference Material
ASME	American Society of Mechanical Engineers
ASTM	ASTM International (formerly the American Society for Testing and Materials)
CCC	Canister Centerline Cooling
CERCLA	Comprehensive Environmental Response, Compensation, and Liability Act
CUA	The Catholic University of America
DCP-AES	Direct Current Plasma Atomic Emission Spectroscopy
DOE	Department of Energy
DWPF-EA	Defense Waste Processing Facility – Environmental Assessment Glass
EDS	Energy Dispersive X-Ray Spectroscopy
HLW	High Level Waste
ICDD	International Centre for Diffraction Data
IDF	Integrated Disposal Facility
ILAW	Immobilized Low Activity Waste
IHLW	Immobilized High Level Waste
LAW	Low Activity Waste
LFRG	Low Level Waste Disposal Facility Federal Review Group
ORP	Office of River Protection
PCT	Product Consistency Test
PA	Performance Assessment
PNNL	Pacific Northwest National Laboratory
PUF	Pressurized Unsaturated Flow Test
NIST	National Institute of Standards and Technology
NQA	Nuclear Quality Assurance
QA	Quality Assurance
QAPP	Quality Assurance Project Plan
QARD	Quality Assurance Requirements and Description
RCRA	Resource Conservation and Recovery Act
ROD	Record of Decision
RSD	Relative Standard Deviation
S/V	Surface to Volume Ratio
SEM	Scanning Electron Microscopy
SPFT	Single-Pass Flow-Through (Test)
TC&WM EIS	Tank Closure & Waste Management Environmental Impact Statement
TST	Transition State Theory
VHT	Vapor Hydration Test
VSL	Vitreous State Laboratory
WRPS	Washington River Protection *Solutions*, LLC
WTP	Hanford Tank Waste Treatment and Immobilization Plant
XRD	X-Ray Diffraction
XRF	X-Ray Fluorescence Spectroscopy

SECTION 1.0
INTRODUCTION

1.1 Background

About 50 million gallons of high-level mixed waste is currently stored in underground tanks at The United States Department of Energy's (DOE's) Hanford site in the State of Washington. The Hanford Tank Waste Treatment and Immobilization Plant (WTP) will provide DOE's Office of River Protection (ORP) with a means of treating this waste by vitrification for subsequent disposal. The tank waste will be separated into low- and high-activity waste fractions, which will then be vitrified respectively into Immobilized Low Activity Waste (ILAW) and Immobilized High Level Waste (IHLW) products. The ILAW product will be disposed in an engineered facility – the Integrated Disposal Facility (IDF) – on the Hanford site, while the IHLW product is designed for deep geological disposal in a national facility for high-level nuclear waste. The ILAW and IHLW products must meet a variety of requirements with respect to protection of the environment before they can be accepted for disposal. The objective of the work described in this report is to perform testing, data collection, and analyses for the ILAW glass product for subsequent use in the performance assessment (PA) of the IDF to assess potential environmental risks associated with long-term storage.

The Record of Decision (ROD) from the Tank Closure & Waste Management Environmental Impact Statement (TC&WM EIS) establishes the current waste streams to be disposed of at the IDF to be located in the 200 East Area which include ILAW, secondary waste associated with ILAW production, and other on-site Hanford Non-Comprehensive Environmental Response, Compensation, and Liability Act (CERCLA) waste. In accordance with the DOE order on radioactive waste management (DOE Order 435.1), the IDF PA is intended to analyze the long-term impacts on human health and the environment of the disposition of waste placed into the facility. Evaluation of the impact of disposed waste requires the ability to predict the long-term release of key radionuclides from the engineered system. In the case of IDF, the engineered system includes a number of components including the proposed Resource Conservation and Recovery Act (RCRA) cap, back fill material, ILAW glass, leachate collection system, etc.

Since 1998, the IDF PA (formerly the ILAW PA) has been supported by a PA maintenance plan focused on collecting the critical data needed to predict long-term performance: site geology, recharge, hydrology, geochemistry (measurement of site specific K_d values for key contaminants of concern), and waste form release. The purpose of the PA maintenance plan is to allow PA revisions to reflect new scientific information that reduces the technical uncertainty associated with critical aspects of the PA. Although many of the components contained in the engineered system and addressed in previous IDF PAs are important in minimizing radionuclide release, arguably one of the most important aspects of the

engineered system is the long-term performance of the ILAW glass. The ILAW glass serves as a primary barrier that controls radionuclide release and the glass is expected to have the highest inventories of radionuclides that pose the greatest potential impact, such as Tc-99 and I-129. The ILAW glass serves as a primary barrier that controls radionuclide release. Therefore, developing robust, scientifically defensible predictions of long-term glass performance for the IDF PA is critical. The technical approach that is currently used to predict long-term release from ILAW glass for the IDF PA previously gained acceptance from the Low-Level Waste Disposal Facility Federal Review Group (LFRG) and the international community evaluating the long-term corrosion of waste glasses [1-8]. It has also been peer reviewed and approved by a panel of independent experts during development of the 1998 IDF PA.

In the early IDF PAs, three prototypic glasses that spanned the range of glass compositions expected to be produced by the WTP (LAWA44, LAWB45, and LAWC22) were selected based upon specific processing constraints and composition projections that were current at the time. However, subsequent work has expanded the range of glass compositions that may be produced at the WTP and this type of composition range expansion is likely to continue through the life of the project. Thus, while the basic technical approach is well developed, there is a need to expand the range of glasses tested in order to span the composition range expected to be disposed in the IDF, and to develop an understanding of the dependence of the underlying model parameters and reaction network on the ILAW glass composition. Washington River Protection *Solutions*, LLC (WRPS) is leading the work to address this need and contracted with Atkins and the Vitreous State Laboratory (VSL) of The Catholic University of America (CUA) to provide scientific and technical support. The work initiated in 2010 includes long-term Product Consistency Tests (PCT-Bs[1]) and Single Pass Flow Through (SPFT) tests. Many of the long-term PCTs started in prior years are on-going with periodic sampling and analysis of the leachates to collect longer-term leach data. Continued sampling and analysis of on-going long-term PCTs were part of the FY2019 work scope for WRPS [9]. The present report provides results from that work, started in FY2018 according to a Test Plan [10] that was responsive to the corresponding FY2018 WRPS scope of work [11], and continued in FY2019. An overarching objective of the present work was to review the accumulated data and perform additional analyses on selected ongoing tests in order to characterize the secondary phases that have formed.

1.2 ILAW Release Approach for the IDF PA

The technical approach that is currently used to predict long-term release from ILAW glass for the IDF PA has been developed, refined, and updated over the past decade or so. The

[1] The PCT method (ASTM C1285) offers two procedures: (1) PCT-A requires testing at 7-day ± 2%, at a temperature of 90 ± 2 °C, in static condition in a 304L stainless steel vessel, using -100 to +200 mesh particles in ASTM Type 1 water and a leachant volume of 10 ± 0.5 cm^3/g sample; and (2) PCT-B offers wide flexibility of varying sampling time, size of sample, temperature, and ratio of sample mass to volume of leachant. In the VSL procedure for PCT-Bs used in the present work the 4 mL of leachant taken for liquid analyses at each sampling time is replaced with 4 mL of deionized water.

approach and the supporting test data for ILAW glasses have been extensively documented [1, 3-7, 12 - 15]. A brief summary is presented in this section.

The underlying premise of the IDF PA is that the source term for radionuclide release is controlled by the long-term weathering of the glass matrix. This engineering-based approach has been used in previous PAs to provide the defense-in-depth required to defend the above premise and demonstrate through computer simulations that the proposed glass waste form will meet the regulatory requirements put forth by the LFRG. The focus of this engineering-based approach is on estimating the model parameters and chemical reaction network needed to provide a robust simulation of glass weathering and the corresponding release of radionuclides over the period of performance (~10,000 years). The overall model incorporates the effects of chemical affinity and ion exchange as discussed in the last paragraph. The model parameters $\vec{k}_o$, η, E_a, and K_g are used to populate a chemical affinity-based kinetic rate law that is based upon Transition State Theory (TST) [16]:

$$r = \vec{k}_o 10^{\eta pH} exp\left(\frac{-E_a}{RT}\right)\left[1 - \left(\frac{Q}{K_g}\right)\right]^{\sigma} \quad (1.1)$$

where r is the dissolution rate [g/(m^2.d)], $\vec{k}_o$ is the forward rate constant [g /(m^2.d)], pH is the negative of the logarithm to base 10 of the hydrogen ion activity, η is the power law coefficient, E_a is the apparent activation energy (kJ/mol), R is the gas constant [kJ/(mo1 K)], T is the temperature (K), Q is the ion activity product (unitless), K_g is the pseudo-equilibrium constant for the rate controlling phase or phases (unitless), and σ is the Temkin coefficient which has been theoretically shown to equal one. Equation (1.1) relates the effect of: (1) pH, (2) temperature, (3) saturation state of the system, and (4) the activities of species that affect the rate of glass dissolution via Q. Equation (1.1) is based on the kinetic rate equation developed by Åagaard and Helgeson [17], as applied to glass by Grambow [18] wherein orthosilicic acid (H_4SiO_4) is the only rate controlling species in Q.

In addition to the dissolution rate equation (1.1), a term is included in the IDF PA calculations to predict the ion-exchange rate (r_{IEX}) between sodium in the glass and hydrogen ions in the aqueous phase, as the glass-water reaction proceeds. In general, the ion exchange rate is thought to be a function of temperature, glass composition, and reaction progress (stage of the glass-water reaction). The potential importance of the contribution from ion exchange in the long-term corrosion mechanism had been emphasized previously by Feng and Pegg [19-21]. In previous glass testing work in support of the IDF PA, the standard approach to estimate this parameter has been that of McGrail et al. [5] and Pierce et al. [7] whereby r_{IEX} is obtained by subtraction of the boron dissolution rate from the sodium dissolution rate; measurement of its temperature dependence also permits estimation of the activation energy of the Na ion exchange reaction E_{IEX}. More recently, various issues with this approach have been identified [22, 23] including: (i) the reliability of this subtraction approach in view of the apparent diffusive release of boron [13, 15]; (ii) an error in the calculation of r_{IEX} that has been propagated through

previous work [23]; and (iii) the use of an r_{IEX} that is independent of time and solution composition [22, 23]. In view of these issues, WRPS has commissioned studies of potential alternative approaches for incorporation of ion exchange into the rate law [22, 23]; some of the recommendations from those studies have been implemented in FY2019 testing at VSL [9, 24].

The use of Equation (1.1) with suitably estimated parameters allows for the source-term to be estimated within a reactive chemical transport modeling framework that takes into account the coupled effects of fluid flow and glass-water reactions on the chemistry of fluids percolating through the disposal facility. Coupling the fluid chemistry with a kinetic rate equation allows the simulations to describe the response of the glass corrosion rate to changes in fluid composition as a function of time and space.

In previous work, the model parameters for Equation (1.1) have been obtained from the analysis of data produced using a variety of experimental techniques. The SPFT test has been the primary technique used to estimate the coefficients of Equation (1.1). The results of the recent work at VSL show that pulsed flow tests can also be used to obtain the parameters of Equation (1.1). Other tests used to evaluate glass durability are long-term high surface to volume ratio (S/V) product consistency test (PCT-B), vapor hydration test (VHT), and pressurized unsaturated flow test (PUF) [1, 3-7, 12-14, 25, 26]. This suite of tests evaluates different aspects of the glass-water reaction over the course of the various regimes of glass weathering: the initial forward rate regime; the decreasing rate regime; the residual rate regime; and the alteration rate renewal regime. These regimes are described below and illustrated in Figure 1.1 [8].

The initial forward rate consists of both ion-exchange and hydrolysis reactions. In dilute to near-saturated solutions, the TST-based model (without the ion-exchange term) successfully accounts for silicate dissolution in terms of temperature, pH, and reactive surface area when hydrolysis is the controlling reaction. However, as the glass-water reaction proceeds and the concentration of glass components (particularly the dissolved silicic acid concentration) increases in solution, the rate of dissolution decreases. For ILAW glasses tested under alkaline conditions, it has been observed that ion exchange becomes the dominant process controlling glass weathering under these near-saturated conditions, as was pointed out earlier for high-level waste (HLW) glasses [21]. The data collected from SPFT experiments conducted as a function of pH, temperature, and silicic acid concentration are used to study these processes and to obtain the model parameters $\vec{k}_o$, η, E_a, and K_g at the nominal constant temperature of 15 °C at the IDF.

As the glass continues to dissolve, the aqueous concentration of dissolved components approaches saturation with respect to the formation of a hydrated surface layer. The combined H^+/Na^+ ion-exchange and hydrolysis of the silicate network lead to the formation of a multi-layered reaction zone including a hydrated layer, a porous gel layer, and crystalline phases that precipitate on the surface. Increasing the ratio of surface area of glass to volume of leachant (S/V) (e.g., in PCT-B) is one method to explore higher reaction progresses and identify the secondary phases that are associated with the alteration rate renewal regime, also referred to as resumption.

The hydrated surface layer forms either as a reorganization of the hydrated layer (phyllosilicates) or when relatively insoluble glass components (e.g., Al, Fe, and Si) accumulate in the bulk solution and precipitate at the glass-water interface (tectosilicate) [25, 26]. The water-glass interface is a multi-layer system that includes phases in which the less soluble components left behind are organized into a hydrated layer of phyllosilicates and tectosilicates from the precipitation of components in solution that exceed their solubility limits [25]. The rate of dissolution then continues at a relatively constant residual rate that has been shown in some cases to be consistent with a process controlled by diffusion through the hydrated surface layer. The key alteration phase is often a clay mineral, such as a smectite or chlorite. The precipitation kinetics associated with these phases can be complex, but in general, the rate of secondary phase growth increases in response to an increase in the magnitude of supersaturation [27, 28].

Finally, depending on the type of alteration phases that form, the glass-water reaction can increase from the residual rate and return to an elevated rate, which is termed resumption. This type of behavior has been observed in accelerated testing, with high temperatures and high solid surface area to volume ratios, for various glasses including US HLW glasses [29-33], other HLW glasses [34-44], as well as Hanford low-activity waste (LAW) glasses [15, 32, 45, 46].

The data collected from VHT, PCT-B, and PUF experiments along with geochemical modeling and solid-phase characterization are used to identify the key alteration phases formed as the glass weathers. The results from these tests provide the additional confirmatory information needed to identify and constrain the appropriate chemical reaction network required for model simulations.

1.3 Test Objectives

One of the mechanisms that affect glass dissolution is the formation of secondary phases, which can either decelerate or accelerate the dissolution process. To be able to analyze the long-term effects of secondary phases, the phases involved in long-term PCT leaching of LAW glasses need to be identified. Some of the tests started earlier with the 20 IDF glasses had reached resumption and the tests were terminated. In FY2019, monitoring and testing continued for the glasses that have very recently reached resumption or that had not yet reached resumption. In addition, a set of higher waste loading LAW glasses, which were selected for PCT-B in FY2018, have now reached one-year sampling duration. Leachate samples, solid precipitates, and reacted glass surfaces have been analyzed. Thus, the objectives of the present work are:

- Compile and review the long-term PCT data on the IDF glasses.
- Based on the above review identify and analyze additional PCT leachates.
- Based on the review identify PCTs for altered glass and secondary phase analysis.

- Open selected vessels and remove and analyze small amounts of the solids by Scanning Electron Microscopy (SEM)/ Energy Dispersive X-Ray Spectroscopy (EDS) and X-Ray Diffraction (XRD).
- Use results from the above analysis to identify, in particular, the onset of leach rate resumption, and associated secondary phase formation.
- Analyze replicates of ANL-LRM standard glass samples that were included in the test sets to assess the long-term reproducibility of PCT results.
- Continue sampling of fifteen new PCT-B on glasses selected from those formulated to develop the Enhanced LAW Glass Correlation for high waste loading glasses.

1.4 Previous Testing at VSL

A large data set of results from long-term PCT-B performed at VSL on WTP LAW glasses was compiled and reported previously [15]. The data set includes glass compositions, leachate compositions and pH at each sampling interval, sampling time, test condition (leachant, temperature, S/V, test protocol, etc.), and associated secondary phase information. Data for a total of 253 LAW glass compositions are included in the data set, which extended up to 3982 days of PCT-B leaching. These glass formulations were developed at VSL in support of the WTP and provided the basis for the present WTP baseline formulations. These glasses span a composition range that is much more extensive than those used in previous performance assessment glass testing work [7]. Selected tests were sampled and analyzed to characterize the secondary phases, which included zeolites such as analcime and phillipsite and phyllosilicates of the smectite group, stevensite and swinefordite [15]. Glasses in the later stages of the reaction progress were included in this analysis.

In addition to the development of the baseline operating envelope for the WTP, since 2003, VSL has been developing a wide range of LAW formulations that achieve considerably higher waste loadings than the WTP baseline formulations [47-49]. As a result, the range of glass compositions that may be produced at the WTP is expanding toward higher sodium and sulfate contents and new glass components such as V_2O_5 (for improved sulfate solubility), SnO_2 (for leach resistance at high alkali concentrations), and Cr_2O_3 (for resistance to K-3 refractory corrosion) that are added as glass former additives, and this type of composition range expansion is likely to continue through the life of the project. In an initial effort to begin to encompass the composition range expected to be disposed at the IDF, a total of 10 glasses, referred to as IDF Phase 1 glasses, were selected as representative bounding glasses for this composition expansion [15]. A second set of ten Phase 2 glasses were added in FY2015 to expand the population of glasses at high alkali contents and fill gaps among lower Na_2O glasses with higher SO_3 contents [50-52]. Seven more glasses selected from those formulated to support development of an Enhanced LAW Glass Correlation for high waste loading glasses [53-55] were added to the test set in FY2018 [56]. Therefore, the IDF glass sets that are the subject of the present report include

27 high waste loading glasses, which complement the earlier set of 253 WTP glasses.

The compositions of Phase 1 and Phase 2 glasses are presented in Table 1.1 and shown in Figure 1.2. The selection was based on an analysis of the compositions and properties of the large number of LAW glasses that have been developed for the WTP at VSL. Multiple batches of these ten selected Phase 1 glasses were prepared for testing at VSL. Samples of three of these glasses were also shipped to Pacific Northwest National Laboratory (PNNL) to support complementary PUF testing (IDF1-B2, IDF2-G9, and IDF3-F7). Long-term PCT-Bs at VSL were conducted under accelerated conditions compared to the IDF in which the glass will be stored at 15 ℃. The first ten of these glasses were subjected to PCT-B at VSL at three temperatures (40 °C, 90 °C, and 120 °C) and two S/V values (2,000 m^{-1} and 20,000 m^{-1}), all in triplicate. Phase 2 glasses were subjected to long-term PCT-B at 90 °C and S/V of 20,000 m^{-1} in triplicate. The results showed that although the LAW glasses selected for this evaluation are compositions that have higher waste loadings than those developed for the WTP baseline, they follow generally similar leaching behavior. It is also evident that an increase in total alkali content alone is not necessarily detrimental to long-term PCT leaching. Furthermore, glass IDF1-B2, which has the highest alkali content of all glasses, and which fails the WTP VHT requirement by a significant margin, is actually one of the better performing glasses over the range of PCT-B conditions investigated. This indicates that the WTP VHT requirement (testing at 200°C) may be conservative with respect to the long-term robustness of the vitrified waste forms under disposal conditions (IDF at 15 °C). Glass IDF1-B2 showed robustness with respect to rate resumption despite increases in test temperature and S/V, both of which promote more reactive leaching conditions that drive the system towards secondary phase formation. This glass was deliberately included in the study to provide such a bounding case, together with the other IDF Phase 1 glasses described above; the rationale for the selection of these glasses has been described previously [15].

Four of the ten selected IDF Phase 1 glasses were also subjected to SPFT testing at VSL; the results were reported earlier [15, 57]. Full-suites of SPFT experiments as a function of pH, temperature, and silicic acid concentration (48 tests) were performed on the selected bounding glass, IDF1-B2. Full-suites of SPFT experiments were conducted later on glass IDF7-E12 [57]. More limited SPFT tests as a function of silicic acid concentration and temperature were performed on two other glasses, IDF2-G9 and IDF3-F7 [15]. Subsequently a full suite of SPFT tests was conducted on glass IDF2-G9 at PNNL [58] as well as on a fifth glass from the IDF Phase 2 set: IDF18-A161. The results of the SPFT tests were analyzed to determine the parameters in the ILAW glass dissolution model [59].

The selected bounding glass IDF1-B2 has a high Na_2O concentration (25 wt%) that significantly exceeds that of the WTP baseline glasses; it also has properties that challenge but are within the WTP limits except for its VHT response. The rate law parameters were generally similar to those for the previously tested WTP baseline glasses, but a number of deviations from that model were identified and discussed [15, 57]. For example, the model worked well for IDF1-B2 tests performed far from saturation, but under near saturation conditions, the data for

glass IDF1-B2 fit the TST rate model with H_4SiO_4 as rate controlling species only at low temperatures. Overall, however, the rate law parameters determined from the SPFT tests on the five high waste loading glasses (IDF1-B2, IDF2-G9, IDF3-F7, IDF7-E12, IDF18-A161) are of the same order of magnitude as those determined for other LAW glasses, such as LAWA44, LAWB45, and LAWC22, which are baseline WTP formulations that have generally lower waste loadings and, therefore, lower alkali contents. The fact that the rate law parameters determined for the bounding glass are close to those for the more typical WTP glasses is of practical significance since it suggests that higher waste loading glasses such as IDF1-B2 will likely still meet the requirements of the IDF PA. Establishing the viability of such high waste loading glasses in this regard is important in realizing their potential benefits in terms of reductions in life cycle costs and mission duration.

Other recent and ongoing SPFT tests have been conducted on glasses selected from 52 formulations (termed ORLEC glasses) spanning the range of alkali and sulfur concentrations in Hanford LAW [60]. These were formulated and characterized to support the development of an Enhanced LAW Glass Correlation [53-55] for the higher waste loading LAW glasses (Table 1.2). Glasses ORLEC28 and ORLEC33 were selected for SPFT testing at PNNL in FY2017 [59]. Glasses used in recent SPFT tests at the VSL include IDF21-EC14, representative of the high-alkali, moderate-sulfur (24 wt% Na_2O and 0.60 wt% SO_3) region of the high waste loading LAW formulations [60], IDF22-EC46 (18 wt% Na_2O and 1.37 wt% SO_3) at higher sulfur content and IDF23-EC52 (23.8 wt% Na_2O and 0.90 wt% SO_3) at intermediate sulfur content [61]. These recent ORLEC glasses were the primary source for the selection of new glass compositions for long-term PCT-B immersed in FY2018 and on which sampling continued this year. Detailed description of the composition algorithm is provided elsewhere [53-55] but a summary of the selection process and its comparison to other LAW glasses is provided in Section 2.

The results from long-term PCT-Bs collected at VSL over the previous eight years for the ten Phase 1 glasses have been reported earlier [50-52, 56]. The data were collected at an S/V of 20,000 m^{-1} at 90 °C and 120 °C, over 272 days, as well as at the nominal PCT S/V of 2000 m^{-1} at temperatures of 90 °C and 40 °C, and reported over ~2900 days, so far. At the lower temperature of 40 °C, the greatest extent of reaction based on boron normalized leaching was for glass IDF8-A125CCC, which reached 10 to 11% reacted glass at 900 days; that glass has stabilized at this level with little further alteration over the past five years. Very little (0.5% to 3%) of the glass has reacted for the other nine glasses tested at 40 °C, all remaining stable over the last four years reported. At 90 °C and S/V 2000 m^{-1}, six of the ten Phase 1 glasses were found to be over 50% reacted (IDF9-A187, IDF6-D6, IDF7-E12, IDF8-A125, IDF4-A15 and IDF3-F7) and percent reacted for the other four remained low. Two high sodium glasses (IDF5-A20 and IDF1-B2) started showing a rising leach rate close to that of the reference glass Argonne National Laboratory – Low-Activity Waste Reference Material (ANL-LRM) [62] at last sampling [56]. However, the high-alkali glass, IDF2-G9 (for Na+K), and the high zirconia glass IDF10-Zr6 remained at low leach rates of 8%, and 6% reacted, respectively, in the eight prior years of leaching [52]. Among the Phase 2 glasses tested at 90 °C and S/V of 20,000 m^{-1}, two reached resumption within the first six months (IDF18-A161 and IDF19-C100), two others (IDF14-A59 and IDF20-F6) and the reference glass ANL-LRM2 [62] reached resumption within

the first year, and two more reached resumption in the second year. These are generally low-zirconia glasses (less than 2 mole% Zr) with high alumina (above 9 mole% Al).

During FY18, PCT-Bs were started on seven glasses selected from those formulated to develop the Enhanced LAW Glass Correlation for high waste loading glasses [53-55]. All seven glasses are being tested at 90 °C and S/V of 20,000 m^{-1}. Two of the glasses are being tested at 90°C and S/V of 1000, 2000, 5000, 10,000 and 20,000 m^{-1}. Results from 7-day and 28-day samplings of the tests remain very low (~0.1 to 1% of reacted glass based on normalized boron release with much decreased leach rate between 7-day and 28-day samplings).

Overall, the PCT-B results reported so far show that although the LAW glasses selected for this evaluation have higher waste loadings than those developed for the WTP baseline, they follow generally similar leaching behavior and the increase in total alkali content alone is not necessarily detrimental to long-term PCT leaching. After eight-year leach testing, glasses IDF2-G9, IDF11-G27, and IDF1-B2, which have the highest alkali content on a molar basis of all 20 glasses, were still the better performing glasses over the range of PCT-B conditions investigated (even though IDF1-B2 fails the WTP VHT requirement by a significant margin). Based on the results available, the most detrimental compositional features in terms of early resumption appear to be high alumina and lower zirconia and silica; high alkali alone is not the determining factor in the relatively rapid alteration.

Selected PCTs were sampled and analyzed to characterize the secondary phases, which included zeolites such as analcime and gobbinsite, and phyllosilicates of the smectite group, saponite, lizardite, tobermorite and kaolinite. Glasses that have reached the later stages of reaction progress show the most abundant secondary phases, which facilitate their identification. High alumina and low ZrO_2 are compositional characteristics of these glasses.

Many of the long-term PCT-Bs initiated in Phase 1 and all of the long-term PCT-Bs initiated on the ten Phase 2 glasses are still ongoing; the objective of the present work was to review the accumulated data and perform additional analyses on selected ongoing tests in order to characterize the secondary phases that have formed. The combined solution analysis and secondary phase determination provide important information needed to identify and constrain the appropriate chemical reaction network required for model simulations.

SECTION 2.0
DESCRIPTION OF THE 27 IDF GLASSES IN COMPOSITIONAL SPACE

The target compositions of the Phase 1 and Phase 2 IDF LAW glasses are given in Table 1.1. They were selected from higher waste loading LAW glasses and the majority of them have been tested for processability in the DM10 melter, as shown in Figure 1.2 (thirteen larger red circles). A few glasses that have been tested only at crucible scale were included to better cover the compositional space for LAW glass compositions (red triangles in the figure). Target compositions of the seven recent (FY18) IDF glasses selected from the Enhanced LAW Glass Correlation for high waste loading glasses are given in Table 1.2. Their compositions in elemental percentage along with a summary of their properties are given in Table 2.1. They are illustrated in red squares in Figure 2.1, which shows ALK (Na_2O + 0.66 × K_2O) and SO_3 concentrations, and in Figure 2.2 where Na_2O concentration is shown on the y-axis. The two glasses tested at various S/V ratios are highlighted in yellow.

All IDF glass batches included a rhenium spike targeted at 0.1 wt% Re_2O_7 if all of it were retained in the glass. To accommodate the rhenium addition, 0.1 wt% SiO_2 was removed in comparison to the original composition. XRF measured rhenium and SO_3 values from the crucible glass melts prepared for IDF tests [50, 56] are used to define the respective Re and SO_3 content of these glasses.

All 27 IDF glasses included in long-term PCTs that are the subject of the present work are presented in Figure 2.3 in terms of their alkali and sodium contents; the higher alkali glasses are found at the upper right corner and the high sulfate-lower sodium glasses at the lower left.

A short compositional description of these glasses is given below.

Phase 1 IDF glasses:

- IDF1-B2 (top right in Figure 2.3), based on ORPLB2 (25.0 wt% Na_2O, 0.1 wt% K_2O, 0.5 wt% SO_3) has the highest mol% alkali oxide content among the selected glasses. This glass shows K-3 refractory corrosion neck loss close to the limit of 0.04 inches and VHT alteration rate slightly more than double the WTP limit. Other glasses evaluated for selection at the highest Na_2O content were rejected as they have viscosity values outside of the acceptable WTP upper limit of 150 poise at 1100 °C or include 3 vol% crystals after heat treatment for 20 hours at 950 °C. Of candidate glasses containing 25 wt% Na_2O, ORPLB2 is one for which properties relevant to processing are close to but within the WTP limits, PCT releases are within the WTP limits, and only VHT response is above the WTP limit; it was therefore selected as the bounding glass composition for the full suite of SPFT testing and for long-term PCT-B.

- IDF2-G9, based on ORPLG9 (21.0 wt% Na_2O, 5.8 wt% K_2O), was selected from the high alkali-high potassium glasses. This glass shows K-3 corrosion neck loss and VHT alteration rate close to, but within WTP limits. This glass was selected for SPFT testing and PCT-B. The sample had not reached resumption based on PCT-B results up to nine years at 90 °C and S/V of 20,00 m^{-1} (see Section 5.2).
- IDF3-F7, based on ORPLF7 has the highest SO_3 and lowest Na_2O concentrations (12.0 wt% Na_2O, 1.5 wt% SO_3) among the glasses selected for IDF Phase 1 testing. This glass also contains the highest lithium concentration of 4.37 wt% Li_2O.
- IDF4-A15 and IDF5-A20, based on ORPLA15 and ORPLA20, respectively, are two glasses with high alkali content (24.0 wt% Na_2O, 0.5 wt% K_2O) that have been used in melter tests at the VSL [63, 64]. These compositions meet all of the WTP contract specifications for LAW glass. These glasses have the second highest sodium concentration (after IDF1-B2), as can be seen in Table 2.1.
- IDF6-D6 (22.0 wt% Na_2O, 0.2 wt% K_2O, 1.2 wt% SO_3) was selected from glasses with intermediate sodium content where waste sodium loading is decreased to accommodate higher sulfate content. The alumina content also is high in this glass (10.1 wt% Al_2O_3) with Al/Si atomic ratio close to $^1/_3$ (see Table 2.1).
- IDF7-E12, based on ORPLE12 (16.0 wt% Na_2O, 0.6 wt% K_2O, 1.5 wt% SO_3), was selected from glasses that could accommodate the highest SO_3 concentration of 1.5 wt%. This glass contains 2.5 wt% Li_2O to improve sulfate solubility. This glass was selected for the full suite of SPFT testing and PCT-B.
- IDF8-A125 based on LAWA125 (20.0 wt% Na_2O, 4.2 wt% K_2O) was selected from high alkali-high potassium glasses with VHT alteration rate and K-3 refractory corrosion neck loss well within the WTP limits. This is a glass with one of the lowest combined alumina and zirconia contents (5.64 wt% Al_2O_3 and 2.91 wt% ZrO_2) but high silica content (42.81 wt% SiO_2), as is evident in Figures 2.4 and 2.5.
- IDF9-A187 (23.0 wt% Na_2O, 0.5 wt% K_2O) was selected from glasses with Na_2O concentrations ranging from 23.0 to 23.5 wt% but with high VHT alteration rate. This glass, as with IDF6-D6, has high Al_2O_3 content and Al/Si ratio close to $^1/_3$ (see Table 2.1).
- IDF10-Zr6 is based on glass LE4H-Zr6 and contains 9.50 wt% ZrO_2. This glass was formulated by increasing the ZrO_2 concentration in the WTP baseline glass LAWE4H by 6 wt%. This glass was included in the set for PCT-B because higher ZrO_2 decreases VHT alteration rate and K-3 neck corrosion, which makes high zirconia of interest for high waste loading LAW glasses. Tests conducted for WRPS [65] to improve technetium retention in LAW glasses showed that ZrO_2 may be beneficial for this application. Accordingly, this glass was selected for PCT-B because none of the other glasses has such high ZrO_2 concentration. Note that this glass has the lowest alumina content (4.95 wt% Al_2O_3), as evident in Figure 2.5.

Among these IDF Phase 1 glasses for which long-term leach tests were initiated in 2010, glasses IDF9-A187CCC and IDF6-D6CCC showed resumption at the earliest, with both showing the formation of analcime and gobbinsite in the alteration products [50]. As noted above, these two glasses have the highest Al_2O_3 content and Al/Si ratio very close to $^1/_3$ (Table 2.1). Zirconium is also relatively low in these two glasses, and in IDF8-A125CCC, which also showed analcime formation in long-term leach test results, as reported earlier [50].

For the Phase 2 IDF glasses, seven were selected from the high-alkali region:

- IDF11-G27, based on ORPLG27 (21.0 wt% Na_2O, 5.8 wt% K_2O); this glass has one of the highest alkali oxide concentrations among all of the glasses selected for testing.
- IDF12-A38, based on ORPLA38-1 (24.0 wt% Na_2O, 0.5 wt% K_2O) includes V_2O_5 as an additive for high alkali glasses to accommodate higher concentrations of SO_3 (0.8 wt%).
- IDF13-A51 based on ORPLA51 (24.0 wt% Na_2O, 0.5 wt% K_2O) investigates the effect of higher TiO_2 concentration.
- IDF14-A59 (24.0 wt% Na_2O, 0.5 wt% K_2O) is a new formulation prepared for the IDF Phase 2 tests; it is based on ORPLA51 but at lower Cl and SO_3 concentrations. Comparison of the long-term PCT responses for IDF13-A51 and IDF14-A59 can therefore show the effect of Cl and SO_3 concentrations.
- IDF15-A57 (24.0 wt% Na_2O, 0.5 wt% K_2O) is also a new formulation prepared for the IDF Phase 2 tests. This glass is based on ORPLA57 and, as with the previous two glasses, was formulated with high alumina, titania, and zinc to control K-3 corrosion in high alkali glasses without adding Cr_2O_3. IDF15-A57 contains 10.65 wt% Al_2O_3, 3.0 wt% TiO_2, 4.0 wt% ZnO, but no MgO.
- IDF16-A58 is based on ORPLA58 (24.0 wt% Na_2O, 0.5 wt% K_2O) and is similar in composition to the previous four glasses (10.65 wt% Al_2O_3, 3.0 wt% TiO_2, 3.0 wt% ZnO) but without CaO.
- IDF17-A60 is based on ORPLA20 with high Na_2O content but with Cl decreased to 0.1 wt% and SO_3 decreased to 0.3 wt%. In this way, the results from PCT-B of this glass can be compared to those from ORPLA20 because the alkali content in both are fixed at 24.0 wt% Na_2O and 0.53 wt% K_2O.

Three Phase 2 glasses were included to fill the composition gaps amongst the lower Na_2O glasses.

- IDF18-A161 is based on LAWA161, which was the enhanced formulation for LAW from Tank AN-105 when the waste definition included higher chlorine content. As a result, the formulation was designed at 20.66 wt% Na_2O and includes 1.17 wt% Cl. This formulation was further tested in a melter at progressively increasing sulfate levels up to

1.10 wt% SO_3 without the formation of secondary sulfate phases [66]. It is also a low zirconium glass (Figure 2.4).

- IDF19-C100 is based on LAWC100 (for Tank AN-102). This formulation is close to LAWA161 in composition but is higher in SO_3 content (1.2 wt%) and lower in Cl content (0.65 wt%). Among the IDF glasses selected for testing, this glass has the highest boron content (13.68 wt%).
- IDF20-F6 is based on ORPLF6, an enhanced formulation for LAW from Tank AZ-101 for which a sodium loading of 13.0 wt% Na_2O would require a sulfate loading of 2.09 wt% SO_3 based on the waste composition [64]. The selected formulation at 13 wt% Na_2O was prepared with a sulfate content of 1.25 wt% SO_3 since that is the sulfate content that was previously evaluated in sulfate oversaturation tests.

The seven FY-18 IDF glasses were selected from 52 high waste loading LAW glasses, termed "ORLEC" glasses, spanning the range of alkali and sulfur concentrations in Hanford LAW formulated and characterized to support the development of an Enhanced LAW Glass Correlation for high waste loading glasses [53-55]. The strategy for the development of this Enhanced LAW Glass Correlation is similar to the one used in the development of the WTP Baseline LAW Glass Correlation [67]. The selection has been described in a previous report [56] and the glass distribution in composition space can be seen in Figure 2.1. The glasses span the range of alkali and sulfate concentrations for the high waste loading Hanford LAW glasses and are marked in Figure 2.1 by a red box around the sample number. Another consideration in making the selection of these ORLEC glasses for long-term PCT is that eight of the ORLEC compositions have already been recommended for SPFT testing. The seven glasses selected for long-term PCT are as described below and their elemental compositions along with a summary of their properties are given in Table 2.1.

- IDF24EC28 (originally ORLEC28) is at the high potassium (3.36 wt% K_2O) and medium SO_3 (0.4 wt%) part of the *Alkali Limited Region (AL)*[2] range where the alkali content of the glass limits waste loading. It bridges the gap between IDF2-G9 (highest K_2O content) and other high alkali glasses with lower K_2O contents.

- IDF28EC50 (originally ORLEC50) is a high sodium (24 wt% Na_2O) glass at the high SO_3 (0.6 wt%) concentration part of the *AL* region. The plot of Na_2O vs. SO_3 in Figure

[2] ORLEC formulations are defined in the range of alkali and sulfate concentrations of Hanford tank wastes as either *Alkali Limited Region (AL)* where ALK = Na_2O (wt%) + 0.66 K_2O (wt%) is limited to 24.33 wt% or as *Alkali & Sulfate Limited Region (ASL)* where both Na_2O and SO_3 concentrations need to be managed to optimize waste loading (curved section in Figure 2.1). If the sulfate concentration in the LAW increases further, waste loading in the glass is limited by sulfate alone at a value of 1.5 wt% SO_3 in a region termed *Sulfate Limited Region (SL)*.

2.2 provides another view of the difference between ORLEC28 and ORLEC50 with different sodium and potassium contents.

- IDF23EC52CCC, ORLEC52, ORLEC34, ORLEC44, ORLEC46, and ORLEC48 are glasses selected at decreasing Na_2O and increasing SO_3 concentrations in the *ASL* region.

Although some overlap appears in Figure 2.3 with some of the earlier IDF glasses and the new selections (e.g., IDF9-A187 and ORLEC34, IDF7-E12 and ORLEC48), the glasses have differences when considering all of the other glass constituents.

Two of these seven glasses were selected to be tested at five different S/V ratios, to total 15 PCTs initiated in FY18. These are divided into two sets of five glasses: two sets for the S/V variation study and one set for the remaining five glasses.

Glass preparation, compositional analyses, evaluation and preparation of the glass powders for long-term PCT have been described in earlier reports: for Phase 1 [15], Phase 2 [50], and FY-18 [56] glasses. All glasses were subjected to canister centerline cooling (CCC) heat treatment [68] before PCT-B, with the suffix CCC added to their name. The LAW Enhanced Correlation (ORLEC) glasses were prepared for PCT-B in the same manner as earlier glasses, and with the same sample nomenclature as given below:

IDF22EC46CCC for formulation ORLEC46
IDF23EC52CCC for formulation ORLEC52
IDF24EC28CCC for formulation ORLEC28
IDF25EC34CCC for formulation ORLEC34
IDF26EC44CCC for formulation ORLEC44
IDF27EC48CCC for formulation ORLEC48
IDF28EC50CCC for formulation ORLEC50

In the data discussion that follows, some of these samples have been simplified to "ECxx".

2.1 Summary of Tests Parameters: Temperature and Variation in S/V Ratio

Long-term PCT-Bs on LAW IDF glasses have been conducted so far at three temperatures (40 °C, 90 °C, and 120 °C) and two S/V values (2,000 m^{-1} and 20,000 m^{-1}). Tests conducted at room temperature on early WTP glasses [69] showed very low alteration, well below 1 g/L, likely requiring decades before the reacted surface would show measurable alteration. Similarly, little alteration has been observed in the long-term PCTs conducted at 40 °C, as described in Section 1.3. In contrast, resumption was reached in many of the tests conducted at 90 °C and 120 °C. At 90 °C, the reacted glass sampled could be well characterized and phases were identified. At the higher temperature of 120 °C, the reacted glass and leachate

quickly became difficult to sample because the entire system gelled together [52]. A test temperature of 90 °C was therefore selected for the FY18 set of tests.

Variation in S/V ratio has been investigated on Phase 1 glasses at two S/V values of 2,000 m^{-1} and 20,000 m^{-1}, while Phase 2 glasses were all tested at 20,000 m^{-1}. The same single S/V ratio of 20,000 m^{-1} was selected for the tests initiated in FY2018, along with a more comprehensive study of the impact of the S/V ratio on glass leaching. In Phase 1 glasses, resumption was observed at both S/V values, but it also affected greatly the resulting solution pH, as reported earlier [15]. Matrix dissolution, ion exchange, and secondary phase formation are intricate mechanisms of the long-term glass leaching, which are all highly affected by the leachate pH [17-21, 25-30, 33, 70, 71]. The contribution from ion exchange and the corresponding pH rise is further enhanced by making more surface area of the glass available to the leach reaction by increasing the surface area of glass per unit volume of leachant. In the present work, the effect of systematic changes in S/V ratio on leachate composition, pH, and on the reacted glass layer and secondary phases are also studied by testing glasses ORLEC28 and ORLEC52 at five different S/V ratios. Studies on the impact of S/V ratio on pH and resumption were previously conducted at VSL on multiple HLW glasses [21].

The selections of the five different S/V ratios were made based on results from long-term PCT of Phase 1 and Phase 2 glasses, which showed that resumption was reached within months to two years at S/V of 20,000 m^{-1} and as early as one year at 2000 m^{-1}. The range selected is from 1000 m^{-1} to 20,000 m^{-1}.

SECTION 3.0
LONG-TERM PCT-B DATA

Long-term PCTs were initiated on ten high waste loading Phase 1 IDF glasses under a test program for WRPS in 2010 [15]. Although funding for that program ended in 2011, most of the long-term PCTs were maintained at VSL's expense and then continued under the 2015 Phase 2 of the IDF program. Also, in Phase 2 tests on ten additional glasses were initiated and are continuing. Finally, in FY18, PCTs were initiated on seven more glasses selected from those formulated to support development of the Enhanced LAW Glass Correlation for high waste loading glasses [53-55]. This section provides an update on the data for the 20 IDF Phase 1 and Phase 2 glasses and the first year of data on the PCTs started in FY18. The long-term tests were subjected to additional leachate sampling and analysis in order to bring the data set up to date. In addition, samples of reacted glass were recovered from selected test vessels for analysis of the secondary phases. Selected tests are being continued (maintenance, sampling, and analysis) in order to further extend the data set to yet longer times. Note that in the figures presented in association with the discussion below, the sample label is often shortened and does not include the "-" separating the IDF number and the original glass code, nor the suffix "CCC," which is part of the sample ID and which denotes the heat treatment that has been imposed on all IDF samples tested herein. It is also noted that ANL-LRM is the PCT reference glass that has undergone PCT-A round robin testing [62]; that glass was tested without the CCC heat treatment.

The product consistency test [72] is used to evaluate the relative chemical durability of glasses by measuring the concentrations of the chemical species released from 100-200 mesh crushed glass (75-149 μm) to the test solution (de-ionized water in this case). PCT-A (90 ºC, 2000 m^{-1} and 7-day) had been performed previously on most of the selected LAW glasses in standard 60-mL 304L stainless steel leach vessels. PCT-B conducted in IDF Phase 1 and Phase 2 work used leach vessels of 150 mL capacity (also 304L stainless steel). These vessels have a bottom plug and a top plug assembly that screw on to each end permitting regular leachate sampling through a top septum without breaking the seal of the vessel, and, if needed, sampling of the glass by dismounting the bottom plug.

The PCT-B was performed in triplicate on all of the glasses [15, 50] in parallel with the ANL-LRM reference glass, which was included in each test set. The tests are generally divided into sub-sets to keep the PCT sets at a manageable size of 20 vessels (five glass tests in triplicate, plus three standard glass samples and two blanks). IDF Phase 1 tests include PCT at S/V of 2000 m^{-1}, with 10 g of glass powder in 100 ml of deionized water per vessel. The 20 IDF Phase 1 and Phase 2 glasses have been tested at 90 °C and the high S/V value of 20,000 m^{-1}; this was selected in order to investigate as early as possible the secondary phases that are formed. In this case, 40 g of glass powder is placed in 40 ml of deionized water. The PCTs started during the FY18 work

included seven glasses at S/V of 20,000 m^{-1}, as well as two of these glasses tested at four additional S/V values of 1000 m^{-1}, 2000 m^{-1}, 5000 m^{-1}, and 10,000 m^{-1}. The mass of glass powder and respective volume of deionized water per vessel for these tests are provided in Table 3.1.

The sampling protocol consisted of removing an aliquot of 4 mL of the leachate at 7, 28, 56, 120, 181, 270, 365, and 547 days, and yearly thereafter; the solution that is removed for analysis is replaced with 4 mL of deionized water. As noted in the data provided below, the effect of the minor dilution (4% at 2000 m^{-1}, or 10% at 20,000 m^{-1}) due to this solution exchange is not detectable between successive samplings. In addition to the effects of glass composition at 90 ºC and S/V of 20,000 m^{-1}, variations in test temperature (40 °C and 90 °C) and S/V (2000 m^{-1} and 20,000 m^{-1}) are represented in the dataset for Phase 1 IDF glasses. The data for the Phase 1 glasses now extend to nine years at S/V of 2000 m^{-1}. PCTs on IDF Phase 2 glasses (90 °C and S/V of 20,000 m^{-1}) have just passed four years of testing, and FY18 IDF glasses reached the first full year of testing. Sampling and analysis of all of the PCTs that have not reached resumption[3] are continuing.

In addition to the leachate concentrations, it is convenient and conventional to also consider the normalized leachate concentrations which are used in discussions in this section. The normalization is performed by dividing the concentration measured in the leachate for any given component by its mass fraction in the glass. Thus, the *normalized concentration* C_i of element i (in g/L) is calculated from the elemental concentration c_i measured in the leachate (in g/L) as:

$$C_i = \frac{c_i}{f_i} \ , \tag{3.1}$$

where f_i is the mass fraction of element i in the glass. The normalized concentrations are a measure of the mass of glass reacted based on the specific element and provides a useful insight into which of the glass constituents contribute to new phase formation. If species are found in solution in proportion to their stoichiometry in the glass, dissolution is congruent. This is usually the case for boron for which the rate of release from the glass is proportional to the glass dissolution rate because it is typically not retained in any reaction product formed during leaching. When alkali and boron in the leachate have similar normalized concentrations, their release is congruent. On the contrary, a strong deviation from congruency likely indicates that the constituent is involved in surface crystallization, or otherwise retained in the altered glass. Under the PCT conditions employed in tests at S/V of 2000 m^{-1} (10 g glass per 100 ml water), a normalized boron release nearing 100 g/L corresponds to 100% reacted glass as it is equivalent to the full glass boron content being released to the solution. At S/V of 20,000 m^{-1}, 1000 g/L corresponds to 100% reacted glass.

[3] Leachate analysis is used to identify resumption: it is identified as a sharp increase in leach rate, after a succession of stable lower leach rates, the latter corresponding to the Residual Rate regime (illustrated in Figure 1.1).

Based on percent relative standard deviations (%RSDs) given in Appendix A1-A3, triplicate results are in good agreement and resumption, when it occurs, takes place for the three replicates at about the same time.

3.1 Long-Term PCT-B at 90 °C and S/V of 20,000 m^{-1}

3.1.1 IDF Phase 1 Data Set

PCT-B at 90 °C and S/V 20,000 m^{-1} was performed on the ten Phase 1 glasses as reported previously [50] and summarized in Section 1.3. No new data were collected on these glasses, but the results are combined in summary Table 3.2 for comparison to other results presented below. As pointed out earlier, the glasses that showed resumption early in that set have the lowest zirconia (such as IDF9-A187), as well as the highest Al_2O_3 contents and Al/Si ratio very close to 1/3 (IDF6-D6). Sampling of the reacted glass samples showed heavy formation of analcime and gobbinsite in the alteration products [50].

3.1.2 IDF Phase 2 Data Set

The leachate sampling duration for the ten IDF Phase 2 glasses has now reached four years. The results from sampling of the two PCT sets (designated ILHC and ILHD) are summarized in Table 3.3. IDF18-A161CCC and IDF19-C100CCC were the first two glasses to reach resumption shortly after the 119-day sampling (Figure 3.1). Next to reach resumption were IDF14-A59CCC and IDF20-F6CCC, at 1-year sampling, along with the reference glass ANL-LRM. IDF14-A59CCC reached 100% altered glass (1087 g/L) but IDF20-F6CCC, IDF18-A161CCC, and IDF19-C100CCC stabilized at around 55-70% altered glass (544 to 702 g/L), staying in the range of 500 to 600 g/L for the last three years. It is possible that the high SO_3 content in these three glasses acts as a pH buffer. Indeed, the pH measured in these three leach tests is a full pH unit below the pH measured in IDF14-A59 in which the SO_3 concentration is 0.1 wt%. However, because high SO_3 glasses generally have high lithium contents, the respective effects are difficult to separate. Also, as shown in Figure 2.4, IDF18-A161CCC and IDF19-C100CCC are the two glasses with the lowest ZrO_2 content among the Phase 2 glasses, comparable to the Phase 1 glasses IDF9-A187CCC and IDF6-D6CCC. They are also high in Al and Ca which, as discussed later in Section 4, are all conditions detrimental to long-term leach resistance because of the alteration phases that they favor. Note also that although Ca remains generally very low in leachate analyses (<<0.1 g/L normalized release) in the early samplings, it rose sharply above 100 ppm (normalized release ~2 g/L) at the 182-day sampling, when resumption was noted, and remained at that concentration thereafter.

In contrast, resumption started for IDF14-A59CCC at later sampling dates (shortly after the 273-day sampling) but the boron release continued to rise sharply over the following two years. Leachate sampling for IDF14-A59CCC at 913 days shows that all available boron has

been released (1087 g/L with 1.7% RSD among triplicates). Note that this is a glass with lower Cl and SO_3 concentrations.

The reference glass ANL-LRM2 also reached resumption around the 1-year sampling period with excellent agreement between both sets of triplicates from sets ILHC and ILHD. The reason for the drop in boron release observed in Figure 3.1 after reaching 100% altered glass can be partially explained by the 10% dilution brought about at sampling and which cannot be compensated for after all the boron from the glass is released. At such large extents of alteration, most of the sample has converted into a gelled mass, which might retain some of the leached constituents. Sampling becomes difficult, and in some cases, the amount of free liquid available for sampling in the vessel is very small. Test vessels containing this glass, as well as IDF14-A59, were sampled and the tests terminated.

Between 300 and 900 days, the leach rates for glasses IDF13-A51CCC and IDF15-A57CCC increase at much slower rates (see Figure 3.1). These are two glasses for which higher amounts of TiO_2 and ZnO, and high alumina content were tested to prevent excessive K-3 refractory corrosion. However, IDF13-A51 reached resumption in the past year, reaching 870 g/L boron release while IDF15-A57 stabilized below 300 g/L normalized boron. Higher TiO_2 and MgO in IDF13-A51, as in IDF14-A59, could be the reason for such increase. Note that the only difference between these two glasses is their chloride and sulfate contents, at 0.7 wt% in IDF13-A51 and at 0.1 wt% in IDF14-A59 which lead to a difference in pH of 0.4 after resumption between the two tests (see Table 3.3).

The remaining four glasses (IDF11-G27CCC, IDF12-A38CCC, IDF16-A58CCC, and IDF17-A60CCC) still show the least altered glass (~5% to 15%) based on normalized boron release. Among these, three glasses are high in silica and low in alumina, which is consistent with the observations from the IDF Phase 1 set (resumption delayed for glasses at Al/Si ratio lower than 1/3). In addition, all four are glasses containing higher than 2.75 wt% SnO_2. Finally, removing calcium entirely in IDF16-A58CCC appears to have delayed the time to resumption as compared to IDF15-A57CCC (no MgO) and IDF14-A59CCC. Note that the composition differences noted in Figure 3.1 and highlighted in the discussion are among many probable sources of differences among the glasses. Analyses of the glass surface in Section 4 will discuss this aspect further.

At this high S/V of 20,000 m^{-1}, liquid sampling has become very difficult in most PCT vessels now containing a large fraction of highly hydrated glass/gel, even when the measured boron in solution remains low; it is likely that most glasses that reached > 50% reaction based on boron (>500 mg/L), and possibly some of the others, will become impossible to sample due to the lack of access to any liquid.

3.2 Long-Term PCT-B at 90 °C and S/V of 2000 m^{-1} on IDF Phase 1 Glasses

The results from the PCT-B at 90 °C and S/V of 2000 m^{-1} on IDF Phase 1 glasses (test sets ILHA and ILHB) show a similar trend in leach rate to those observed at high S/V [50], but they occur at longer times and in a slightly different order (Figure 3.2; note that at this S/V a normalized boron concentration of 100 g/L corresponds to 100% of the boron content in the glass in solution). In the first six years of the total of nine years of testing, six of the ten glasses have exhibited elevated rates indicative of resumption. First was IDF9-A187CCC, followed by IDF6-D6CCC (shortly after samplings at 365 and 545 days, respectively). For these two glasses, the order is the same as in the respective higher S/V tests. Resumption was observed next with IDF8-A125CCC, between 720 and 1800 days, but the alteration rate is not as high. For IDF7-E12CCC, resumption occurred around 1200 days with a sharp rise in rate. Resumption of IDF4-A15CCC was observed between 1200 and 1800 days; it has now reached 80 g/L normalized boron release. Finally, glass IDF3-F7CCC reached resumption with a sharp rise at 1925 days and stabilized at 90 g/L normalized boron release. It has become difficult to obtain a liquid sample from these last four glasses, which are all nearly fully reacted, and these tests were terminated at the same time as when solid samples were collected. As noted in Figure 3.2, tests for IDF9-A187CCC and IDF6-D6CCC have been terminated and the solid phases were collected and analyzed previously [50]. Small amounts of the altered glass were also collected from one of the triplicate vessels from all eight remaining tests. Analyses of samples of IDF8-A125CCC, IDF7-E12CCC, and IDF4-A15CCC were reported earlier [50].

IDF5-A20CCC has reached 2886 days of testing as of the 2018 sampling. It showed increase in boron normalized release from 8.2 g/L at year 5 to 14.5 g/L at year 6 and 23.5 g/L at year 7 but seems to have plateaued in the past two years. It is not clear what could have delayed the increase in release rate, but it is possible that the 4% liquid replenishment is affecting the solution when so much of the liquid is immobilized in the alteration gel. Large solid masses showing agglomeration of glass grains and gels that are likely trapping the solution also were observed in these samples (see Section 4).

IDF1-B2CCC, which has the highest sodium (Na is 38.4 cation%; see Table 2.1), has now reached resumption: the boron normalized release more than doubled in the past two years and now has reached 58 g/L. IDF2-G9CCC, the high potassium glass, is actually higher than IDF1-B2 in total alkali content but it appears to be the most durable among this series of high alkali glasses (Na + K is 38.5 cation% in IDF1-B2 and 38.9 cation% in IDF2-G9 – see Table 2.1). It remains stable at about 7-9% alteration based on boron. It is comparable to the lowest alteration observed for the high zirconia glass IDF10-Zr6CCC (medium alkali), which remained at 6% altered glass (boron normalized release of 5.6 to 6.4 g/L) in the last twelve samplings. This test was also difficult to sample, which may be the reason for the apparent decrease in normalized release. Here again, solid evaluation given in Section 4 provided clues to the reason for this difficulty: large agglomeration of altered glass grains and gel.

The ANL-LRM reference glass [62] continues to show a consistently high rate of alteration, with a higher rise at the last two sampling, with good reproducibility between replicates (now at 39 and 41 g/L boron normalized release, with 1.1% RSD and 1.6% RSD for the two triplicate datasets).

3.3 Long-Term PCT-B at 40 °C and S/V of 2000 m^{-1}

At the lower test temperature of 40 °C (test sets ILLA and ILLB), all ten Phase 1 glasses and the ANL-LRM2 reference glass show much less alteration and none of the glasses have reached resumption over the period of testing. As shown in Figure 3.3, the alteration rates remain nearly unchanged in the past five years of leach testing. Based on normalized boron release, for nine of the glasses, less than 0.5% to 3% of the glass has reacted, all remaining stable over the last four years. For IDF8-A125CCC, 10 to 11% of the glass had reacted at 900 days and the reaction appears to have stabilized at this level up to 3270 days as of the latest sampling. As shown in Figure 3.4, the normalized releases for the two alkalis (Na and K) follow the same trend but sodium shows a small deviation from congruence with boron (~8.6 g/L on average over the last 6 years) and potassium is found at only a third of the boron release. As noted in the figure, the pH continues to increase slowly at each successive sampling, indicating that water ingress and ion exchange continues. Yet, slight decreases in sodium and potassium releases are noticeable at the last sampling, possibly because they are held in pores of a gel that formed or associated with mineral phases at the glass surface.

In an effort to identify similarities and differences in the phases that have developed in the various leach tests (analyses in Section 4.0), samples of the solid phases developed on the glasses were collected from all vessels of the following tests:

- ILLA and ILLB: Ten Phase 1 glasses at 40 °C and S/V of 2000 m^{-1},
- ILHA and ILHB: Eight Phase 1 glasses at 90 °C and S/V of 2000 m^{-1},
- ILHC and ILHD: Ten Phase 2 glasses at 90 °C and S/V of 20,000 m^{-1}.

3.4 PCT Data on IDF Glasses Immersed in FY18

3.4.1 Long-Term PCT-B on FY18 IDF Glasses at 90 °C and S/V of 20,000 m^{-1}

Five of the seven FY-18 IDF glasses described in Section 2 were tested together in one PCT-B set at 90 °C and S/V of 20,000 m^{-1} designated ILHE. Glasses ORLEC52 and ORLEC28, in tests designated ILHF and ILHG, respectively, were tested at various S/V ratios, including an S/V ratio of 20,000 m^{-1}; the discussion herein compares the results from all seven glasses at S/V of 20,000 m^{-1}.

PCT leachate analyses up to 365 days are reported for these samples in Table 3.4. At this high temperature and high S/V ratio, the leaching was already well beyond the early stages of alteration (inter-diffusion and hydrolysis) at the 7-day sampling reported last year [56]. As sampling proceeded through the year, tests for glasses ORLEC46 and ORLEC50 were reduced from a triplicate to a duplicate when the interval between sampling exceeded one month because the evaporation from one vessel in each triplicate exceeded 10% of original leachant weight, the maximum acceptable per VSL procedure.

As evident in the three plots in Figure 3.5 all boron normalized releases during the first 56 days range between 2 g/L and 13 g/L (less than 1.3 % reacted glass) and follow the "residual rate" regime depicted in Figure 1.1. At this high S/V of 20,000 m^{-1}, none of the ORLEC glasses exhibited an early resumption as was the case for the Phase 1 glass IDF6-D6 at 56 days. Sodium normalized release is less than that of boron for the higher alkali glasses (in ORLEC52 and ORLEC50, boron is at 13 g/L and sodium at 9 g/L) but, in general, sodium release is at or above congruence with boron, and higher in the three glasses that also contain lithium, ORLEC44, ORLEC46 and ORLEC48. Rhenium release is always lower than boron release.

During the following samplings at 4 and 6 months, resumption was detected in the four higher SO_3 glasses: ORLEC34, ORLEC44, ORLEC46, and ORLEC48 (Figure 3.6). These are glasses in which SnO_2 was not used as a glass former additive and ZrO_2 was kept between 3.5 and 4 wt% to improve sulfate solubility in the glass. On the other hand, the three high alkali glasses ORLEC28, ORLEC50, and ORLEC52 show less than 25 g/L boron release (<2.5% reacted per boron release) after a full year of testing. They remain in the residual rate regime up to 270 days but a slight increase in normalized release is detectable at the 365-day sampling, indicating that resumption may occur in the near future. Sodium release follows a similar trend for all glasses: regardless of resumption it remains at about 60 to 70% below congruence with boron.

3.4.2 Tests ILHF and ILHG at Varying S/V Ratios

Glasses IDF23-EC52CCC and IDF24-C28CCC, in tests designated ILHF and ILHG, respectively, were tested at various S/V ratios. Both tests are conducted at 90 °C and five S/V ratios of 1000, 2000, 5000, 10,000 and 20,000 m^{-1}, in triplicate. These two glasses are in the high alkali composition range, containing 23.80 wt% Na_2O, 0.50 wt% K_2O, and 0.90 SO_3 for IDF23-EC52CCC, and 22.11 wt% Na_2O, 3.36 wt% K_2O, and 0.40 SO_3 for IDF24-C28CCC. PCT leachate analysis at 7 days and 28 days are reported for these samples in Table 3.4, and for the ANL-LRM reference glass in Table 3.5.

The effect of variations in S/V ratio on PCT releases can be seen in Figures 3.7 and 3.8 for glasses IDF23-EC52CCC and IDF24-EC28CCC, respectively. As suggested from previous tests on other waste glass formulations in long-term PCT [21], an increase in S/V ratio produces

an increase in leaching for the main glass components. Normalized boron release is shown as a function of time in Figures 3.7 and 3.8; similar trends are observed for Na, K, Re, and Si. Boron exhibits the highest releases for both glasses, but it is lower in IDF24-EC28CCC. In IDF23-EC52CCC PCT sodium release is about 3/4 of that of boron, potassium about 1/3, and silicon less than 10% of that of boron. Because boron leaches less in the higher potassium glass IDF24-EC28CCC, deviations from congruence are slightly lower (sodium release is about 80% of boron release, potassium 45 to 50% of boron, and silicon varies between 25% to 7% of boron). The pH increased over the first four samplings (7 days to 120 days) and stabilized after 180 days.

Normalized releases of the main glass components and the rhenium spike are shown as a function of S/V in Figures 3.9 and 3.10 for the two glasses IDF23-EC52CCC and IDF24-EC28CCC, respectively. One point excluded was the last sampling at 365 days for 20,000 m^{-1}, which appears to show a possible transition to resumption. The releases fit a power law function of S/V, which follows the previously demonstrated dependence with pH [21]. The region II pH shows a linear relationship with log(S/V), as shown in 3.11.

Rhenium is often used as a non-radioactive surrogate for Tc. Because Tc is a major contributor to the overall dose calculations in the IDF PA, it is important to understand the behavior of Tc as it relates to glass corrosion. For this reason, the release behavior of the 0.1 wt% Re spike from IDF23-EC52CCC and IDF24-EC28CCC was evaluated for all samplings between 7-day to 365-day and compared to the release behavior of the other components, as shown in Figures 3.12 and 3.13. Previously reported 7- and 28-day samplings showed that at the lowest S/V and 7-day sampling for IDF24-EC28CCC, rhenium release was nearly congruent to that of boron (0.55 g/L Re and 0.67 g/L B) but it quickly decreases to about 1/3 of that of boron (3.29 g/L Re and 9.47 g/L B), and close to the release of potassium (4.21 g/L) [56]. Similar near congruence for IDF23-EC52CCC at S/V of 1000 m^{-1} (0.40 g/L Re and 0.58 g/L B) was observed at the 7-day sampling, which decreased to about 1/3 of boron at the 28-day sampling (0.65 g/L Re and 1.85 g/L B), close to the release of potassium (0.64 g/L). Evaluation of all leachates up to 365-day sampling showed that rhenium normalized release remains well below 5 g/L while boron release rises to above 15 g/L. Overall, on average, rhenium release is 27% that of boron in IDF23-EC52CCC and 22% in IDF24-EC28CCC.

It is anticipated that sampling and evaluation of the glass leached layers after corrosion will be conducted at the next sampling, particularly since the 365-day sample indicated that resumption is imminent at the highest S/V of 20,000 m^{-1}.

SECTION 4.0
SECONDARY PHASE ANALYSIS OF IDF PCT-B SAMPLES

Samples of altered glass were collected from 28 ongoing PCT-Bs immersed in prior years (8 glasses from tests ILHA and ILHB at 90 °C and S/V of 2,000 m^{-1}, 10 glasses from tests ILLA and ILLB at 40 °C and S/V of 2,000 m^{-1}, and 10 glasses from tests ILHC and ILHD at 90 °C and S/V of 20,000 m^{-1}). None of the vessels from the triplicate sets were sacrificed. A small amount of the altered glass was removed from one of the triplicate vessels (which was then so identified) and the test was continued. Sampling was done in this manner to allow for the possibility that phases developed at the glass surface would be insufficiently crystallized for characterization and, therefore, later sampling would be required. Between 0.04 and 1.76 g of sample was taken out of a total of 10 g per vessel in tests ILHA, ILLA, ILHB, and ILLB, and between 0.11 to 0.82 g out of 40 g per vessel in tests ILHC and ILHD. The powder was triple-rinsed with warm (near 90°C or 40°C according to the leach test) de-ionized water and dried prior to preparation for analysis by SEM/EDS and XRD. XRD evaluations were completed, reported previously [56], and are now complemented with SEM evaluation. The results are provided in Tables 4.1 and 4.2, where earlier sampling evaluations are also collected to complement and compare with the SEM findings described below.

Sample nomenclature for glass powders after their sampling from a leach vessel was as follows: the leach test ID (e.g. ILHA, ILHB, etc.) followed by the sampling time and the vessel number. For example, IDF1-B2 in ILHA-18-5 is IDF1-B2 altered glass taken from vessel #5 at the 18^{th} time the leachate was sampled.

In prior evaluation of IDF Phase 1 and Phase 2 glasses [50-52, 56] that have reached resumption, the phases identified in the leached glass samples are tecto- or sorosilicates, as identified using XRD by well-defined sharp diffraction peaks. In SEM, structures that developed above the glass surface were observed. Phyllosilicates, if present, could not be identified on IDF Phase 2 glasses in earlier samplings [52]. In contrast, phyllosilicates were identified in IDF Phase 1 glasses, even when alteration remained low, together with tectosilicates in glasses that underwent resumption. Sampling of the other IDF Phase 2 glasses that had not reached resumption had been reserved for future years in order to allow longer time for the alteration products to develop sufficiently and crystallization to mature to more identifiable forms. Many glasses sampled last year from PCTs had already reached resumption or resumption seemed impending. The present results assist in identification of abundant crystalline phases concomitant with resumption. The results of SEM evaluation provided below complement the XRD results presented earlier.

SEM analyses where conducted following two different sample preparations of each collected altered glasses: (1) grains were mounted on a small carbon-impregnated tape to observe the morphology of crystallization; (2) the altered glass was embedded in epoxy and polished to

expose a cross-sectional view in SEM.

For XRD analysis, dried samples of altered glasses were crushed and then deposited onto a sample holder. This was necessary to avoid preferential crystal orientation, which would hinder phase identification by XRD. The amount collected for XRD was very small for some of the samples (due to agglomeration of the glass sample in the leach vessel) and care was taken to avoid loss of material during grinding. The XRD powder patterns have been reported previously [56]; typical phases have included nontronite and saponite, smectites of the phyllosilicate mineral group, and, for glasses that have reached resumption, phillipsite, gobbinsite, and analcime (all zeolites of the tectosilicate mineral group) [15, 50]. A summary of previous findings is included here for convenience.

4.1 Summary of XRD Results from Prior Report [56]

XRD powder patterns were collected and evaluated on eight glasses from tests ILHA and ILHB at 90 °C and S/V of 2,000 m^{-1}, ten glasses from tests ILLA and ILLB at 40 °C and S/V of 2,000 m^{-1}, and ten glasses from tests ILHC and ILHD at 90 °C and S/V of 20,000 m^{-1}.

4.1.1 IDF Phase 1 Glass Samples Tested at 90 °C and S/V of 2,000 m-1

Out of ten samples immersed for PCT-B in June and July of 2010 (tests ILHA and ILHB), two were terminated after early resumption and eight remained for sampling. Among these, four glasses have reached resumption and are now showing 80-90 g/L boron normalized release (IDF7-E12CCC, IDF3-F7CCC, IDF4-A15CCC, and IDF8-A125CCC) and one is undergoing resumption with a rise from 34 to 58 g/L boron normalized release (IDF1-B2CCC), as can be seen in Figure 3.2.

From the XRD powder pattern of IDF7-E12CCC subjected to PCT-B at 90 °C and S/V of 2000 m^{-1} for 2912 days best matches were found for the zeolite analcime and for the phyllosilicate tobermorite with trace of Al ($Ca_{4.9}(Si_{5.5}Al_{0.5}O_{16.3})(OH)_{0.7}(H_2O)_5$) or without any Al ($Ca_5Si_6O_{17}(H_2O)_5$), which is a common calcium-rich hydrothermal alteration product that was also detected at prior sampling [50]. This phase identification was not surprising since this glass has the highest CaO content among IDF glasses. Based on this XRD pattern, which contains very little of the rounded hump between 20 and 40° typical of the amorphous glass phase, this is the glass sample containing the most secondary phases in this series of glasses.

The sample containing the second most crystallization, based on intensity of XRD peaks, was from glass IDF3-F7CCC subjected to PCT-B at 90 °C and S/V of 2000 m^{-1} for 2912 days. In this case, two zeolites were matched to the powder pattern, $Na_{3.555}(Al_{3.6}Si_{12.4}O_{32})(H_2O)_{10.556}$ and analcime $NaAl(SiO_6)(H_2O)$. In addition, the pattern of the phyllosilicate nontronite is strong and its characteristic broad peaks indicate possible substitutions (for example Zn^{2+} instead of Fe^{2+}) in

the formula given in the match as $Na_{0.3}Fe_2Si_4O_{10}(OH)_{2.4}H_2O$. Such substitutions lead to changes in unit cell dimensions and the superposition of multiple substitutions gives the appearance of broader peaks for smectites.

The third most abundant amount of crystallization was found in IDF4-A15CCC after 2886 days of PCT-B leaching at 90 °C and S/V of 2000 m^{-1}. In this case, the XRD spectrum primarily showed peaks for two tectosilicates close in composition, the zeolite $Na_6(Al_6Si_{10}O_{32})(H_2O)_{12}$, and gobbinsite $Na_5(Al_5Si_{11}O_{32})(H_2O)_{11}$. Other possible matches for minor crystalline components include the zeolite garronite $Ca_{3.49}(Al_6Si_{10}O_{32})(OH)_{0.49}(H_2O)_{12.07,}$ or the sodalite nosean $Na_7(SO_4)(Al_5Si_7O_{24})$. The amorphous hump typical of the glass phase is still clearly visible and many small but broad diffraction peaks indicate the presence of phyllosilicates; the kaolinite halloysite $Al_2Si_2O_5(OH)_4$ and the clinochlore $(Mg_5Al)(Si,Al)_4O_{10}(OH)_8$ were two possible matches for phyllosilicates but the number of matching diffraction peaks is small compared to the zeolites.

The diffraction pattern taken on sample IDF8-A125CCC after 2912 days of PCT-B leaching at 90 °C and S/V of 2000 m^{-1} showed broad diffraction patterns assigned to smectite minerals and sharper peaks matched to two zeolites: analcime and chabazite $Na_{0.44}K_{3.02}(Al_{3.6}Si_{6.4}O_{24})(H_2O)_{10.02}$.

The diffraction pattern taken on sample IDF1-B2CCC after 2912 days of PCT-B leaching at 90 °C and S/V of 2000 m^{-1} shows predominantly an amorphous phase but very small peaks of smectites (broad peaks at 20° and 62° 2θ) and the zeolite chabazite $Ca_2Al_4Si_8O_{24}(H_2O)_{12}$ were present. The presence of such phases may be symptomatic of the resumption that is on-going with this sample. Very similar observations are made on sample IDF5-A20CCC in which the zeolite was clearly identified with sharp peaks attributable to analcime.

Neither IDF2-G9CCC nor IDF10-Zr6CCC showed any sign of crystallization being present in the long-term leached samples.

4.1.2 IDF Phase 2 Glass Samples Tested at 90 °C and S/V of 20,000 m-1

The XRD pattern from IDF14-A59CCC after 1087 days [56] of PCT-B leaching at 90 °C and S/V of 20,000 m^{-1} and that previously obtained on the 548-day sample [50] showed in both cases the pattern for the zeolite phillipsite $(K,Na)_2(Si,Al)_8O_{16}\cdot 4H_2O$ or the zeolite $Na_6(Al_6Si_{10}O_{32})(H_2O)_{12}$, which are both likely present.

The XRD patterns for five other glasses that have reached resumption in tests ILHC and ILHD showed that the crystal content followed the level of alteration reflected by the boron normalized release, consistent with the observed resumptions. The pattern of the zeolite $Na_6(Al_6Si_{10}O_{32})(H_2O)_{12}$ provided a good match for all five patterns and, in samples with more alteration, a second set of diffraction peaks was also visible. These were assigned to phillipsite

$(K,Na)_2(Si,Al)_8O_{16}\cdot 4H_2O$ in earlier samples of IDF18-A161CCC but not in IDF19-C100CCC and IDF20-F6CCC. Other XRD peaks also visible in IDF18-A161CCC, IDF19-C100CCC, and IDF20-F6CCC were matched by phyllosilicates of the chlorite and smectite groups; with smaller amounts of zeolite in the previous samples, the XRD pattern [50] showed aliettite ($Ca_{0.9}Mg_6(Si,Al)_8O_{22}(OH)_4\cdot 4(H_2O)$), beidellite ($Na_{0.3}Al_2(Si,Al)_4O_{10}(OH)_2\cdot 2(H_2O)$), and swinefordite ($Ca_{0.1}(Li,Al)_3Si_4O_{10}(OH)_2\cdot 2(H_2O)$ as three possible smectites that are present in these samples.

The four glasses for which alterations remain at less than 10% of the glass (boron normalized release of 50 to 109 g/L) showed no sign of crystallization from their XRD patterns.

4.1.3 IDF Phase 1 Glass Samples Tested at 40 °C and S/V of 2,000 m-1

This is the first time that the samples from sets ILLA and ILLB subjected to PCT-B at the lower temperature of 40°C have been sampled. XRD did not detect crystallization in any of the glass samples.

4.2 SEM Evaluation of Altered Glass Samples from IDF Phase 1 and Phase 2

4.2.1 IDF Phase 1 Glass Samples Tested at 90 °C and S/V of 2,000 m-1

IDF1-B2 in ILHA-18-5:

In surface evaluation, the glass grains of IDF1-B2 in ILHA-18-5 appear to be moderately coated with micro-crystalline material, indicative of a glass undergoing resumption. One type of crystal identified is a phase containing predominantly calcium (oxide, carbonate or hydroxide) as subhedral trapezohedrons or dodecahedrons, ~15 to 20 μm in size (Figures 4.1a and 4.1b). A moderate coating of platy, octahedral crystals are also found throughout the surface of the glass grains (Figures 4.1c and 4.1d). The Na-aluminosilicate crystals, with Al:Si ratio of ~1:2, are identified as a zeolite of formula $Na_{2.5}Al_{2.7}Si_{6.1}O_{18}$ (with traces of Mg, Zn, and Zr, which may be from the crystalline phases or the glass below). Finally, a phyllosilicate forms a thin, vesicular, coating on all grains. This phyllosilicate is predominantly a Na-aluminosilicate, with Al:Si ratio of ~ 1:4 (likely a smectite), and also contains high levels of Mg, Zn, Zr, significant amounts of Ca and Fe, and minor amount of V. Another platy thin tabular crystal (Figure 4.1d), commonly ~0.5 to 1 μm by ~3-4 μm, is also a Na-aluminosilicate with Al:Si ratio of 1:4, which may also contain minor amounts of Mg, Ca, Cr, Fe, Zn. The minor components could also be interference from the glass matrix. These thin crystals are not visible in back-scattered electron images (insert in Figures 4.1d).

In cross-section (Figures 4.1 e, f, and Figure 4.2) the glass particles show minor to moderate alteration layers consisting of hydrated alteration gel layers of varying compositions

and an outer deposit of mostly analcime. Transition layers are thin, (~4-5 μm, but up to 20 μm), covered with the analcime coatings generally <10 μm in thickness. A set of EDS spectra taken across the layers from glass - to alteration gel - to zeolite (Figure 4.2) gives the following insight. First, by looking at the main glass constituents, Al, Na, and Si, three compositional zones can be identified: the unaltered glass in which the Al:Si rato is ~1:4 and where Na remains at the nominal level; in the following zone, Na decreases continuously but Al remains unchanged while Si increases slightly to compensate for the change in Na; the ratio of Al:Si remains ~1:4, as it is in many smectites identified by XRD in other more altered glasses [56]. Finally, at the outer most zone, the Al content nearly doubles to an Al:Si ratio of ~1:2, compositionally matching the zeolite clinoptilolite $(Na,K)_{1.4}Al_{2.7}Si_{6.5}O_{18}$. The sodium depletion is accompanied in the smectite by increases in M^{2+}, M^{3+}, and M^{4+} metals Zr, Ca, Fe, Mg, and Zn, as shown in Figure 4.2. Such substitutions, not uncommon in smectites, lead to the empirical formula $(Na,K)_{1.9}(Mg_{0.2}Ca_{0.3}Cr_{0.1}Fe_{0.1}Sn_{0.1}Zn_{0.3}Zr_{0.6})Al_{1.5}Si_{6.2}O_{18}$. Mg and Zn are particularly enriched in a thin layer at the transition between the smectite and the zeolite with the composition $(Na,K)_2(Mg_{0.3}Ca_{0.2}Fe_{0.3}Zn\ Zr_{0.4})Al_{1.9}Si_{5.8}O_{18}$.

IDF2-G9 in ILHA-18-8:

The glass grains of IDF2-G9 in ILHA-18-8 appear to be relatively free of crystalline material and the alteration products detected on the surface are rare and isolated (Figure 4.3). Two types of crystals were detected: a zeolite, possibly chabazite, and small cubic crystals ~2-5 μm in size and of composition $CaSnO_{10.7}$ (Figure 4.3d). The morphology and composition match a calcium stannate or calcium hydroxystannate, a perovskite-type material documented for its catalytic and luminescent properties [73, 74].

In cross-section (Figure 4.3 e-f) an alteration layer of ~2-3 μm thickness (but occasionally up to 12-20 μm) is seen, similar to what was observed in IDF1-B2. The outermost layer is enriched in Mg and Zn and depleted in Al, Si, K, Zr, and Ca. The second, inner layer is depleted in Mg and Zn with relative enrichment in the remaining elements. Both alteration layers are severely depleted in Na. The center is unaltered glass, with enrichment in Si, Na, O, K, Ca, and Sn relative to the alteration layers. Although no resumption is detected in IDF2-G9, these are signs that it is nearing resumption.

IDF3-F7 in ILHA-18-11:

In low magnification surface evaluation, IDF3-F7 in ILHA-18-11 shows the overall texture of glass grains but appear to be moderately coated with a micro-crystalline material (Figure 4.4 a-b). Ubiquitous crystals of phyllosilicates form a consistent coating on the majority of glass grains with small, an-subhedral globular/botryoidal crystals, ~1-2 μm in diameter. Their composition is that of a Zr-aluminosilicate, (Al:Si ratio of ~1:4) with large amounts of Zn, Na, and Ca, and smaller but significant amounts Cr and Mg, and minor amounts of K and Fe.

Although uncommon, clustered acicular crystals of a calcium silicate ~0.3 to 0.5 µm by ~4-6 µm are also found (Figure 4.4 d). The composition is predominantly Ca-silicate with significant amounts of Al, trace to minor amounts of Na, Mg, Zn and Zr, and traces of K and Fe. A zeolite, possibly Na-chabazite (Al:Si ratio of ~1:2 with K, Ca, Zn, Zr), which forms tabular, euhedral crystals ~10 by 3µm in size, also were found.

In cross-section (Figure 4.4 e, f) the alteration of glass particles appears to form up to four disctinct phases: a) inner, high-contrast, low-Ca Mg-Zr aluminosilicate, b) middle, low-contrast, Na-Ca aluminosilicate, c) moderate-contrast, high-Al Mg-Zr aluminosilicate, and d) an outer binding matrix, possibly a tobermorite gel. The outer phase is amorphous, anhedral, with sparsely distributed crystals of analcime and rounded high Ca, low Si, silicate phase.

IDF4-A15 in ILHB-18-5:

Low magnification micrographs of IDF4-A15 in ILHB-18-5 (Figure 4.5 a-c) show the overall texture of the glass grains, which appear to be moderately coated with micro-crystalline material and cubic crystals of $CaSnO_3$, 25-30 µm in size. Hexagonal Na-aluminosilicate crystals, ~5µm in size and of formula $(Na,K_{0.1})(Mg_{0.1}Ca_{0.3}Fe_{0.1}Zn_{0.2}Zr_{0.2})AlSi_{3.3}O_{10}$ are shown in Figure 4.5d. The grains are also coated with a sub-micron phase that is too thin for obtaining any spectra but is likely a phyllosilicate based on their recognizable morphology.

In cross-section, the fully reacted glass (based on boron release, but only 6% of silica released), grains show large (20 to 50 µm) sections of two types of phases: a higher contrast Na-Ca-Zr-silicate (top left in Figure 4.5 e) and one of lower contrast (darker in Figure 4.5 e-f) of composition $Na_{1.5}Al_2S_4O_{12}$, which is probably highly hydrated based on the cracks developed on drying and preparation of the SEM sample.

IDF5-A20 in ILHB-18-8:

Observations on IDF5-A20 in ILHB-18-8 reveal phases similar to those in IDF4-A15; at lower magnification, the grains show moderate coating of crystals (Figure 4.6a). The phyllosilicate layer appears spalled in places (Figure 4.6b-c), thus providing access to the structure across this layer. EDS analyses of this phase are given in Table 4.3. The analysis collected on the outer layer (upper right in Figure 4.6b) is distinctly higher in Mg and Zn while the inner layer is higher in Zr and Ca with Mg absent. This would indicate that there is more than one phyllosilicate in development during alteration, with diffusion between layers, particularly in Ca and Mg. Euhedral analcime crystals, mostly trapezoidal in shape, but a few tablet shaped ~10 µm size, are visible in Figure 4.6 c-d. Cubic $CaSnO_3$ crystals were also detected (Figure 4.6d).

In cross-section, the images show a ~15 µm zeolite layer covering mostly fractured grains. EDS analyses of this phase are given in Table 4.4.

IDF7-E12 in ILHA-18-14:

Particles of IDF7-E12 in ILHA-18-14 (Figure 4.7) are highly irregular, agglomerated from secondary phase formation (2-500 μm in size), slightly rounded in shape and are mostly aggregates of analcite, Ca/Na-hydroxides, and other silicates. A fibrous crystal is a major alteration product. EDS analysis indicates that this crystal is probably a Ca-silicate or Ca-hydroxide. Large icositetrahedral analcime particles of size up to 30 μm are inundated with the fibrous Ca-bearing phase. IDF7-E12 is the glass with the highest calcium content tested (10 wt% or 11.5 mol% CaO). Calcium was increased in this glass to increase sulfate solubility and it appears to also favor early resumption by formation of a large amount of the calcium-bearing phase tobermorite. XRD patterns of tobermorite were identified in sampling and evaluation of the sample conducted in 2015 and in 2018 with various degrees of hydration and Ca/Si ratios as $Ca_4(Si_6O_{15})(OH)_3(H_2O)_5$ [50] or $Ca_{4.9}(Si_{5.5}Al_{0.5}O_{16.3})(OH)_{0.7}(H_2O)_5$ [56].

IDF8-A125 in ILHA-18-17:

Particles of IDF8-A125 in ILHA-18-17 (Figure 4.8) are coated with micro-crystalline K-Na-aluminosilicate hexagonal/trigonal crystals, ~10-15 μm across. This is likely the chabazite previously identified by XRD [56]. EDS analysis provides a slightly different composition, $Na_{1.6}K_{0.7}Mg_{0.2}Ca_{0.1}Ti_{0.2}Fe_{0.3}Zn_{0.4}(Al_{2.1}Si_{6.3}O_{18})$. This glass was designed for high-potassium waste and contains 4.2 wt% K_2O. Two other high potassium glasses (IDF2-G9 an IDF11-G27), which contain higher potassium concentrations, did not reach resumption as early as IDF8-A125, possibly because this glass has much less Zr and more Fe, Mg, and Ti.

SEM analysis of the cross-section showed that the altered layer spalled in most places; EDS profiles show Na depletion and Al enrichment up to 45 μm and the maximum concentration of O (possibly due to hydration) at 30 to 45 μm.

IDF10-Zr6 in ILHB-18-17:

This glass, which contains 9.5 wt% ZrO_2, has been one of the most leach resistant so far. Particles of IDF10-Zr6 in ILHB-18-17 (Figure 4.9) appear to be relatively free of crystalline material. However, small analcime crystals, ~10 μm in diameter, were detected on a few grains indicating that resumption might be forthcoming.

4.2.2 IDF Phase 2 Glass Samples Tested at 90 °C and S/V of 20,000 m-1

IDF11-G27 in ILHC-11-3:

Glass IDF11-G27 is compositionally close to IDF2-G9, with moderate decreases in B, Mg, and Zn and increases in Si, Sn, and Zr. Tetragonal to orthorhombic crystals appear

ubiquitous on the surface of the ILHC-11-3 altered glass, as shown in Figure 4.10a. They vary in size with dimensions of ~2 to 3 μm by 0.5 μm, up to ~30 μm by 4 to 5 μm. EDS analyses of the crystals lead to the empirical formula $Na_2K(Al_{2.5}Si_{6.3}O_{18})$ with traces of Ca, Sn, Zn, and Zr, which suggests chabazite. Little alteration is detected in cross-section but the presence of chabazite could portend upcoming resumption.

IDF12-A38 in ILHC-11-6:

Little alteration is detected in IDF12-A38, and no phases other than glass could be identified by XRD [56]. Yet some octahedral/di-pyramidal crystals, ~10 μm up to 30 μm in size, are detected on a few grain surfaces (Figure 4.11). Compositionally they are nearly pure Na-aluminosilicate with minor amounts of Mg, Ca, Zr, and Sn. The Al:Si ratio is ~2:5 indicating likely zeolite, possibly analcime based on morphology.

IDF13-A51 in ILHC-11-9:

A sample of IDF13-A51 in ILHC-11-9 was taken when boron release in IDF13-A51 was measured at 30% reacted glass. Since it rose sharply to 90% reacted at the following leachate sampling, the solid phases observed are concomitant with incipient resumption. This resumption of alteration was slower than for IDF14-A59, although these are two very similar glasses, both with larger amounts of TiO_2 (4 wt%) and MgO (2 wt%), which convert to 3.3 mol% MgO and 3.4 mol% TiO_2. The only difference is the higher Cl and SO_3 concentrations in IDF13-A51 (both 0.7 wt% instead of 0.1 wt% in IDF14-A59). As mentioned in Section 3.1.2, this Cl and SO_3 increase caused a small decrease in the leachate pH, which could be the cause of the delay in the time to reach resumption. As seen in Figures 4.12 a and b, the glass surface is coated with a fine, sub-micron scaly secondary phase, but the layer was too thin to collect a useful EDS spectrum without the underlying glass. Crystalline phases observed on the suface (Figure 4.12b) of ~10 μm size are primarily Na-aluminosilicate, most likely analcime.

In cross-section, three distinct layers are observed (Figure 4.12c) and EDS analyses show the following compositional variations: (1) the first three spectra are taken in the unaltered glass where the Na concentration is stable and the Si:Al ratio is ~3 to 4; (2) a layer of sodium depletion in which Al also decreases slightly (Si:Al ratio ~6.5 to 7) associated with increases in Zr, Ca, Mg, and Sn, likely a phyllosilicate (smectite) layer; and (3) a thick zone of higher contrast indicating higher Al and Si (Si:Al ratio ~2.2) in which Mg, Ca, Zr, and Sn are absent, with only Zn remaining. In the smectite layer, Ca and Mg profiles are anti-correlated, suggesting different roles in the formation of smectite. At the edge of what appears to be a gap between phyllosilicate and zeolite, at ~60 μm from spectrum (1), there is an enrichment in Ti. The average zeolite composition, $Na_{6.4}Al_{10}Si_{22}O_{62,}$ indicates it could be from the heulandite family, a zeolite commonly formed as an alteration product of silicic volcanic glasses [75].

IDF14-A59 in ILHC-11-12:

A sample of IDF14-A59 in ILHC-11-9 was taken a full year after the phillipsite was already identified in this test after 548 days. The morphology of the phillipsite seen after 1087 days (Figure 4.13a,b) is much more developed than it was in 2017 (Figure 4.13d) [52] but comparable to others identified in magmatic minerals alteration products [76, 77] and seen in other samples of glasses at advanced stage of alteration [52].

In cross section evaluation, there does not seem to be any smectite layer but again, the apparent gap between the reacted glass and the zeolite shows a sharp enrichment in Ti (~11 at%).

IDF15-A57 in ILHC-11-15:

The sample of IDF15-A57 in ILHC-11-15 shows evidence of phyllosilicate and tiny zeolite crystals in surface evaluation (Figure 4.14a-c). In cross section, a few grains show a thin layer, only about 1.5 μm thick (Figure 4.14d), with enrichment in Zr, Si, and Ca (formula $NaK_{0.2}Ca_{0.3}Ti_{0.3}Zn_{0.5}Zr_{0.6}AlSi_5O_{15}$), which appears denser than the hydrated layer behind it. The zeolite layer is evident in Figure 4.14e, and in that grain there is no transition smectite layer between the glass and the zeolite. This glass was selected for testing because Mg and Sn were removed from the formulation. The present observation is in agreement with prior observations that magnesium addition triggers the precipitation of magnesium silicate and drives the glass to resumption [78].

IDF16-A58 in ILHD-11-3:

In glass IDF16-A58, CaO was removed from the formulation. The glass showed about 10% alteration based on the boron release at the time of sampling. It is therefore not surprising to find little sign of alteration in sample IDF16-A58 in ILHD-11-3 (Figure 4.15a). At large magnification (Figure 4.15b), there is evidence of zeolite crystals and phyllosilicates underneath. Both types of crystals are also detected in the cross section (Figure 4.15c-d) with the sharp rise in Al concentration, which is a distinctive sign of zeolite, and a slight enrichment in Zr and depletion in sodium between the zeolite and pristine glass. Comparing this sample to other samples containing both calcium and magnesium described above, it appears that together, the two alkaline-earths contribute to the formation of silicates detrimental to long-term leaching.

IDF17-A60 in ILHD-11-6:

Glass IDF17-A60 was formulated to be similar to IDF5-A20; it contains CaO and MgO in moderate amounts (3.4 and 0.9 wt% respectively) but is much lower in Al_2O_3 in comparison to

the previous four glasses, and does not contain TiO_2. Its alteration is very low, as can be evaluated from the leachate (~6% reacted based on boron) or from evaluation of the glass sample. The grains are covered with multiple very thin (4-5 μm or less) layers. As shown in Figure 4.16a, three layers are identified on the surface, all of them at Si:Al ratios of around 5.5, very close to the ratio in the glass. EDS analysis of the inner and outer layers are given in Table 4.3. The outer layer (marked with red circles in the figure) is enriched in Ca and Mg, the middle layer is high in Mg only, and the inner layer closest to the glass is lowest in Mg and slightly higher in Ca. EDS analyses on grain cross-section shown in Figure 4.16c gives similar results. Overall, observations made on this glass after three years at S/V of 20,000 m^{-1} are very similar to the observations on glass IDF5-A20 (see Figure 4.6) after nine years at S/V of 2000 m^{-1}.

IDF18-A161 in ILHD-11-9 and IDF19-C100 in ILHD-11-12:

Both of these glasses contain ~20 wt% Na_2O and were designed to accommodate higher sulfate content (> 1.1 wt% SO_3). To facilitate SO_3 solubility, their CaO content is 8 wt% and to control K-3 corrosion Al_2O_3 is more than 10 wt%. The solids were collected from the vessels about two years after the tests reached resumption. As seen in Figures 4.17 and 4.18, the gains appear mostly reacted and bound together. The alteration layer is mainly composed of analcite aggregates, which are showing some cleavage (Figure 4.17b-c). All particles are bound with a calcium silicate gel, likely a tobermorite gel based on the EDS spectrum shown in Figure 4.17. Very similar observations were collected on the two samples. In cross section, the particles appear hollow (Figure 4.18c). EDS analyses from center of the grain to the edge of the crystals show highly variable compositions, reflected in the irregular texture.

IDF20-F6 in ILHD-11-15:

This glass, which has high SO_3, high CaO, and high Li_2O, appears almost completely altered. The components remaining in the glass particles are predominantly Si, Na, and Al, with considerable amounts of Ti, Zr, and Zn and trace amounts of of Cl, Mg, and K. The layers also contain anhedral grains of a Zn-Zr aluminosilicate. The majority of particles are agglomeratied, and the binding phases are analcime and a Ca-silicate, likely tobermorite.

For these last three glasses, the boron normalized release in the leachate indicated that resumption was reached within the first year of testing, after which the release plateaued around 60 to 70% of the total available boron. SEM images show abundant calcium silicate gel that developed around the reacted particles. This gel layer could very well be collecting the boron and some of the other leachate constituents as well as some of the water in the crystals.

4.2.3 IDF Phase 1 Glass Samples Tested at 40 °C and S/V of 2,000 m-1

As shown in Figure 4.20, the glass grains collected from the leach tests at 40 °C remain angular and relatively uniform in shape and size (~100-150 μm). At larger magnification, a few 1-1.5 μm particles were detected on the surface (Figure 4.20b) but their composition was not distinguishable from that of the glass. Some layer spalling ~1-2 μm thick, up to 5 μm, was detected on IDF2G9 and IDF5A20, two glasses for which the normalized boron release is slightly higher than for the others presented in Figure 4.20. The composition was slightly variable when taken on the fractured section, showing some depletion in Na, Mg, Al, and enrichment in Ca and Si relative to the glass below (Figures 4.20d and h). In IDF6D6 the grains appear to be sparsely coated with micro-crystalline material, which was too thin to obtain any analysis. In the micrograph of IDF7-E12 (Figure 4.20l) which contains some pre-existing sulfate sodalite crystals, the dendritic-skeletal structure of these crystals is visible, indicating that they have leached out preferentially. No alteration was detectable in cross-section.

Glass IDF8-A125 was naturally of particular interest because it is one that showed a larger increase in release, even if modest in comparison to tests at 90 °C (10 g/L of normalized boron release in the first three years of leaching at 40 °C compared to ~1-2 g/L for other glasses), which then plateaued at that level. XRD did not reveal any crystallization but SEM showed the presence of a thin layer, which fractured on some of the grains (Figure 4.21 a-d). At higher magnification, the layer displays the typical morphology of phyllosilicates (Figure 4.21c). In cross-section and even larger magnification (the size-bar is 5 μm in Figures 4.21 e and f), a darker layer of several hundred nm in thickness indicates the enrichment in heavier elements and depletion in lighter ones. The EDS analyses of the phases in Figures 4.21 e and f are given in Figure 4.22. Results are arranged to show all the EDS spectra from the core glass separately from the points in the surface layer and to place the points closest to the outer edge (near leachate) closest to the right in the figure. Silicon (not shown in the figure) increases from 24.0 at% to 25.5 at% from the glass to the alteration layer, probably as a consequence of the decrease in other components. Sodium shows the most depletion in the altered layer. When Al and Zr are slightly enriched in the surface area, Fe and Zn are depleted, and vice versa. The variations in Ca, Mg, and Ti are much smaller. Chlorine remains in the layer but not sulfur. These are all variations in compositions that can be captured in phyllosilicate crystal structures. Their silicate sheets offer sites for a variety of cations, in octahedral or tetrahedral sites and even between sheets, which due to swelling with interstitial water, can accommodate many larger ionic species. It appears to develop here as an evolution of the altered gel-layer, the hydrated glass structure providing the backbone for its formation. It is not surprising that Fe plays a predominant role in the phase developing on glass IDF8-A125, which is the only low-Zr glass with over 5 wt% Fe_2O_3. Enrichments in Fe and Zn (and to lesser extent in Mg) at the outer edge closest to the solution correspond to the more developed phyllosilicate crystals. Closer to the unaltered glass is found a layer rich in Zr and Al where Na decreases more slowly. In that area, the transition between hydrated altered glass or gel to smectite may still be ongoing.

4.3 Conclusions from Solids Evaluation

Two very distinct types of phases have been identified on grains of altered glasses collected after long-term PCTs:

Phyllosilicates have been observed in almost all samples, generally in earlier stages of alteration at 90 °C, or after eight years at 40 °C, and in direct contact with the glass. They are, however, no longer seen in glasses having undergone resumption and which have been fully reacted for years. The phyllosilicates identified here are members of the smectite clay mineral family, such as nontronite $Na_{0.3}Fe_2Si_4O_{10}(OH)_{2.4}H_2O$ or $Na_{3.6}(Al_{3.6}Si_{12.4}O_{32})(H_2O)_{10.6}$ and beidellite $(Na_{0.3}Al_2(Si,Al)_4O_{10}(OH)_2.2H_2O$ [52]. However, the broad XRD features indicated composition variations due to structural substitutions and expansion. Phyllosilicates are so named because their crystal structures are comprised of silicate sheets, with alternating tri-octahedral sheets that contain divalent cations (Mg^{2+}, Fe^{2+}, Zn^{2+}) or with alternating di-octahedral sheets that contain trivalent cations (Al^{3+}, Fe^{3+}, …). Isomorphic substitution with Zr^{4+}, which has a similar ionic radius to Mg^{2+} (radii of $^{VI}(Zr^{4+})$ = 0.72 Å, $^{VI}(Mg^{2+})$ = 0.72 Å) [79] are also possible when hydration provides the required charge compensation. Swelling with interstitial water also permits accommodation of larger ionic species (K^+ 1.42 Å, Cs^+ 1.81 Å). These phyllosilicates appear to crystallize within the altered gel-layer formed during glass leaching, as evident with the progressive change in composition seen in EDS analyses of glass grain cross-sections. As a result of boron release from the glass (likely replaced by water molecules) and sodium depletion, the layered intergrowth of micron to sub-micron sized smectite crystals is favored and keeps evolving as the hydration front progresses. Besides the sodium-aluminosilicate base composition, SEM/EDS evaluations show contributions of K, Mg, Ca, Fe, Ti, Zn, Zr, and Sn (Table 4.3) and occasional traces of Cr. The variety of interstitial metals, some with strong structural bonds such as Zr, probably contributes to the diffusion barrier and passivating character of the reacted gel layer.

In this alteration gel layer transitioning to phyllosilicates, the atomic ratio of Si/Al is always close to that of the glass, in the range of 4 to 7 (Table 4.3), and rises as distance from the hydration front increases. Most components of the glass also participate in the composition of smectite, another indication that its formation is more likely a rearrangement of the hydrated glass after removal of boron and sodium than precipitation of insoluble components. Zn, Mg, and Fe are often found in higher concentrations near the solution. Ca and Mg are often opposite in concentration profiles. These are also signs of rearrangements taking place within the gel. All these observations are in agreement with Bleam's statement in the introduction to his book chapter on clay mineralogy and chemistry [80]: "Mineralogists studying chemical weathering have come to realize clay minerals form in direct contact with igneous silicate minerals by solid-state rearrangement, appearing early in the chemical weathering sequence and disappearing only in the later stages."

One particular phase was found in six samples (most importantly in IDF18-A161 and IDF19-C100, but also in IDF3-F7, IDF6-D6, and IDF7-E12 of Phase 1, and IDF20-F6 of Phase 2), associated with severe alteration and long after resumption: a calcium silicate of composition ($Ca_5Si_6O_{17}(H_2O)_5$) without Al, but which may also contain trace amounts of Al as ($Ca_{4.9}(Si_{5.5}Al_{0.5}O_{16.3})(OH)_{0.7}(H_2O)_5$). This phase identified as tobermorite is classified as a phyllosilicate (2-D sheets) and often found in nature as the product of limestone weathering. It is also known in cement chemistry as CSH and indeed acts in the present case as a cementing material, binding together the altered glass grains and the zeolites that may have formed. It was found in altered glass originally containing 8 to 10 wt% CaO, added to improve SO_3 solubility (all with greater than 6 at% Ca in Table 2.1). The fact that tobermorite is identified only well after resumption indicates that it is probably formed only at that time, once calcium becomes extensively available. As noted in Section 3.1.2, a sharp Ca increase in solution was noted for IDF18-A161 and IDF19-C100 at the time of resumption but stopped increasing as crystallization proceeded. Its presence also explains the near absence of liquid in the leach vessels of these samples because this is a phase that consumes many hydration molecules.

Zeolites are the other crystals found in the glass alteration products. In contrast with smectite phases, zeolites are clearly identified in XRD by sharp well defined diffraction patterns characteristic of euhedral crystals. Their well-formed crystal faces are also clearly identifiable in SEM. Analcime dominates many of the XRD patterns collected from the most reacted glass samples, but SEM revealed that zeolites of different morphologies are present in many cases. These include phillipsite ($(K,Na)_2(Si,Al)_8O_{16}\cdot 4(H_2O)$), chabazite $Na_{0.44}K_{3.02}(Al_{3.6}Si_{6.4}O_{24})(H_2O)_{10.02}$, and gmelinite ($Ca(Al_2Si_4O_{12})\cdot 5.8(H_2O)$), based on the best phase matches to the XRD powder patterns [15, 52, 56], but possibly others such as gaultite ($Na_4Zn_2Si_70_{18}.5H_20$) or thomsonite. However, these latter crystals are smaller, about one-fifth of the size of the analcime dodecahedral crystals, which are frequently seen as large as ~50 μm in size.

Tectosilicate crystals have been found in large quantities only in glasses that had reached resumption. It is likely that these crystals are concomitant with and probably responsible for the resumption. We found herein a few instances of glasses that, based on leachate evaluation are still far from resumption (IF2-G9, IDF10-Zr6, IDF11-G27, IDF12-A38), but where SEM evaluation showed that a few euhedral crystals have started to appear. They are generally found on a few grains of material only and not all over the glass surfaces as is the case after resumption, and the crystals are still quite small. Upcoming analyses will confirm whether resumption follows shortly after zeolites are identified.

In SEM cross-section evaluation, Al increases sharply (the ratio of Si/Al drops abruptly) at the transition from smectite to zeolites. As seen in Table 4.4, zeolites are compositionally very distinct from the smectites and different from the glass, with a ratio of Al:Si ~1:2. This sheds light on the evident role of Al in the tendency of the glass to produce zeolite in alteration. From the Phase 1 and Phase 2 compositions in Table 2.1, we find that the four

glasses with the lowest Si/Al ratios (~3 or below) are IDF9-A187, IDF18-A161, IDF19-C100, and IDF6-D6, all four reaching resumption early. Trends could be compared to the work of previous authors [81, 82] who also considered the role of Al glass content on the formation of analcime in leach tests. However, these earlier simplified glasses covered a composition region favoring resumption below a limit of 35 at% Si, which all IDF glasses exceed. In addition, the ratio of Si/(Si+Al) specified by those authors does not accurately predict the difference in time to reach resumption observed for the IDF glasses to the IDF glass compositions.

Zr and Sn are two glass components that have been found effective in delaying resumption or decreasing depth of alteration in VHT [13, 83]. For example, IDF8-A125 is one of three high potassium glasses tested among Phase 1 and Phase 2 formulations (together with IDF1-G9 an IDF11-G27) that showed a much earlier resumption than the other two glasses. One essential difference between these glasses is a lower Zr content in IDF8-A125. However, Zr is not found in the composition of zeolites but remains in the smectites. So the role of Zr in preventing early resumption is via formation of smectite. Similarly, Sn is found in smectites formed in glasses where it is used as a glass former, but contrary to Zr, it was also found to crystallize as a calcium stannate or calcium hydroxystannate close to the composition $CaSnO_3$ (see Table 4.4). This well-formed cubic crystal was found in altered Phase 1 glasses IDF2-G9, IDF4-A15, and IDF5-A20, all formulated with 2.75 wt% SnO_2, but not in Phase 2 glasses that include similar tin additions. However, occurrences of such crystals are less frequent than those of zeolites.

No zeolite crystallization has been detected in any glass sample evaluated from leach tests conducted at 40 °C.

SECTION 5.0
SUMMARY AND CONCLUSIONS

This report provides results of work performed to collect information on the corrosion behavior of LAW glasses to support the IDF PA. In addition to the development of the baseline operating envelope for the WTP, since 2003, VSL has been developing a wide range of LAW glass formulations that achieve considerably higher waste loadings than the WTP baseline formulations. As a result, the range of glass compositions that may be produced at the WTP is expanding toward higher sodium and sulfate contents and new glass forming additives, and this type of composition range expansion is likely to continue through the life of the project. In an initial effort (Phase 1) started to encompass the composition range expected to be disposed at the IDF, a total of 10 IDF Phase 1 glasses were selected for this composition expansion [15]. The selection was based on an analysis of the compositions and properties of the large number of LAW glasses that have been developed for the WTP at VSL. Those glasses were subjected to testing using the long-term PCT-B, and selected glasses were tested according to the SPFT method to determine rate law parameters. The Phase 1 program ended in 2011 but most long-term PCTs were maintained at VSL's expense. Work conducted under Phase 2 offered the opportunity to report the leachate data from those tests that were continued and to characterize the alteration phases [50]. A second objective of the Phase 2 work was to extend the Phase 1 study by adding ten new high waste loading glasses in order to further span the expanded glass composition range, taking into consideration more recent high waste loading compositions that have been developed at VSL. The IDF Phase 1 and Phase 2 glasses include compositions that are bounding with respect to performance on the WTP leach test specifications (PCT and VHT), that are higher in waste loading than the baseline WTP glasses, and that include variations in significant minor components such as sulfate and chlorine, as well as glass constituents that are not present in the baseline glasses. The IDF Phase 2 series also includes one glass (IDF15-A57CCC) with a VHT response that exceeds the WTP contract limit.

Many of the long-term PCT-Bs initiated in Phase 1 and most of the long-term PCT-Bs initiated on the ten Phase 2 glasses are ongoing and yet longer-term data will be collected. The most recent data show that among the ten Phase 1 glasses tested at 90 °C and S/V of 2000 m^{-1}, seven are now over 50% reacted and one (IDF5-A20) showed a rising leach rate over the past years which then plateaued at ~25% reacted. However, one of the two high-alkali glasses, IDF2-G9, and the high zirconia glass IDF10-Zr6 are still showing low leach rates of 9% and 6% reacted, respectively. In contrast, no change in alteration rate has been observed for the Phase 1 glasses being tested at 40 °C and S/V of 2000 m^{-1}. Among the IDF Phase 2 glasses tested at 90 °C and S/V of 20,000 m^{-1}, two reached resumption within the first six months, two others and the reference glass ANL-LRM2 reached resumption within the first year, and two more reached resumption in the past year, and have plateaued at around 50% reacted glass. These are generally low-zirconia glasses (less than 2 mole% Zr) with high alumina (above 9 mole% Al). All glasses

that have reached resumption at the earliest time in each set of tests are found in the lower section of Figure 2.4 with low Zr concentrations of about 2 mol% or less. Since these are not the glasses with the highest alkali content, high-alkali alone is not the determining factor in the relatively rapid alteration. These are observations that can be used to improve the relative performance of glasses under the test conditions. However, the test conditions with higher temperatures (40 – 90 °C) and higher S/V values are expected to lead to much faster glass alteration than under the conditions of storage at the IDF, where both the S/V in the event of water intrusion and the temperature are expected to be lower.

SEM/EDS evaluation of solid samples taken from the leach tests of IDF Phase 1 and Phase 2 glasses confirmed and enhanced XRD analyses from last year [56]. XRD permitted identification of phases present on the glass surface, for the most part, tecto- and sorosilicates crystallizing on top of phyllosilicates covering the gel layer of glass alteration. The phyllosilicate phases observed are members of the smectite clay mineral family and encompass a broad range of compositions. Although both are aluminosilicate minerals, smectites and zeolites have very distinguishable features. Smectites are anhedral and zeolites are euhedral. SEM cross-sectional evaluation primarily defines smectites by their Si/Al elemental ratio in the range of 4 to 7, much higher than is found in zeolites, typically ~ 2. In smectites, SEM/EDS revealed an evolution of elemental profiles with enrichments in Fe, Zn, and Mg in layers closest to the solution and higher Zr close to the hydration front towards the pristine glass. Ca, Sn, and Ti are also found in significant amounts in smectites. A parallel can be drawn to chemical weathering of igneous silicates in which solid-state rearrangement forms the clay minerals observed on their surface [78].

The phyllosilicate tobermorite was identified in previous XRD analyses of Hanford LAW glass alteration products. SEM micrographs now reveal that the phase is abundant in severely altered samples rich in CaO (8 to 10 wt%). This calcium silicate hydrate is also known in cement chemistry as CSH and appears in altered LAW glasses after resumption takes place. It acts as a cementing material, binding together the altered glass grains and the zeolites that may have formed and also consumes most of the free leachate.

Analcime is the zeolite identified most frequently but other common ones are chabazite, phillipsite, and gmelinite. The morphology of some of these zeolite crystals identified in earlier samplings of the altered glasses [50] had not been observed before in Hanford LAW glass alteration products (long-term PCT, VHT). However, more of the same morphology has been seen in the present study, and phases of similar morphology were previously identified in alteration of basaltic glass formed from volcanic activity 15 to 20 million years ago [75]. The alteration in these natural analogues results in the formation of various zeolites during hydrothermal alteration (<150 °C) under alkaline conditions and provides a good resource for identification of crystal morphologies also observed in the present LAW glass samples.

It must be noted also that based on previous XRD evaluation, none of the glasses tested at 40 °C showed any sign of alteration phases having developed after eight years of PCT-B. High

magnification SEM micrographs revealed a sub-micron size gel layer where compositional changes point to nascent formation of a smectite, but no zeolites. Since the glass stored at IDF will be at temperatures well below 40 °C, it is important to verify that all the alteration phases identified in the accelerated 90 °C tests are pertinent to the actual storage situation.

During FY18, PCT-Bs were started on seven new glasses selected from those formulated to develop the Enhanced LAW Glass Correlation for high waste loading glasses [53-55]. All seven glasses are being tested at 90 °C and S/V of 20,000 m^{-1}. Two of the glasses are being tested at 90 °C and S/V of 1000, 2000, 5000, 10,000, and 20,000 m^{-1}. All have now reached a full year of leach testing. The 7-day samplings showed that the PCT release results are consistent with results from prior testing of the same glasses without CCC heat treatment [53-55]. Results from 7-day to 365-day samplings of the tests at different S/V ratios show that the PCT releases follow a power law function of S/V (see Figures 3.9 and 3.10), which was suggested by earlier observations on various HLW glasses [21]. However, this observation was made also on tests conducted at 90 °C. Similar tests with variations in S/V ratios at temperatures between 90 °C and 40 °C are recommended for future work since it will help identify changes in the time for resumption and phases formed on the glass surfaces with S/V and temperature. In particular, it will help identify the conditions that promote zeolite formations as pH and leachate compositions vary. At S/V of 20,000 m^{-1}, four glasses have reached resumption at about six months of testing and the three higher alkali formulations have not after one year; however, they appear to start to show a mild increase in release at the last sampling. As previously seen among Phase 1 and Phase 2 glasses, high-alkali alone is not the determining factor in reaching relatively rapid alteration at earlier time. The planned frequency of sampling after 365 days is at 547 days and yearly thereafter; however, the reaction may advance rapidly to resumption in that interval, particularly at the high S/V of 20,000 m^{-1}. For that reason, additional samplings were included in tests ILHC and ILHD at 6-month intervals, but the sampling intervals may still be too large. Sampling at ~450 days would be highly beneficial and would provide the opportunity to collect some of the altered glass samples for solid analyses at about the same time resumption occurs; results from the last leachate sampling suggests incipient resumption.

5.1 Major Observations on Resumption and Secondary Phase Formation

- Tectosilicates of the zeolite group (analcime predominantly, but also chabazite, phillipsite, and gmelinite) in which sodium is the dominant extra framework cation, crystallize on the altered glass when resumption is observed or is incipient based on leachate analysis.
- High temperature (90°C, and 120°C) and high S/V (20,000 m^{-1}) favor zeolite formation and earlier occurrence of resumption.
- No evidence of zeolite formation was observed at 40°C.

- High sodium and/or potassium alone are not responsible for the occurrence of early resumption. Other glass constituents play an essential role.
- Glasses with low zirconia content (< 2 mol%) are likely to reach resumption early.
- Glasses high in alumina (> 9 mol% or atomic ratio Si/Al ≅ 3) are likely to reach resumption early.
- High sulfate waste formulated with higher Li_2O and CaO concentrations favor the formation of a tobermorite gel agglomerating the altered glass grains and the zeolites.
- Smectites of great diversity were observed to form at 40°C and 90°C. Their compositions vary with glass composition, including in particular Zr, Sn, K, Na, Al, Fe, Zn, Ti, Ca and Mg. These phases are characterized by an atomic ratio of Si/Al close to 6 or greater, with a progressive change in composition from the altered glass to the outer layer, indicating formation by restructuring of the hydrated altered glass.
- The Group IV elements (Zr, Sn, Ti) are always found to remain in the altered glass gel and are enriched in the smectite layer. When smectites rich in Zr, Sn, and Ti are present, resumption is delayed.
- Group III (Fe) and Group II glass constituents (Ca, Mg, and Zn) are also found in the smectites but only Zn-smectites appear to retard glass leaching. Ca and Mg appear to have similar and even synergistic roles in the smectites. However, the Ca/Mg interaction in the altered gel layer and smectite still requires more study to understand their respective role in leaching.

SECTION 6.0
QUALITY ASSURANCE

This work was conducted under a quality assurance (QA) program compliant with the applicable criteria of 10 CFR 830.120; the American Society of Mechanical Engineers (ASME) Nuclear Quality Assurance (NQA)-1-2008 including NQA-1a-2009 addenda; and DOE Order 414.1D, Quality Assurance. These QA requirements are implemented through a Quality Assurance Project Plan (QAPP) for WRPS work [82] that is conducted at VSL. Test and procedure requirements by which the testing activities are planned and controlled are also defined in this plan. The program is supported by VSL standard operating procedures that were used for this work [83]. This is LAW work and is not subject to the requirements of DOE/RW-0333P, Office of Civilian Waste Management Quality Assurance Requirements and Description (QARD).

SECTION 7.0
REFERENCES

[1] "Experimentally Determined Dissolution Kinetics of Na-rich Borosilicate Glasses at Far-From-Equilibrium Conditions: Implications for Transition State Theory," J.P. Icenhower, B.P. McGrail, W.J. Shaw, E.M. Pierce, P. Nachimuthu, D.K. Shuh, E.A. Rodriguez, and J.L. Steele, *Geochimica Cosmochimica Acta* **72**, 2767-2788 (2008).

[2] "Measurement of Kinetic Rate Law Parameters on a Na-Ca-Al Borosilicate Glass for Low-Activity Waste," B.P. McGrail, W.L. Ebert, A.J. Bakel, and D.K. Peeler, *J. Nucl. Mater.* **249**, 175-189 (1997).

[3] "A Strategy to Conduct an Analysis of the Long-Term Performance of Low-Activity Waste Glass in a Shallow Subsurface Disposal System at Hanford," B.P. McGrail, W.L. Ebert, D.H. Bacon and D.M. Strachan, PNNL-11834, Pacific Northwest National Laboratory, Richland, WA, (1998).

[4] "Low-Activity Waste Glass Studies: FY2000 Summary Report," B.P. McGrail, J.P. Icenhower, P.F. Martin, D.R. Rector, H.T. Schaef, E.A. Rodriguez, and J.L. Steele, PNNL-13381, Pacific Northwest National Laboratory, Richland, WA (2000).

[5] "Waste Form Release Data Package for the 2001 Immobilized Low-Activity Waste Performance Assessment," B.P. McGrail, J.P. Icenhower, P.F. Martin, H.T. Schaef, M.J. O'Hara, E.A. Rodriguez, and J.L. Steele, PNNL-13043, Rev. 2, Pacific Northwest National Laboratory, Richland, WA (2001).

[6] "Laboratory Testing of Bulk Vitrified Low-Activity Waste Forms to Support the 2005 Integrated Disposal Facility Performance Assessment," E.M. Pierce, B.P. McGrail, L.M. Bagaasen, E.A. Rodriguez, D.M. Wellman, K.N. Geiszler, S.R. Baum, L.R. Reed, J.V. Crum, and H.T. Schaef, PNNL-15126, Rev. 2, Pacific Northwest National Laboratory, Richland, WA (2005).

[7] "Waste Form Release Data Package for the 2005 Integrated Disposal Facility Performance Assessment," E.M. Pierce, B.P. McGrail, E.A. Rodriguez, H.T. Schaef, K.P. Saripalli, R.J. Serne, K.M. Krupka, P.F. Martin, S.R. Baum, K.N. Geiszler, L.R. Reed, and W.J. Shaw, PNNL-14805, Pacific Northwest National Laboratory, Richland, WA (2004).

[8] "An International Initiative on Long-Term Behavior of High-Level Nuclear Waste Glass", S. Gin, A. Abdelouas, L.J. Criscenti, W.L. Ebert, K. Ferrand, T. Geisler, M.T. Harrison, Y. Inagaki, S. Mitsui, K.T. Mueller, J.C. Marra, C.G. Pantano, E.M. Pierce, J.V. Ryan, J.M. Schofield, C.I. Steefel and J.D. Vienna, *Materials Today* **16**(6) 243-248 (2013).

[9] Request for Off-Site Services (Technical) Statement of Work, "ILAW Glass Durability Testing to Support IDF PA," Rev. 0, Requisition #314744, Washington River Protection Solutions, LLC (WRPS), 10/17/18.

[10] "FY2018 Long-Term PCT of ILAW Glasses," I.S. Muller and I.L. Pegg, Test Plan, VSL-17T4510-1, Rev. 0, Vitreous State Laboratory, The Catholic University of America, Washington DC, 2/6/18.

[11] Request for Off-Site Services (Technical) Statement of Work, "ILAW Glass Durability Testing to Support the IDF PA - SPFT, PCT, Ion Exchange Model and Technical Support for ILAW Glass," Requisition #305361, Rev. 1, Washington River Protection *Solutions*, LLC (WRPS), 10/11/17.

[12] "An Experimental Study of the Dissolution Rates of Simulated Aluminoborosilicate Waste Glasses as a Function of pH and Temperature under Dilute Conditions," E.M. Pierce, E.A. Rodriguez, L.J. Calligan, W.J. Shaw, and B.P. McGrail, *Applied Geochemistry* **23**, 2559-2573 (2008).

[13] "A Strategy to Conduct an Analysis of the Long-Term Performance of Low-Activity Waste Glass in a Shallow Subsurface Disposal System at Hanford," J.J. Neeway, E.M. Pierce, V.L. Freedman, J.V. Ryan, and N.P. Qafoku, PNNL-23503, Rev. 0, Pacific Northwest National Laboratory, Richland, WA (2014).

[14] "Immobilized Low-Activity Waste Glass Release Data package for the Integrated Disposal Facility Performance Assessment," V.L. Freedman, J.V. Ryan and D.H. Bacon, PNNL-24615, RPT-IGTP-005, Rev. 0, Pacific Northwest National Laboratory, Richland, WA, September, 2015.

[15] "ILAW Glass Testing for Disposal at IDF: Phase 1 Testing," A.E. Papathanassiu, I.S. Muller, M. Brandys, K. Gilbo, A. Barkatt, I. Joseph and I.L. Pegg, VSL-11R2270-1, Rev. 0, Vitreous State Laboratory, The Catholic University of America, Washington, DC, 6/6/11.

[16] "The Activated Complex in Chemical Reactions," H. Eyring, *J. Chem. Phys.* **3**, 107-114 (1935).

[17] "Thermodynamic and Kinetic Constraints on Reaction Rates among Minerals and Aqueous Solutions. I. Theoretical Considerations," P. Åagaard and H.C. Helgeson, *Am. J. Sci.* **282**, 237-285 (1982).

[18] "A General Rate Equation for Nuclear Waste Glass Corrosion," B. Grambow, *Material Research Symposium Proceedings* **44**, 15-27 (1985).

[19] "Kinetic Ion Exchange Salt Effects on Glass Leaching," X. Feng and I.L. Pegg, *Energy, Environment and Information Management*, Eds. H. Wang, S. Chang, and H. Lee, Argonne, IL, p. 7-9, (1992).

[20] "Effects of Salt Solutions on Glass Dissolution," X. Feng and I.L. Pegg, *Phys. Chem. Glasses*, **35**, 1 (1994).

[21] "A Glass Dissolution Model for the Effects of S/V on Leachate pH," X. Feng and I.L. Pegg, J. *Non-Cryst. Solids*, **175**, 281 (1994).

[22] "Survey of Literature on the Role of Ion Exchange in Glass Corrosion," A.E. Papathanassiu, W. Gong, W. Lutze, and I.L. Pegg, Final Report, VSL-17L4320-1, Rev. 0, Vitreous State Laboratory, The Catholic University of America, Washington DC, 8/2/17.

[23] "A Critical Review of Ion Exchange in Nuclear Waste Glasses to Support the Immobilized Low-Activity Waste Integrated Disposal Facility Rate Model," C.E. Lonergan, RPT-IGTP-018, Rev A.0, Pacific Northwest Laboratory, Richland, WA, August 2017.

[24] "FY 2019 ILAW Glass Ion Exchange Rate Testing," I.S. Muller, C. Viragh, and I.L. Pegg, Final Report, VSL-19R4620-2, Rev. A, Vitreous State Laboratory, The Catholic University of America, Washington DC, 8/13/19.

[25] "Characterization of Alteration Phases on HLW Glasses after 15 Years of PCT Leaching," I.S. Muller, S. Ribet, I.L. Pegg, S. Gin, and P. Frugier, *Ceramic Transactions*, Vol. 176 (2005).

[26] "Long-Term PCT Data for LAW Glasses," I.S. Muller, D.A. McKeown, X. Xie, I.L. Pegg, and I. Joseph, Final Report, VSL-17R4090-1, Rev. 0, Vitreous State Laboratory, The Catholic University of America, Washington, DC, 05/30/17.

[27] "Dissolution and Precipitation Kinetics of Sheet Silicates," K.L. Nagy, *Reviews in Mineralogy and Geochemistry*, **31**, 173-233, Mineralogical Society of America, Chantilly, VA (1995).

[28] "Letter: Simultaneous Precipitation Kinetics of Kaolinite and Gibbsite at 80°C and pH 3," K.L. Nagy, and A.C. Lasaga, *Geochimica et Cosmochimica Acta* **57**, 4329 – 4335 (1993).

[29] "Preliminary Results of Durability Testing with Borosilicate Glass Compositions," M. Adel-Hadadi, R. Adiga, Aa. Barkatt, X. Feng, I.L. Pegg, et al., Tech. Info. Center, Office of Sci. and Tech. Info., USDOE, DOE/NE/44139-34, (1988).

[30] "Compositional Effects on Chemical Durability and Viscosity of Nuclear Waste Glasses – Systematic Studies and Structural Thermodynamic Models," X. Feng, Ph.D. Thesis, The Catholic University of America (1988).

[31] "Leach Rate Excursions in Borosilicate Glasses: Effects of Glass and Leachant Composition," Aa. Barkatt, S.A. Olszowka, W. Sousanpour, M.A. Adel-Hadadi, R. Adiga, Al. Barkatt, G.S. Marbury, and S. Li, Mat. Res. Soc. Symp. Proc., 212, 65 (1991).

[32] "Alteration Layers on Glasses After Long-Term Leaching," A.C. Buechele, S.T.- Lai, and I.L. Pegg, *Ceramic Transactions*, Eds. D.K. Peeler and J.C. Marra, vol. 87, p. 423, American Ceramic Society (1998).

[33] "Compositional Effects on the Long-Term Durability of Nuclear Waste Glasses: A Statistical Approach," S. Ribet, I.S. Muller, I.L. Pegg, S. Gin, and P. Frugier, Mat. Res. Soc. Symp. Proc. Vol. 824 (2004).

[34] "The Long-Term Corrosion and Modeling of Two Simulated Belgian Reference High-Level Waste Glasses – Part II," J. Patyn, P. Van Iseghem, and W. Timmermans, Mat. Res. Symp. Soc. Proc., 176, 299 (1990).

[35] "New Insight into the Residual Rate of Borosilicate Glasses: Effect of S/V and Glass Composition", S. Gin, P. Frugier, P. Jollivet, F. Bruguier, E. Curti, Int. J. Appl. Glass Sci., 4, 371-382 (2013).

[36] "Nuclear Glass Durability: New Insight into Alteration Layer Properties," S. Gin, C. Guittonneau, N. Godon, D. Neff, D. Rebiscoul, M. CabieS. Mostefaoui, J. Phys. Chem. C 115, 18696-18706, (2011).

[37] "An International Initiative on Long-Term Behavior of High-Level Nuclear Waste Glass," S. Gin, A. Abdelouas, L.J. Criscenti, W.L. Ebert, K. Ferrand, T. Geisler, M.T. Harrison, *et al.*, Mater. Today 16, 243–248 (2013).

[38] "Origin and Consequences of Silicate Glass Passivation by Surface Layers", S. Gin, P. Jollivet, M. Fournier, F. Angeli, P. Frugier, T. Charpentier, Nat. Commun., 6 (2015).

[39] "The Fate of Silicon During Glass Corrosion Under Alkaline Conditions: A Mechanistic and Kinetic Study with the International Simple Glass," S. Gin, P. Jollivet, M. Fournier, C. Berthon, Z. Wang, A. Mitroshkov, Z. Zhu, J. V. Ryan, Geochim. Cosmochim. Acta, 151, 68–85 (2015).

[40] "Resumption of Nuclear Glass Alteration: State of the art," M. Fournier, S. Gin, P. Frugier, J. Nucl. Mater., 448, 348–363 (2014).

[41] "Open Scientific Questions About Nuclear Glass Corrosion," S. Gin, Procedia Materials Science, 163-171 (2014).

[42] "Current Understanding and Remaining Challenges in Modeling Long-Term Degradation of Borosilicate Nuclear Waste Glasses," J.D. Vienna, J.V. Ryan, S. Gin, and Y. Inagaki, Int. J. Appl. Glass Sci., 4, 283–294 (2013).

[43] "Contribution of Atom-Probe Tomography to a Better Understanding of Glass Alteration Mechanisms: Application to a Nuclear Glass Specimen Altered 25 years in a Granitic Environment," S. Gin, J.V. Ryan, D.K. Schreiber, J. Neeway, and M. Cabie, Chem. Geol. 349, 99–109 (2013).

[44] "Effect of Composition on the Short-Term and Long-Term Dissolution Rates of Ten Borosilicate Glasses of Increasing Complexity from 3 to 30 Oxides", S. Gin, X. Beaudoux, F. Angeli, C. Jegou, N. Godon, J. Non-Cryst. Solids, 358, 2559–2570 (2012).

[45] "Development of the Vitrification Compositional Envelope to Support Complex-Wide Application of MAWS Technology," I.S. Muller, H. Gan, A.C. Buechele, S.T. Lai, and I.L. Pegg, DOE/CH-9601, September 1996.

[46] "Alteration Phases on High Sodium Waste Glasses after Short- and Long-Term Hydration," A.C. Buechele, S.-T. Lai, and I.L. Pegg, *Ceramic Transactions*, vol. 107, p. 251 (2000).

[47] "Waste Loading Enhancements for Hanford LAW Glasses," I.S. Muller, K.S. Matlack, H. Gan, I. Joseph, and I.L. Pegg, Final Report, VSL-10R1790-1, Rev. 0, Vitreous State Laboratory, The Catholic University of America, Washington, DC, 12/01/10.

[48] "Improved High-Alkali Low-Activity Waste Formulations," I.S. Muller, M. Chaudhuri, H. Gan, A. Buechele, X. Xie, I.L. Pegg, and I. Joseph, Final Report, VSL-15R3290-1, Rev. 0, Vitreous State Laboratory, The Catholic University of America, Washington, DC, 08/12/15.

[49] "Enhanced LAW Glass Property-Composition Models – Phase 2," I.S. Muller, K. Gilbo, I. Joseph, and I.L. Pegg, Final Report, VSL-14R3050-1, Rev. 0, Vitreous State Laboratory, The Catholic University of America, Washington, DC, 8/29/14.

[50] "FY15 ILAW Glass Testing for Disposal at IDF", I.S. Muller, and I.L. Pegg, VSL-15R3790-1, Rev. 0, Vitreous State Laboratory, The Catholic University of America, Washington, DC, 4/15/16.

[51] "FY2016 update on ILAW Glass Testing for Disposal at IDF", I.S. Muller, and I.L. Pegg, VSL-16S4170-1, Rev. 0, Vitreous State Laboratory, The Catholic University of America, Washington, DC, 2/1/17.

[52] "LAW Glass Testing by Long-Perm PCT to Support Disposal at IDF", I.S. Muller, and I.L. Pegg, VSL-17R4320-1, Rev. 0, Vitreous State Laboratory, The Catholic University of America, Washington, DC, 9/28/17.

[53] "Enhanced LAW Glass Correlation – Phase 1," I.S. Muller, K. Matlack, I.L. Pegg and I. Joseph," Final Report, VSL-16R4000-1, Rev. 0, Vitreous State Laboratory, The Catholic University of America, Washington, DC, 12/01/16.

[54] "Enhanced LAW Glass Correlation – Phase 2," I.S. Muller, K. Matlack, I.L. Pegg and I. Joseph," Test Plan, VSL-17R4140-1, Rev. 0, Vitreous State Laboratory, The Catholic University of America, Washington, DC, 6/30/17.

[55] "Enhanced LAW Glass Correlation – Phase 3," I.S. Muller, K. Matlack, I.L. Pegg and I. Joseph," Test Plan, VSL-17R4230-1, Rev. 0, Vitreous State Laboratory, The Catholic University of America, Washington, DC, 11/15/17.

[56] "FY2018 Long-Perm PCT of ILAW Glasses", I.S. Muller, and I.L. Pegg, VSL-18R4510-1, Rev. 0, Vitreous State Laboratory, The Catholic University of America, Washington, DC, 12/19/18.

[57] "FY2016 ILAW Glass SPFT Testing for Disposal at IDF," A.E. Papathanassiu, C. Viragh, I.S. Muller, and I.L. Pegg, VSL-17R3860-1, Rev. 0, Vitreous State Laboratory, The Catholic University of America, Washington, DC, 7/12/17.

[58] "FY2016 ILAW Glass Corrosion Testing with the Single-Pass Flow-Through Method," J.J. Neeway, R.M. Asmussen, B.P. Parruzot, E.A. Cordova, B.D. Williams, I.L. Leavy, J.R. Stephenson, and E.M. Mcelroy, PNNL-26169, RPT-IGTP-013 Rev. 0.0, Pacific Northwest National Laboratory, Richland, WA (2017).

[59] "FY2017 ILAW Glass Corrosion Testing with the Single-Pass Flow-Through Method," J.J. Neeway, R.M. Asmussen, E.A. Cordova, C.E. Lonergan, B.D. Williams, I.L. Leavy, and E.M. Mcelroy, PNNL-27098, RPT-IGTP-015, Rev. 0, Pacific Northwest National Laboratory, Richland, WA, February, 2018.

[60] "FY2017 ILAW Glass SPFT Testing for Disposal at IDF: Glass IDF21-EC14," C. Viragh, H. Abramowitz, I.S. Muller, A. E. Papathanassiu, and I.L. Pegg, VSL-17R4320-2, Rev. 0, Vitreous State Laboratory, The Catholic University of America, Washington, DC, 2/27/18.

[61] "FY2018 ILAW Glass SPFT Testing for Disposal at IDF: Glasses ORLEC46 and ORLEC52," C. Viragh, H. Abramowitz, I.S. Muller, A. E. Papathanassiu, and I.L. Pegg, VSL-18R4510-2, Rev. 0, Vitreous State Laboratory, The Catholic University of America, Washington, DC, 12/27/18.

[62] "Round Robin Testing of a Reference Glass for Low-Activity Waste Forms," W.L. Ebert and S.F. Wolf, Department of Energy Report ANL-99/22, Argonne National Laboratory, Argonne, IL (1999).

[63] "Enhanced LAW Glass Formulation Testing," K.S. Matlack, I. Joseph, W. Gong, I.S. Muller, and I.L. Pegg, Final Report, VSL-07R1130-1, Rev. 0, Vitreous State Laboratory, The Catholic University of America, Washington, DC, 10/05/07.

[64] "Glass Formulation Development and DM10 Melter Testing with ORP LAW Glasses," K.S. Matlack, I. Joseph, W. Gong, I.S. Muller, and I.L. Pegg, Final Report, VSL-09R1510-2, Rev. 0, Vitreous State Laboratory, The Catholic University of America, Washington, DC, 6/12/09.

[65] "Improving Technetium Retention in Hanford LAW Glass – Phase 1," K.S. Matlack, I.S. Muller, I. Joseph and I.L. Pegg, Final Report, VSL-10R1920-1, Rev. 0, Vitreous State Laboratory, The Catholic University of America, Washington, DC, 03/19/10.

[66] "Glass Formulation Testing to Increase Sulfate Incorporation," K. S. Matlack, M. Chaudhuri, H. Gan, I.S. Muller, W. Gong, and I.L. Pegg, Final Report, VSL-04R4960-1, Rev. 0, Vitreous State Laboratory, The Catholic University of America, Washington, DC, 2/28/05.

[67] "Proposed Approach for Development of LAW Glass Formulation Correlation," I.S. Muller, G. Diener, I. Joseph, and I.L. Pegg, Letter Report, VSL-04L4460-1, Rev. 2, Vitreous State Laboratory, The Catholic University of America, Washington, DC, 10/29/04.

[68] "LAW Container Centerline Cooling Data," RPP-WTP Memorandum, L. Petkus to C. Musick, CCN# 074181, River Protection Project−Waste Treatment Plant, Richland, WA, 10/16/03.

[69] "Glass Formulation and Testing with TWRS LAW Simulants," I.S. Muller, I.L. Pegg, A.C. Buechele, H. Gan, C. Kim, S.T. Lai, G. Del Rosario and Q. Yan, Final Report, VSL-10R1790-1, Rev. 0, Vitreous State Laboratory, The Catholic University of America, Washington, DC, 1/16/1998.

[70] "Role of Neoformed Phases on the Mechanisms Controlling the Resumption of SON68 Glass Alteration in Alkaline Media", S. Ribet and S. Gin, Journal of Nuclear Materials **324,** 152-164 (2004).

[71] "Aqueous Alteration of Japanese Simulated Waste Glass P0798: Effects of Alteration-Phase Formation on Alteration Rate and Cesium Retention" Y. Inagaki, A. Shinkai, K. Idemistu, T. Arima, H. Yoshikawa, M. Yui, J. Nucl. Mater. 354 (2006) 171–184.

[72] "Standard Test Methods for Determining Chemical Durability of Nuclear, Hazardous, and Mixed Waste Glasses and Multiphase Glass Ceramics: The Product Consistency Test (PCT)," ASTM C 1285-14, American Society for Testing and Materials, West Conshohocken, PA, 2014.

[73] "Synthesis of biodiesel and acetins by transesterification reactions using novel $CaSn(OH)_6$ heterogeneous base catalyst" S.Sandesh, P.R.Kristachar, P. Manjunathan, A.B.Halger, Applied Catalysis A: General 523-1 (2016).

[74] "Nano cube of $CaSnO_3$: Facile and green co-precipitation synthesis, characterization and photocatalytic degradation of dye", S. Moshtaghi S. holamrezaei M. Salavati Niasari, Journal of Molecular Structure, 1134, P 511-519, (2017).

[75] D. B. Hawkins, "Kinetics of Glass Dissolution and Zeolite Formation Under Hydrothermal Conditions", December 1980 Clays and Clay Minerals 29(5):331-340 (1981).

[76] "Hydrothermal Alteration and Zeolitization of the Fohberg Phonolite, Kaiserstuhl Volcanic Complex, Germany", T. Weisenberger and N. Spürgin, Int J Earth Sci (Geol Rundsch) (2014) 103:2273–2300.

[77] "Zeolites in Alkaline Rocks of the Kaiserstuhl Volcanic Complex, SW Germany – New Microprobe Investigation and the Relationship of Zeolite Mineralogy to the Host Rock" T. Weisenberger and N. Spürgin, Geologica Belgica (2009) 12/1-2: 75-91.

[78] "SON68 glass dissolution driven by magnesium silicate precipitation" B. Fleury, N. Godon, A. Ayral, S. Gin, Journal of Nuclear Materials 442 (2013) 17–28.

[79] "Synthetic Smectite Colloids: Characterization of Nanoparticles after Co-Precipitation in the Presence of Lanthanides and Tetravalent Elements (Zr, Th)", M Bouby, N. Finck and H. Geckeis, *Chromatography* 2015, *2*, 545-566.

[80] "Soil and Environmental Chemistry (2nd Edition), Chapter 3: Clay Mineralogy and Chemistry", William Bleam, ISBN 9780128041789, Pages 87-146, Academic Press, 2017.

[81] P. Van Iseghem, B. Grambow, in: M.J. Apted, R.E. Westerman (Eds.), Scientificc Basis for Nuclear Waste Management XI, Materials Research Society, Pittsburgh, PA, 1988, p. 631.

[82] Strachan, D.M. and Croak, T.L., "Compositional Effects on Long-Term Dissolution of Borosilicate Glass." *Journal of Non-Crystalline Solids*, *272*, (1), 2000, 22-33.

[83] "First Investigations of the Influence of IVB Elements (Ti, Zr, and Hf) on the Chemical Durability of Soda-lime Borosilicate Glasses," B. Bergeron, L. Galoisy, P. Jollivet, F. Angeli, T. Charpentier, G. Calas and S.Gin, *Journal of Non-Crystalline Solids*, 356, 2315-2322 (2010).

[84] "Quality Assurance Project Plan for WRPS Support Activities Conducted by VSL," Vitreous State Laboratory, QAPP-WRPS, Rev. 4, Vitreous State Laboratory, The Catholic University of America, Washington, DC, 9/14/16.

[85] "Master List of Controlled VSL Manuals and Standard Operating Procedures in Use," QA-MLCP, Rev. 164, Vitreous State Laboratory, The Catholic University of America, Washington, DC, 6/25/19.

Table 1.1. Target Compositions of the Twenty Phase 1 and Phase 2 IDF Glasses (wt%).

Glass ID	IDF1-B2[#]	IDF2-G9[#]	IDF3-F7[#]	IDF4-A15	IDF5-A20	IDF6-D6	IDF7-E12[#]	IDF8-A125	IDF9-A187	IDF10-4HZr
Tank	AN-107	AP-101	AZ-102	AN-105	AN-105	AN-102	AZ-101	AP-101	AN-105	AN-105
Loading	27%	29%	15%	31%	31%	26%	20%	27%	30%	28%
Al_2O_3	10.00	6.76	8.65	9.45	6.65	10.09	7.58	5.64	10.57	4.95
B_2O_3	7.30	8.51	9.53	8.60	8.74	9.85	9.82	9.55	12.77	11.77
CaO	1.10	2.70	9.77	3.32	3.32	7.89	10.02	1.94	6.47	2.43
Cr_2O_3	0.52	0.59	0.56	0.49	0.50	0.50	0.50	0.02	0.52	0.08
Cs_2O spike	0.15	-	-	0.14	-	-	0.15	0.18	-	-
Fe_2O_3	1.10	0.20	0.23	0.92	0.19	0.28	0.24	5.39	0.90	6.70
K_2O	0.12	5.76	0.50	0.54	0.53	0.17	0.55	4.21	0.51	0.54
Li_2O	-	-	4.37	-	-	-	2.49	-	-	-
MgO	1.10	0.96	0.98	0.92	0.92	1.00	1.04	1.44	0.90	1.45
Na_2O	25.00	21.00	12.00	24.00	24.00	22.00	16.00	20.00	23.00	21.27
NiO	0.04	0.01	-	-	-	0.04	-	-	-	0.01
PbO	-	0.01	-	-	-	0.01	-	-	-	0.01
SiO_2	39.88	40.82	42.38	39.17	42.24	37.14	41.19	42.81	34.70	38.89
SnO_2	1.08	2.84	-	2.73	2.74	-	-	-	1.00	-
TiO_2	-	-	-	-	-	-	-	1.94	-	-
V_2O_5	2.00	-	2.50	-	-	1.96	1.74	-	0.97	-
ZnO	3.65	3.40	2.92	2.43	2.74	2.96	3.21	2.88	2.99	1.50
ZrO_2	5.44	5.68	3.92	5.91	5.96	3.98	3.53	2.91	2.99	9.50
Cl	0.11	0.23	0.01	0.68	0.67	0.35	0.02	0.22	0.64	0.20
F	0.49	0.09	0.08	0.00	0.00	0.18	0.20	0.32	-	0.08
P_2O_5	0.23	0.14	0.04	-	-	0.30	0.12	0.08	-	0.12
SO_3	0.52	0.20	1.50	0.60	0.70	1.20	1.50	0.37	0.95	0.41
Re_2O_7 Spike	0.10	0.10	0.10	0.10	0.10	0.10	0.10	0.10	0.10	0.10
MnO_2	0.06	-	-	-	-	-	-	-	-	-
Sum	100.0	100.0	100.0	100.0	100.0	100.0	100.0	100.0	100.0	100.0

- Empty data field
[#] SPFT tested

Table 1.1. Target Compositions of the 20 IDF Phase 1 and Phase 2 Glasses (wt%) (cont'd).

Glass ID	IDF11-G27	IDF12-A38	IDF13-A51	IDF14-A59	IDF15-A57	IDF16-A58	IDF17-A60	IDF18-A161[#]	IDF19-C100	IDF20-F6
Tank	AP-101	AN-105	AN-105	AN-105	AN-105	AN-105	AN-105	AN-105	AN-102	AZ-102
Loading	29%	32%	31.52%	31.52%	31.52%	31.52%	31.52%	26%	24%	16.06%
Al_2O_3	6.03	6.94	10.15	10.31	10.65	10.65	6.75	10.04	10.16	8.48
B_2O_3	7.92	8.21	8.02	8.15	8.05	8.75	8.87	13.51	13.68	9.36
CaO	2.69	3.12	1.00	1.02	1.50	-	3.37	7.90	8.02	9.58
Cr_2O_3	0.59	0.49	0.02	0.02	0.02	0.02	0.51	0.02	0.02	0.56
Cs_2O spike	-	-	-	-	-	-	-	0.15	-	-
Fe_2O_3	0.28	0.26	0.19	0.19	0.05	0.25	0.19	0.99	1.00	0.29
K_2O	5.75	0.53	0.530	0.53	0.53	0.53	0.53	0.44	0.15	0.54
Li_2O	-	-	-	-	-	-	-	-	-	3.45
MgO	0.44	0.98	1.93	1.96	-	1.55	0.93	0.99	1.00	0.97
Na_2O	21.00	24.00	24.00	24.00	24.00	24.00	24.00	20.66	20.00	13.00
NiO	0.01	-	-	-	-	-	-	-	0.03	-
PbO	0.01	-	-	-	-	-	-	-	0.01	-
SiO_2	42.00	41.52	38.93	39.55	40.73	40.78	42.75	36.05	36.52	42.28
SnO_2	3.19	2.66	1.00	1.02	-	-	2.78	-	-	0.84
TiO_2	-	-	4.00	4.06	3.00	3.00	-	-	-	-
V_2O_5	-	0.91	-	-	-	-	-	0.99	1.00	2.47
ZnO	2.69	2.80	2.80	2.84	4.00	3.00	2.78	2.95	3.00	2.87
ZrO_2	6.44	6.00	5.96	6.05	6.00	6.00	6.05	2.95	3.00	3.83
Cl	0.23	0.67	0.67	0.10	0.67	0.67	0.10	1.17	0.65	0.01
F	0.09	-	-	-	-	-	-	-	0.190	0.089
P_2O_5	0.14	-	-	-	-	-	-	-	0.27	0.04
SO_3	0.41	0.80	0.70	0.10	0.70	0.70	0.30	1.10	1.20	1.25
Re_2O_7 Spike	0.10	0.10	0.10	0.10	0.10	0.10	0.10	0.10	0.10	0.10
Sum	100.0	100.0	100.0	100.0	100.0	100.0	100.0	100.0	100.0	100.0

- Empty data field
[#] SPFT tested

Table 1.2. Target Composition of Seven ORLEC Glasses Selected for Long-Term PCT (wt%).

Glass ID	**ORLEC14**	**ORLEC28**	**ORLEC50**	**ORLEC52**	**ORLEC33**	**ORLEC34**	**ORLEC44**	**ORLEC46**	**ORLEC48**
IDF batching	**IDF21-EC14**	**IDF24-EC28**	**IDF28-EC50**	**IDF23-EC52**	**PNNL Test**	**IDF25-EC34**	**IDF26-EC44**	**IDF22-EC46**	**IDF27-EC48**
Testing for IDF PA	SPFT	SPFT & Long Term PCT	Long Term PCT	SPFT & Long Term PCT	SPFT	Long Term PCT	Long Term PCT	SPFT & Long Term PCT	Long Term PCT
Al_2O_3	10.00	10.00	10.00	9.92	8.36	8.36	7.60	7.60	7.60
B_2O_3	10.00	10.00	11.00	11.00	11.00	11.00	11.00	11.00	11.00
CaO	1.95	1.95	1.95	1.95	3.64	3.64	5.49	6.94	8.14
Cr_2O_3	0.34	0.44	0.34	0.20	0.08	0.08	0.08	0.08	0.08
Fe_2O_3	0.34	0.60	0.34	0.20	0.20	0.20	0.20	0.20	0.20
K_2O	0.50	**3.36**	0.50	0.50	0.50	0.50	0.50	0.50	0.50
Li_2O	0.00	0.00	0.00	0.00	0.00	0.00	0.99	1.86	2.58
MgO	1.00	1.00	1.00	1.00	1.00	1.00	1.00	1.00	1.00
Na_2O	**24.00**	**22.11**	**24.00**	**23.80**	**22.00**	**22.00**	**20.00**	**18.00**	**16.00**
NiO	0.01	0.01	0.01	0.01	0.01	0.01	0.01	0.01	0.01
PbO	0.01	0.01	0.01	0.01	0.01	0.01	0.01	0.01	0.01
SiO_2*	38.71	37.66	38.49	38.51	42.31	42.31	42.43	41.93	41.91
SnO_2	2.33	2.33	1.00	0.80	0.00	0.00	0.00	0.00	0.00
TiO_2	0.34	0.60	0.34	0.00	0.00	0.00	0.00	0.00	0.00
V_2O_5	0.35	0.00	0.90	1.88	2.27	2.27	2.44	2.50	2.50
ZnO	3.00	3.00	3.00	3.00	3.00	3.00	3.00	3.00	3.00
ZrO_2	6.03	6.03	6.03	5.83	4.03	4.03	3.50	3.50	3.50
Cl	0.20	0.20	0.20	0.20	0.20	0.20	0.20	0.20	0.20
F	0.08	0.08	0.08	0.08	0.08	0.08	0.08	0.08	0.08
P_2O_5	0.12	0.12	0.12	0.12	0.12	0.12	0.12	0.12	0.12
SO_3	**0.60**	**0.40**	**0.60**	**0.90**	**1.10**	**1.10**	**1.25**	**1.37**	**1.47**
Re_2O_7 Spike*	0.10	0.10	0.10	0.10	0.10	0.10	0.10	0.10	0.10
Sum	100.0	100.00	100.00	100.00	100.00	100.00	100.00	100.00	100.00

* Re_2O_7 was not added to the crucible glasses characterized in the ORP Enhanced LAW Glass Correlation tests, but was added at the expense of SiO_2 for long-term PCT samples.

Table 2.1. Elemental Compositions and Properties of the Twenty-Seven IDF Glasses.

Glass ID / Atom %	IDF1-B2	IDF2-G9	IDF3-F7	IDF4-A15	IDF5-A20	IDF6-D6	IDF7-E12	IDF8-A125	IDF9-A187	IDF10-Zr6	IDF11-G27	IDF12-A38	IDF13-A51	IDF14-A59	IDF15-A57	IDF16-A58	IDF17-A60	IDF18-A161	IDF19-C100	IDF20-F6
Al	9.34	6.45	7.84	8.87	6.25	9.37	6.95	5.31	9.57	4.72	5.81	6.56	9.49	9.65	9.97	9.87	6.36	9.13	9.28	7.83
B	9.99	11.89	12.66	11.82	12.04	13.39	13.18	13.17	16.94	16.45	11.18	11.37	10.98	11.17	11.04	11.87	12.24	17.99	18.30	12.66
Ca	0.93	2.34	8.05	2.83	2.84	6.66	8.35	1.66	5.33	2.11	2.36	2.68	0.85	0.87	1.28	0.00	2.89	6.53	6.66	8.05
Fe	0.66	0.12	0.13	0.55	0.11	0.17	0.14	3.24	0.52	4.08	0.17	0.16	0.11	0.11	0.03	0.15	0.11	0.57	0.58	0.17
K	0.12	5.95	0.49	0.55	0.54	0.17	0.55	4.29	0.50	0.56	6.00	0.54	0.54	0.54	0.54	0.53	0.54	0.43	0.15	0.54
Li	0.00	0.00	13.52	0.00	0.00	0.00	7.79	0.00	0.00	0.00	0.00	0.00	0.00	0.00	0.00	0.00	0.00	0.00	0.00	10.88
Mg	1.30	1.16	1.12	1.09	1.09	1.17	1.21	1.72	1.03	1.75	0.54	1.17	2.28	2.32	0.00	1.82	1.11	1.14	1.16	1.13
Na	38.42	32.95	17.90	37.05	37.13	33.60	24.12	30.99	34.27	33.38	33.30	37.32	36.90	36.96	36.98	36.58	37.20	30.90	30.05	19.76
Si	31.61	33.03	32.60	31.18	33.70	29.25	32.02	34.21	26.67	31.48	34.34	33.30	30.87	31.41	32.36	32.05	34.17	27.81	28.30	33.14
Sn	0.34	0.92	0.00	0.87	0.87	0.00	0.00	0.00	0.31	0.00	1.04	0.85	0.32	0.32	0.00	0.00	0.89	0.00	0.00	0.26
Ti	0.00	0.00	0.00	0.00	0.00	0.00	0.00	1.17	0.00	0.00	0.00	0.00	2.39	2.43	1.80	1.78	0.00	0.00	0.00	0.00
V	1.05	0.00	1.27	0.00	0.00	1.02	0.89	0.00	0.49	0.00	0.00	0.48	0.00	0.00	0.00	0.00	0.00	0.50	0.51	1.28
Zn	2.14	2.03	1.66	1.43	1.61	1.72	1.84	1.70	1.70	0.90	1.62	1.66	1.64	1.67	2.35	1.74	1.64	1.68	1.72	1.66
Zr	2.10	2.24	1.47	2.29	2.32	1.53	1.34	1.13	1.12	3.75	2.57	2.35	2.30	2.34	2.32	2.30	2.36	1.11	1.13	1.46
Cl	0.15	0.32	0.01	0.92	0.91	0.47	0.03	0.30	0.83	0.27	0.32	0.91	0.90	0.13	0.90	0.89	0.14	1.53	0.85	0.01
F	1.23	0.23	0.19	0.00	0.00	0.45	0.49	0.81	0.00	0.20	0.23	0.00	0.00	0.00	0.00	0.00	0.00	0.00	0.47	0.22
S	0.31	0.12	0.87	0.36	0.42	0.71	0.88	0.22	0.55	0.25	0.25	0.48	0.42	0.06	0.42	0.41	0.18	0.64	0.70	0.74
Others*	0.32	0.27	0.20	0.19	0.17	0.32	0.24	0.08	0.17	0.10	0.27	0.17	0.02	0.02	0.02	0.02	0.17	0.04	0.15	0.20
Sum**	100.0	100.0	100.0	100.0	100.0	100.0	100.0	100.0	100.0	100.0	100.0	100.0	100.0	100.0	100.0	100.0	100.0	100.0	100.0	100.0
Properties																				
PCT-A (B) (g/m^2)	0.84	0.74	0.17	0.66	0.72	0.56	0.25	0.96	1.71	0.70	0.66	0.73	0.37	–	0.21	0.31	–	0.67	0.52	0.16
PCT-A (Na) (g/m^2)	0.77	0.77	0.36	0.68	0.73	0.67	0.40	0.81	1.46	0.55	0.77	0.68	0.54	–	0.50	0.49	–	0.67	0.43	0.34
VHT 24-day rate ($g/m^2/d$)	110	41 to 50$	18	25	7	5 to 18$	31 to 41$	38	25 to 73$	0.6	13 to 57$	8 to 32$	2 to 32$	22	63 to 75$	25 to 33$	5	25 to 68$	10 to 14$	13 to 17$
Viscosity (P) 1100°C	131	86	32	112	95	48	34	104	33	58	102	98	119	–	150	150	–	44	52	40
Conductivity (S/m) 1100°C	0.644	0.464	0.349	0.598	0.444	0.392	0.457	0.327	0.47	0.433	0.451	0.552	0.568	–	0.504	0.477	–	0.311	0.240	–
K3 Neck Loss (inch)	0.039	0.038	0.01	0.036	0.033	0.0395	0.031	0.0255	0.0325	–	0.034	0.043	0.0315	–	0.027	0.022	–	0.0325	0.036	0.012

*Cs, Cr, Ni, Pb, P, Re; ** Atom % excludes oxygen; - Empty data field; $ Duplicate test results; highlights denote values discussed in the text.

Table 2.1. Elemental Compositions and Properties of the Twenty-Seven IDF Glasses (cont'd).

Glass ID / Atom %	IDF24-EC28	IDF28-EC50	IDF23-EC52	IDF25-EC34	IDF26-EC44	IDF22-EC46	IDF27-EC48
Al	9.38	9.15	9.21	7.74	6.97	6.92	6.90
B	13.73	14.85	14.83	14.92	14.77	14.68	14.63
Ca	1.66	1.63	1.63	3.06	4.57	5.75	6.72
Fe	0.36	0.12	0.20	0.12	0.12	0.12	0.12
K	3.41	0.50	0.50	0.50	0.50	0.49	0.49
Li	0.00	0.00	0.00	0.00	3.11	5.79	8.01
Mg	1.19	1.17	1.16	1.17	1.16	1.15	1.15
Na	34.11	36.10	36.35	33.51	30.16	26.98	23.91
Si	30.04	30.20	30.14	33.32	33.07	32.48	32.37
Sn	0.74	0.25	0.31	0.00	0.00	0.00	0.00
Ti	0.36	0.00	0.20	0.00	0.00	0.00	0.00
V	0.00	0.97	0.46	1.18	1.26	1.28	1.27
Zn	1.76	1.73	1.73	1.74	1.72	1.71	1.71
Zr	2.34	2.22	2.30	1.54	1.33	1.32	1.32
Cl	0.27	0.27	0.26	0.27	0.26	0.26	0.26
F	0.20	0.20	0.20	0.20	0.20	0.20	0.19
S	0.24	0.53	0.35	0.65	0.73	0.79	0.85
Others*	0.20	0.12	0.17	0.08	0.08	0.08	0.08
Sum**	100.00	100.00	100.00	100.00	100.00	100.00	100.00
Properties							
PCT-A (B) (g/m^2)	0.51	0.80	0.84	0.90	0.49	0.34	0.27
PCT-A (Na) (g/m^2)	0.51	0.58	0.71	0.68	0.52	0.41	0.43
VHT 24-day rate ($g/m^2/d$)	6.5	2.1	17.1	27.1	30.0	26.6	45.8
Viscosity (P) 1100°C	113	90	77	90	58	43	36
Conductivity (S/m) 1100°C	0.408	0.509	0.519	0.406	0.363	0.378	0.347
K3 Neck Loss (inch)	0.0300	0.0180	0.0330	0.0195	0.0350	0.0400	0.0330

* Cr, Ni, Pb; ** Atom % excludes oxygen; - Empty data field

Table 3.1. Mass of Glass and Volume of Leachant Used in Long-Term PCT at Various S/V Ratios.

S/V ratio (m^{-1})	1,000	2,000	5,000	10,000	20,000
Mass of glass (g)	5	10	15	20	40
Volume of leachant (ml)	100	100	60	40	40

Table 3.2. Summary of Long-Term PCT on the Twenty IDF Phase 1 and Phase 2 Glasses.

Glass ID	IDF1-B2	IDF2-G9	IDF3-F7	IDF4-A15	IDF5-A20	IDF6-D6	IDF7-E12	IDF8-A125	IDF9-A187	IDF10-Zr6	IDF11-G27	IDF12-A38	IDF13-A51	IDF14-A59	IDF15-A57	IDF16-A58	IDF17-A60	IDF18-A161	IDF19-C100	IDF20-F6
Tests at 120°C and S/V 20,000 m^{-1}																				
Immersion date	09/21/2010	09/21/2010	06/24/2010	09/21/2010	09/21/2010	09/22/2010	09/22/2010	09/22/2010	09/22/2010	09/22/2010	Not tested									
Duration (d)	119	119	56	119	119	56	56	119	56	119										
Resumption (d)	Nearing	NO	56	NO	NO	56	56	Slow rise	56	NO										
Status	Terminated after 272 days																			
Tests at 90°C and S/V 20,000 m^{-1}																				
Immersion date	06/24/2010	06/24/2010	06/24/2010	07/15/2010	07/15/2010	07/15/2010	06/24/2010	06/24/2010	07/15 2010	07/15/2010	06/09/2015	06/09/2015	06/09/2015	06/09/2015	06/09/2015	06/10/2015	06/10/2015	06/10/2015	06/10/2015	06/10/2015
Duration (d)	272	272	272	272	272	180	181	272	180	272	1449	1449	1449	1087	1449	1449	1449	1449	1449	1449
Resumption(d)	Nearing	NO	NO	Nearing	NO	56	120	Plateau	56	NO	NO	NO	734	318	653	NO	NO	179	216	326
Status	Terminated after 272 days										O	O	T	T	O	O	O	T	T	T
Tests at 90°C and S/V 2,000 m^{-1}																				
Immersion date	06/16/2010	06/16/2010	06/16/2010	07/13/2010	07/13/2010	07/13/2010	06/16/2010	06/16/2010	07/13/2010	07/13/2010	Not tested									
Duration (d)	2912	2912	2912	2886	2886	1877	2912	2912	1877	2886										
Resumption (d)	2647	NO	1925	1617	2390	574	1171	963	438	NO										
Status*	O	O	O	O	O	T	O	O	T	O										
Tests at 40°C and S/V 2,000 m^{-1}																				
Immersion date	06/22/2010	06/22/2010	06/22/2010	07/14/2010	07/14/2010	07/14/2010	06/22/2010	06/22/2010	07/14/2010	07/14/2010	Not tested									
Duration (d)	2541	2541	2541	2526	2526	2526	2541	2541	2526	2526										
Status	Ongoing tests – No resumption – steady at 1% alteration							O/steady at 10%	O/steady at 1%											

* O=Ongoing, T=Terminated

Table 3.3. Long-Term PCT-B Results at 90 °C and S/V of 20,000 m^{-1} (Tests ILHC and ILHD).

Glass ID	Test	Immersion Date	Sampling Date	Period	pH#	B* Norm. Release [g/L]	K* Norm. Release [g/L]	Li* Norm. Release [g/L]	Na* Norm. Release [g/L]	Si* Norm. Release [g/L]
IDF11-G27CCC	ILHC	6/9/2015	6/16/2015	7	12.31	5.41	4.47	-	7.35	0.91
			7/7/2015	28	12.61	8.25	6.16	-	10.64	1.42
			8/4/2015	56	12.65	9.54	6.84	-	11.09	1.64
			10/6/2015	119	12.71	10.06	7.79	-	12.59	1.66
			12/8/2015	182	12.83	12.41	9.31	-	16.42	2.08
			3/8/2016	273	12.91	13.68	10.19	-	17.03	2.42
			6/7/2016	364	12.93	15.64	10.34	-	23.62	3.00
			12/8/2016	548	13.26	35.67	20.10	-	32.92	10.07
			6/8/2017	730	13.28	41.71	18.98	-	37.71	11.30
			12/8/2017	913	13.32	51.69	26.55	-	57.01	16.93
			2/13/2019	1345	12.67	23.30	13.49	0.00	20.55	5.50
			5/28/2019	1449	12.68	25.72	13.23	0.00	24.08	6.79
IDF12-A38CCC	ILHC	6/9/2015	6/16/2015	7	12.16	4.59	3.02	-	5.47	0.90
			7/7/2015	28	12.41	6.85	4.08	-	8.82	1.33
			8/4/2015	56	12.47	7.94	4.97	-	9.11	1.51
			10/6/2015	119	12.53	8.08	4.95	-	9.94	1.48
			12/8/2015	182	12.66	13.96	9.75	-	14.16	2.70
			3/8/2016	273	12.71	20.64	13.01	-	21.47	4.11
			6/7/2016	364	12.75	29.94	12.93	-	26.47	5.02
			12/8/2016	548	12.87	41.59	20.77	-	34.99	6.50
			6/8/2017	730	12.94	58.12	32.69	-	37.55	9.53
			12/8/2017	913	12.97	84.89	38.72	-	63.41	15.26
			5/31/2018	1087	12.87	93.95	39.61	0.00	60.60	15.60
			2/13/2019	1345	12.86	99.72	49.38	0.00	58.49	10.77
			5/28/2019	1449	12.93	98.90	38.04		77.88	10.33
IDF13-A51CCC	ILHC	6/9/2015	6/16/2015	7	12.05	3.08	2.06	-	4.07	0.61
			7/7/2015	28	12.33	5.61	2.79	-	6.31	0.92
			8/4/2015	56	12.43	6.61	3.55	-	6.87	1.01
			10/6/2015	119	12.50	8.51	3.51	-	8.27	1.08
			12/8/2015	182	12.64	9.97	4.51	-	9.70	1.20
			3/8/2016	273	12.70	11.54	5.08	-	11.94	1.29
			6/7/2016	364	12.73	16.88	7.08	-	19.65	1.79
			12/8/2016	548	12.86	104.36	38.01	-	62.76	5.70
			6/8/2017	730	13.33	197.31	71.53	-	79.53	8.10
			12/8/2017	913	13.37	323.17	133.51	-	180.51	10.28
			2/13/2019	1345	13.37	861.27	377.06	0.00	324.51	27.03
			5/28/2019	1449	13.43	870.56	261.37		347.79	27.78
IDF14-A59CCC	ILHC	6/9/2015	6/16/2015	7	12.11	2.64	2.09	-	4.25	0.64
			7/7/2015	28	12.37	5.03	2.54	-	7.13	1.05
			8/4/2015	56	12.48	6.39	3.77	-	7.43	1.25
			10/6/2015	119	12.54	9.53	4.88	-	10.38	1.33
			12/8/2015	182	12.77	22.09	9.65	-	17.67	2.37
			3/8/2016	273	12.81	132.61	52.46	-	65.30	6.45
			6/7/2016	364	12.85	268.65	97.56	-	188.44	10.54
			12/8/2016[$]	548[$]	13.16	740.66	289.77	-	289.54	25.93
			6/8/2017	730	13.66	1,003.04	426.20	-	413.12	40.60
			12/8/2017	913	13.67	1,087.05	447.96	-	498.61	46.04
			5/31/2018	Solid sampling and terminated						

- Below detection limit; *Normalized release calculated from average of triplicate tests with less than 10% RSD (median 0.6% RSD); [$]Altered glass removed from one of the triplicate vessels; [#] Measured at room temperature

Table 3.3. Long-Term PCT-B Results at 90 °C and S/V of 20,000 m^{-1} (Tests ILHC and ILHD) (continued).

Glass ID	Test	Immersion Date	Sampling Date	Period	pH[#]	B* Norm. Release [g/L]	K* Norm. Release [g/L]	Li* Norm. Release [g/L]	Na* Norm. Release [g/L]	Si* Norm. Release [g/L]
IDF15-A57CCC	ILHC	6/9/2015	6/16/2015	7	12.04	2.05	1.74	-	3.85	0.60
			7/7/2015	28	12.33	3.63	2.31	-	5.86	0.97
			8/4/2015	56	12.45	4.71	2.80	-	6.45	1.14
			10/6/2015	119	12.51	6.29	3.10	-	7.80	1.04
			12/8/2015	182	12.74	9.28	4.00	-	9.15	1.36
			3/8/2016	273	12.81	23.67	8.15	-	16.29	2.42
			6/7/2016	364	12.86	58.46	16.48	-	46.18	5.07
			12/8/2016	548	13.16	140.46	48.64	-	76.18	11.07
			6/8/2017	730	13.68	244.16	85.55	-	132.40	25.82
			12/8/2017	913	13.68	293.00	96.98	-	165.63	20.69
			5/31/2018	1087	13.21	265.95	73.67	-	126.36	15.02
			2/13/2019	1345	13.33	270.61	99.32	-	121.37	15.70
			5/28/2019	1449	13.46	286.09	67.33	-	142.17	15.18
IDF16-A58CCC	ILHD	6/10/2015	6/17/2015	7	12.17	3.76	1.55	-	4.00	0.58
			7/8/2015	28	12.32	7.64	2.84	-	6.57	0.79
			8/5/2015	56	12.44	8.75	3.11	-	7.24	0.93
			10/7/2015	119	12.51	10.46	3.39	-	8.29	1.05
			12/9/2015	182	12.65	12.71	4.02	-	9.89	1.24
			3/9/2016	273	12.71	16.38	5.11	-	12.12	1.70
			6/9/2016	365	12.74	18.68	5.46	-	14.16	2.00
			12/8/2016	547	12.84	23.69	8.21	-	15.47	2.27
			6/9/2017	730	12.93	41.06	11.85	-	21.68	3.49
			12/11/2017	915	12.96	109.28	30.86	-	57.13	5.05
			2/14/2019	1345	12.85	165.19	47.85	-	74.65	6.57
			5/29/2019	1449	12.93	173.21	47.78	-	109.15	7.21
IDF17-A60CCC	ILHD	6/10/2015	6/17/2015	7	12.26	4.30	2.46	-	5.43	0.95
			7/8/2015	28	12.42	6.77	4.07	-	8.46	1.42
			8/5/2015	56	12.48	7.31	4.37	-	8.91	1.58
			10/7/2015	119	12.54	7.69	4.67	-	9.94	1.74
			12/9/2015	182	12.74	11.07	5.86	-	12.58	2.48
			3/9/2016	273	12.81	16.15	9.66	-	15.44	3.64
			6/9/2016	365	12.84	24.79	12.59	-	24.65	5.19
			12/8/2016	547	12.94	38.48	21.01	-	27.50	6.62
			6/9/2017	730	12.98	46.84	23.63	-	32.46	8.38
			12/11/2017	915	13.02	49.86	31.64	-	44.07	8.27
			5/31/2018	1086	12.91	59.76	16.65	-	38.50	5.13
			2/14/2019	1345	12.91	60.24	30.93	-	38.47	9.29
			5/29/2019	1449	12.98	60.39	25.74	-	50.87	9.22
IDF18-A161CCC	ILHD	6/10/2015	6/17/2015	7	11.53	7.30	3.17	-	6.28	0.50
			7/8/2015	28	11.87	8.77	4.48	-	7.66	0.65
			8/5/2015	56	11.98	9.23	4.76	-	8.16	0.87
			10/7/2015	119	12.22	14.84	7.82	-	12.17	1.24
			12/9/2015	182	12.33	210.83	112.87	-	139.43	1.40
			3/9/2016	273	12.41	394.29	196.67	-	225.99	1.87
			6/9/2016	365	12.43	544.32	227.03	-	340.78	1.93
			12/8/2016	547	12.77	684.90	343.36	-	376.92	2.64
			6/9/2017	730	12.88	564.15	288.33	-	401.11	2.89
			12/11/2017	915	12.92	676.30	341.62	-	435.99	3.77
			2/14/2019	1345	11.67	602.02	288.77	-	314.48	2.91
			5/29/2019	1449	11.68	463.69	262.52	-	345.44	2.69

- Below detection limit; *Normalized release calculated from average of triplicate tests with less than 10% RSD (median 0.6%RSD);
[#] Measured at room temperature

Table 3.3. Long-Term PCT-B Results at 90 °C and S/V of 20,000 m^{-1} (Tests ILHC and ILHD) (continued).

Glass ID	Test	Immersion Date	Sampling Date	Period	pH#	B* Norm. Release [g/L]	K* Norm. Release [g/L]	Li* Norm. Release [g/L]	Na* Norm. Release [g/L]	Si* Norm. Release [g/L]
IDF19-C100CCC	ILHD	6/10/2015	6/17/2015	7	11.58	5.81	4.17	-	4.88	0.43
			7/8/2015	28	11.92	7.85	5.09	-	6.85	0.61
			8/5/2015	56	12.03	8.69	5.75	-	7.22	0.80
			10/7/2015	119	12.32	10.67	6.02	-	8.94	0.96
			12/9/2015	182	12.43	71.58	47.17	-	49.32	1.39
			3/9/2016	273	12.52	419.94	328.34	-	241.22	2.27
			6/9/2016	365	12.55	420.48	272.00	-	284.94	2.13
			12/8/2016	547	11.86	485.63	318.15	-	331.13	2.60
			6/9/2017	730	11.93	454.48	307.74	-	348.67	2.92
			12/11/2017	915	11.92	544.33	391.16	-	379.52	2.91
			2/14/2019	1345	11.62	510.20	348.87	-	285.44	3.43
			5/29/2019	1449	11.66	439.42	353.43	-	366.07	2.50
IDF20-F6CCC	ILHD	6/10/2015	6/17/2015	7	11.54	1.60	1.37	2.35	2.26	0.47
			7/8/2015	28	11.85	1.94	1.53	3.08	3.22	0.65
			8/5/2015	56	11.94	2.04	1.67	3.35	3.52	0.74
			10/7/2015	119	12.15	2.44	1.66	3.99	4.51	0.82
			12/9/2015	182	12.26	3.74	2.38	5.57	5.73	1.04
			3/9/2016	273	12.32	11.35	6.59	10.99	11.08	1.59
			6/9/2016	365	12.35	337.31	107.88	196.55	233.60	2.63
			12/8/2016	547	11.66	459.43	192.73	232.94	299.54	3.37
			6/9/2017	730	11.86	641.69	212.38	276.99	378.30	4.95
			12/11/2017	915	11.81	701.72	297.35	295.66	401.25	5.10
			5/31/2018	1086	11.93	554.24	249.81	291.02	361.61	4.49
			2/14/2019	1345	11.96	558.38	249.42	228.10	307.15	4.08
			5/29/2019	1449	12.05	569.10	264.50	235.56	459.46	4.12
ANL-LRM-2	ILHC	6/9/2015	6/16/2015	7	12.02	6.60	2.07	-	5.83	0.88
			7/7/2015	28	12.31	13.34	3.35	-	11.13	1.28
			8/4/2015	56	12.42	17.06	3.93	-	11.72	1.36
			10/6/2015	119	12.47	22.76	4.79	3.12	18.44	2.50
			12/8/2015	182	12.57	41.77	10.40	7.30	27.94	8.61
			3/8/2016	273	12.61	143.10	28.47	74.81	96.66	27.56
			6/7/2016	364	12.66	699.96	125.34	404.69	496.12	9.61
			12/8/2016$	548	12.43	918.89	169.37	599.61	710.94	205.39
			6/8/2017	730	12.47	729.60	157.64	605.12	527.29	18.20
			Test terminated							
ANL-LRM-2	ILHD	6/10/2015	6/17/2015	7	12.03	6.80	1.90	-	5.88	0.91
			7/8/2015	28	12.31	13.22	3.40	-	11.00	1.28
			8/5/2015	56	12.43	17.22	3.99	-	12.02	1.37
			10/7/2015	119	12.47	23.12	5.11	2.54	18.55	2.12
			12/9/2015	182	12.54	47.98	10.61	11.30	30.81	9.73
			3/9/2016	273	12.61	119.70	22.95	61.66	75.74	22.92
			6/9/2016	365	12.66	581.49	106.92	354.90	453.58	8.17
			12/8/2016$	547	12.45	1000.19	191.78	594.14	767.94	177.58
			6/9/2017	730	12.48	789.10	173.24	589.47	580.22	46.24
			Test terminated							

- Below detection limit; *Normalized release calculated from average of triplicate tests with less than 10% RSD (median 0.6%RSD); # Measured at room temperature; $Altered glass removed from one of the triplicate vessels

Table 3.4. Long-Term PCT-B Results at 90 °C and Various S/V Ratios (Tests ILHE, ILHF and ILHG).

Glass ID	Sample ID	Test	S/V (m^{-1})	Immersion Date	Sampling Date	Period	pH[#]	B* Norm. Release [g/L]	K* Norm. Release [g/L]	Li* Norm. Release [g/L]	Na* Norm. Release [g/L]	Si* Norm. Release [g/L]
IDF22 EC46CCC	22EC46	ILHE	20000	6/4/2018	6/11/2018	7	11.78	3.61	1.88	2.86	4.29	0.91
					7/2/2018	28	11.85	4.02	2.38	3.26	5.07	1.06
					7/30/2018	56	11.92	4.88	3.28	3.51	6.50	1.17
					10/2/2018	120	12.07	67.05[$]	33.11[$]	46.48[$]	45.12[$]	3.53[v]
					11/30/2018	179	11.82	486.72	241.88	262.49	275.67	6.80
					3/1/2019	270	11.81	712.21	371.47	280.30	411.39	9.32
					6/4/2019	365	11.86	714.50	278.54	264.44	464.99	8.13
IDF25 EC34CCC	25EC34				6/11/2018	7	11.91	8.10	2.66	0.00	6.68	1.10
					7/2/2018	28	11.93	8.66	3.05	0.00	7.61	1.11
					7/30/2018	56	12.00	9.76	4.44	0.00	8.20	1.10
					10/2/2018	120	12.04	35.03*	43.25[$]	0.00	33.21[$]	3.62[$]
					11/30/2018	179	12.22	158.78	70.22	0.00	86.77	6.45
					3/1/2019	270	11.82	518.54	184.75	0.00	233.80	13.72
					6/4/2019	365	11.88	592.30	149.76	0.00	347.44	18.07
IDF26 EC44CCC	26EC44				6/11/2018	7	11.82	5.09	2.22	2.75	5.01	1.07
					7/2/2018	28	11.86	5.45	2.71	2.69	5.69	1.19
					7/30/2018	56	11.96	5.42	3.49	2.52	6.41	1.19
					10/2/2018	120	12.02	35.06[$]	14.73[$]	26.75	25.18	3.37
					11/30/2018	179	12.10	315.96[$]	154.98[$]	187.70[$]	192.26[$]	8.64[$]
					3/1/2019	270	11.82	687.89	327.12	273.13	391.23	16.55
					6/4/2019	365	11.88	774.53	258.90	244.37	489.01	17.72
IDF27 EC48CCC	27EC48				6/11/2018	7	11.70	2.42	1.59	2.69	3.44	0.78
					7/2/2018	28	11.84	2.66	2.03	3.13	4.11	0.89
					7/30/2018	56	11.91	2.87	2.49	3.27	4.43	0.95
					10/2/2018	120	11.97	6.92	3.86	7.64	7.92	1.63
					11/30/2018	179	12.10	77.12[$]	34.12[$]	49.03[$]	100.86[$]	1.63
					3/1/2019	270	11.59	652.16	260.76	277.14	329.05	5.35
					6/4/2019	365	11.55	806.51	297.04	314.75	584.67	5.79
IDF28 EC50CCC	28EC50				6/11/2018	7	12.01	8.25	2.77	0.00	6.04	0.62
					7/2/2018	28	12.13	11.25	3.59	0.00	8.36	0.79
					7/30/2018	56	12.17	13.06	6.03	0.00	8.95	0.91
					10/2/2018	120	12.24	13.53	4.67	0.00	9.81	0.89
					11/30/2018	179	12.32	14.60	5.05	0.00	10.02	0.85
					3/1/2019	270	12.32	16.27	5.65	0.00	12.54	0.98
					6/4/2019	365	12.45	24.44	5.87	0.00	17.98	1.45

- Empty data field; *Normalized release calculated from average of triplicate tests with less than 10% RSD; [#] Measured at room temperature;
[$]Average evaluated by hand as standard deviation between triplicate or duplicate exceeded 10%RSD.

Table 3.4. Long-Term PCT-B Results at 90 °C and Various S/V Ratios (Tests ILHE, ILHF and ILHG) (cont'd).

Glass ID	Sample ID	Test	S/V (m^{-1})	Immersion Date	Sampling Date	Period	pH[#]	B* Norm. Release [g/L]	K* Norm. Release [g/L]	Na* Norm. Release [g/L]	Si* Norm. Release [g/L]
IDF23 EC52CCC	1K23 EC52	ILHF	1000	6/5/2018	6/12/2018	7	10.48	0.58	0.00	0.57	0.23
					7/3/2018	28	10.90	1.85	0.64	1.39	0.34
					7/31/2018	56	11.38	2.14	0.90	1.49	0.35
					10/3/2018	120	11.13	2.60	0.85	1.81	0.40
					12/3/2018	181	11.35	2.60	1.04	1.84	0.42
					3/4/2019	272	11.39	2.54	0.88	1.97	0.42
					6/5/2019	365	11.46	2.84	1.03	2.32	0.47
	2K23 EC52		2000		6/12/2018	7	11.26	1.85	0.54	1.30	0.32
					7/3/2018	28	11.31	3.13	0.94	2.09	0.41
					7/31/2018	56	11.29	3.40	1.40	2.23	0.41
					10/3/2018	120	11.47	3.75	1.18	2.58	0.43
					12/3/2018	181	11.68	4.01	1.51	2.77	0.47
					3/4/2019	272	11.66	3.98	1.27	2.96	0.48
					6/5/2019	365	11.78	4.42	1.42	3.65	0.54
	5K23 EC52		5000		6/12/2018	7	11.58	3.49	0.98	2.33	0.38
					7/3/2018	28	11.65	5.72	1.78	3.57	0.52
					7/31/2018	56	11.80	6.38	2.48	4.35	0.57
					10/3/2018	120	11.79	6.65	1.98	4.59	0.57
					12/3/2018	181	11.98	6.56	2.35	4.50	0.57
					3/4/2019	272	11.92	6.34	2.04	4.88	0.57
					6/5/2019	365	11.99	6.78	1.99	5.68	0.64
	10K23 EC52		10000		6/12/2018	7	11.88	6.06	1.71	4.07	0.48
					7/3/2018	28	11.82	8.53	2.41	5.22	0.60
					7/31/2018	56	11.95	8.84	3.20	6.04	0.64
					10/3/2018	120	11.95	9.34	2.60	6.72	0.65
					12/3/2018	181	12.12	9.57	3.21	7.71	0.68
					3/4/2019	272	12.10	9.82	2.85	7.55	0.68
					6/5/2019	365	12.11	9.64	2.74	8.05	0.79
	20K23 EC52		20000		6/12/2018	7	12.07	9.99	2.99	6.70	0.63
					7/3/2018	28	12.01	12.36	3.56	7.84	0.70
					7/31/2018	56	12.13	13.22	4.68	8.68	0.75
					10/3/2018	120	12.13	15.60	4.35	10.82	0.82
					12/3/2018	181	12.33	15.67	5.57	10.54	0.87
					3/4/2019	272	12.25	15.84	4.76	11.10	0.92
					6/5/2019	365	12.30	21.38	5.38	15.21	1.59

- Empty data field; *Normalized release calculated from average of triplicate tests with less than 10% RSD
[#] Measured at room temperature

Table 3.4. Long-Term PCT-B Results at 90 °C and Various S/V Ratios (Tests ILHE, ILHF and ILHG) (cont'd).

Glass ID	Sample ID	Test	S/V (m^{-1})	Immersion Date	Sampling Date	Period	pH[#]	B* Norm. Release [g/L]	K* Norm. Release [g/L]	Na* Norm. Release [g/L]	Si* Norm. Release [g/L]
IDF24 EC28CCC	1K24 EC28	ILHG	1000	6/5/2018	6/12/2018	7	10.98	0.67	0.45	0.74	0.25
					7/3/2018	28	11.11	1.47	0.75	1.24	0.36
					7/31/2018	56	11.20	1.83	0.86	1.43	0.39
					10/3/2018	120	11.30	1.96	0.98	1.73	0.41
					12/4/2018	182	11.47	2.19	1.09	1.81	0.47
					3/5/2019	273	11.52	2.17	1.12	1.91	0.47
					6/6/2019	366	11.57	2.27	1.11	2.33	0.51
	2K24 EC28		2000		6/12/2018	7	11.32	1.12	0.68	1.12	0.28
					7/3/2018	28	11.41	2.32	1.10	1.78	0.39
					7/31/2018	56	11.58	2.98	1.34	2.37	0.47
					10/3/2018	120	11.62	3.26	1.50	2.70	0.48
					12/4/2018	182	11.66	3.59	1.68	2.82	0.54
					3/5/2019	273	11.78	3.49	1.68	2.83	0.54
					6/6/2019	366	11.84	3.65	1.65	3.57	0.59
	5K24 EC28		5000		6/12/2018	7	11.69	2.45	1.32	2.31	0.37
					7/3/2018	28	11.74	4.45	2.12	3.32	0.53
					7/31/2018	56	11.86	4.90	2.23	3.84	0.54
					10/3/2018	120	11.92	5.70	2.72	4.80	0.60
					12/4/2018	182	12.03	6.05	2.91	4.83	0.63
					3/5/2019	273	12.12	6.28	2.94	4.97	0.65
					6/6/2019	366	12.08	6.12	2.65	5.91	0.67
	10K24 EC28		10000		6/12/2018	7	11.90	3.99	2.02	3.57	0.44
					7/3/2018	28	11.90	6.34	2.73	4.45	0.60
					7/31/2018	56	12.04	7.22	3.27	5.76	0.62
					10/3/2018	120	12.09	8.47	3.81	7.13	0.65
					12/4/2018	182	12.19	9.12	4.18	8.40	0.73
					3/5/2019	273	12.19	8.90	4.16	7.70	0.73
					6/6/2019	366	12.24	9.81	3.68	8.61	0.80
	20K24 EC28		20000		6/12/2018	7	12.08	5.97	3.31	5.72	0.51
					7/3/2018	28	12.11	9.47	4.21	7.39	0.67
					7/31/2018	56	12.25	11.20	5.60	9.01	0.77
					10/3/2018	120	12.27	12.78	6.31	10.92	0.78
					12/4/2018	182	12.41	13.66	6.93	10.72	0.90
					3/5/2019	273	12.37	13.54	6.65	10.80	0.90
					6/6/2019	366	12.43	15.80	6.21	13.97	1.04

- Empty data field; *Normalized release calculated from average of triplicate tests with less than 10% RSD
[#] Measured at room temperature

Table 3.5. Long-Term PCT-B Results for Reference Glass ANL-LRM at 90 °C and S/V of 2,000 m^{-1} (Tests ILHE, ILHF and ILHG).

Glass ID	Test	S/V (m^{-1})	Immersion Date	Sampling Date	Period	pH#	B* Norm. Release [g/L]	K* Norm. Release [g/L]	Li* Norm. Release [g/L]	Na* Norm. Release [g/L]	Si* Norm. Release [g/L]
ANL-LRM-2	ILHE	2000	6/4/2018	6/11/2018	7	10.64	1.09	0.29	0.00	1.01	0.33
				7/2/2018	28	11.19	2.66	0.57	3.55	2.06	0.46
				7/30/2018	56	11.49	3.74	0.95	4.39	2.72	0.54
				10/2/2018	120	11.47	4.97	0.84	6.11	3.33	0.57
				11/30/2018	179	11.56	5.04	1.03	5.64	3.40	0.61
				3/1/2019	270	11.67	5.74	1.17	4.97	4.44	0.64
				6/4/2019	365	11.82	6.65	1.22	5.22	5.84	0.83
	ILHF		6/5/2018	6/12/2018	7	10.83	1.33	0.30	0.00	1.12	0.35
				7/3/2018	28	10.93	2.34	0.52	3.12	1.76	0.43
				7/31/2018	56	11.16	3.34	0.75	4.39	2.39	0.50
				10/3/2018	120	11.35	4.59	0.83	5.34	3.29	0.58
				12/3/2018	181	11.59	4.97	1.00	6.26	3.34	0.62
				3/4/2019	272	11.61	5.18	1.00	6.03	3.88	0.63
				6/5/2019	365	11.58	5.84	0.99	6.00	4.41	0.74
	ILHG		6/5/2018	6/12/2018	7	10.57	1.15	0.24	0.00	1.06	0.32
				7/3/2018	28	10.99	2.50	0.54	3.10	1.86	0.43
				7/31/2018	56	11.35	3.89	0.85	3.64	2.94	0.54
				10/3/2018	120	11.56	5.36	1.06	4.69	4.09	0.61
				12/4/2018	182	11.64	5.80	1.09	6.65	3.96	0.66
				3/5/2019	273	11.59	5.82	0.99	8.29	3.98	0.66
				6/6/2019	366	11.70	6.59	1.17	8.00	5.62	0.96

*Normalized release calculated from average of triplicate tests with less than 10% RSD

Measured at room temperature

Table 4.1. Summary of Phases Identified on Solid Samples Taken from PCT Vessels of the Ten IDF Phase 1 Glasses [50, 56].

Sample ID	Resumption?	Phyllosilicates	Tecto- and Soro-silicates	Others
Sampled from PCT-B at 90°C and S/V 20,000 m^{-1}				
IDF1-B2CCC in IHHA-6-5	272 days	Saponite	Lazurite	-
IDF2-G9CCC in IHHA-6-8	No	None detected		
IDF3-F7CCC in IHHA-6-11	No	None detected		$^{\$}ZnCr_2O_4$
IDF4-A15CCC in IHHB-6-3	272 days	None detected	Phillipsite and Lazurite	-
IDF5-A20CCC in IHHB-6-8	No	None detected	Gehlenite	-
IDF6-D6CCC	56 to 120 days	Agglomeration– sampling not possible		
IDF7-E12CCC	180 days	Agglomeration– sampling not possible		
IDF8-A125CCC in IHHA-6-15	No	None detected	Analcime	-
IDF9-A187CCC	56 to 120 days	Agglomeration – sampling not possible		
IDF10-Zr6CCC in IHHB-6-17	No	None detected		
Sampled from PCT-B at 90°C and S/V 2,000 m^{-1}				
IDF1-B2CCC in ILHA-18-5	2546 days and on-going	Various possible phyllosilicates	Chabazite $Ca_2Al_4Si_8O_{24}(H_2O)_{12}$	
IDF2-G9CCC in ILHA-18-8	No	No crystallization detected in XRD		
IDF3-F7CCC (in ILHA-18-11	2546 days	Nontronite	$Na_{3.555}(Al_{3.6}Si_{12.4}O_{32})(H_2O)_{10.556}$ and analcime $NaAl(SiO_6)(H_2O)$	$^{\$}ZnCr_2O_4$
IDF4-A15CCC in ILHB-18-5	1445 days	Various possible phyllosilicates	Zeolite, gobbinsite at last sampling + Phillipsite and lazurite	-
IDF5-A20CCC in ILHB-18-8	2546 days and on-going	Various possible phyllosilicates	Analcime $NaAl(SiO_6)(H_2O)$	
IDF6-D6CCC in ILHB-15-(9,10,11) Terminated	545 to 727 days	Lizardite	Analcime and Gobbinsite	-
IDF7-E12CCC in ILHA-18-14	1266 days	Tobermorite and Kaolinite	Analcime + Phillipsite and Coesite	-
IDF8-A125CCC in ILHA-18-17	727 to 1630 days	None detectable	Analcime and chabazite	-
IDF9-A187CCC in ILHB-15-(12,13,14) & Terminated	364 to 727 days	Lizardite	Analcime and gobbinsite	-
IDF10-Zr6CCC in ILHB-18-17	No	No crystallization detected in XRD		

$^{\$}$Trace amount of zincochromite ($ZnCr_2O_4$) originally identified in the CCC glass prior to leach test; - Empty data field

Table 4.2. Summary of Phases Identified on Solid Samples Taken from PCT Vessels of the Ten IDF Phase 2 Glasses.

Sample ID	Resumption?	Phyllosilicates	Tecto- and Soro-silicates
Sampled from PCT-B at 90°C and S/V 2,000 m^{-1}			
IDF11-G27CCC in ILHC-11-3	No	No crystallization detected in XRD	
IDF12-A38CCC in ILHC-11-6	No	No crystallization detected in XRD	
IDF13-A51CCC in ILHC-11-9	Slow rise – ongoing for 1 yr	Various possible phyllosilicates	Zeolite $Na_6(Al_6Si_{10}O_{32})(H_2O)_{12}$ Analcime $NaAl(SiO_6)(H_2O)$
IDF14-A59CCC in ILHC-12	273 days	None clearly identified	Zeolite $Na_6(Al_6Si_{10}O_{32})(H_2O)_{12}$ + in prior sampling Phillipsite $(K,Na)_2(Si,Al)_8O_{16}\cdot 4H_2O$ in XRD; $(Na_{6.7}K_{0.1}Mg_{0.4}Ca_{0.2}Ti_{0.8}Zn_{0.4})Al_2Si_7O_{24}$ in SEM
IDF15-A57CCC in ILHC-11-15	Slow rise – ongoing for 1 yr	Various possible phyllosilicates	Zeolite $Na_6(Al_6Si_{10}O_{32})(H_2O)_{12}$
IDF16-A58CCC in ILHD-11-3	No	No crystallization detected in XRD	
IDF17-A60CCC in ILHD-11-6	No	No crystallization detected in XRD	
IDF18-A161CCC in ILHD-11-9	119 days	Aliettite $(Ca_{0.9}Mg_6(Si,Al)_8O_{22}(OH)_4\cdot 4H_2O)$ or beidellite $(Na_{0.3}Al_2(Si,Al)_4O_{10}(OH)_2\cdot 2H_2O)$ in XRD	Zeolite $Na_6(Al_6Si_{10}O_{32})(H_2O)_{12}$ + in prior sampling Phillipsite $(K,Na)_2(Si,Al)_8O_{16}\cdot 4H_2O$ in XRD; Multiple morphologies, phillipsite or albite in SEM: $Na_6CaFe_{0.1}Zn_{0.3}Zr)Al_3Si_{10}O_{24}$
IDF19-C100CCC in ILHD-11-12	119 days	Aliettite $(Ca_{0.9}Mg_6(Si,Al)_8O_{22}(OH)_4\cdot 4H_2O)$ or beidellite $(Na_{0.3}Al_2(Si,Al)_4O_{10}(OH)_2\cdot 2H_2O)$ in XRD	Zeolite $Na_6(Al_6Si_{10}O_{32})(H_2O)_{12}$ + in prior sampling Phillipsite $(K,Na)_2(Si,Al)_8O_{16}\cdot 4H_2O$ in XRD; Multiple morphologies, phillipsite or albite in SEM: $Na_6CaFe_{0.1}Zn_{0.3}Zr)Al_3Si_{10}O_{24}$
IDF20-F6CCC in ILHD-11-15	365 days	Swinefordite $(Ca_{0.1}(Li,Al)_3Si_4O_{10}(OH)_2\cdot 2(H_2O)$ in XRD; Possibly cavansite $Ca(VO)Si_4O_{10}(H_2O)_4$ in SEM	Zeolite $Na_6(Al_6Si_{10}O_{32})(H_2O)_{12}$ + in prior sampling Phillipsite $(K,Na)_2(Si,Al)_8O_{16}\cdot 4H_2O$ smaller in XRD Possibly hemimorphite $Zn_4Si_2O_7(OH)_2\cdot H_2O$ in SEM
ANL-LRM2 in ILHC-11-18 and ILHD-11-18 & Terminated	272 days	None detected	Phillipsite $(K,Na)_2(Si,Al)_8O_{16}\cdot 4H_2O$ and possibly analcime in XRD; Multiple morphologies, generally small in SEM: $(Na_{3.7}K_{0.1}Mg_{0.2}Ca_{0.6}Fe_{0.1}Zn_{0.41}Zr_{0.3})Al_{1.5}Si_{4.8}O_{16}$

Table 4.3. EDS Analyses of Phyllosilicate Crystals Observed on Altered Glasses.

Elemental at%	Na	Mg	Al	Si	Cl	K	Ca	Cr	Fe	Ti	Zn	Zr	Sn	O	Si/Al
IDF1-B2 in ILHA-18-5 (90°C)															
Middle layer*	7.7	0.4	5.1	20.9	–	–	1.4	0.2	0.3	–	1.0	2.2	–	60.9	4.1
Outer layer	5.7	0.8	5.1	21.1	–	–	1.5	0.3	0.5	–	1.4	2.1	–	61.5	4.1
IDF5-A20 inILHB-18-8															
Inner layer	5.8	0.8	4.4	22.1	0.2	1.7	1.4	0.2	0.1	–	0.9	2.1		60.3	5.0
Outer layer	7.0	3.2	3.2	20.2	–	–	1.7	–	–	–	2.3	1.7	0.4	60.2	6.3
Inner layer	6.7	–	3.3	21.6	–	0.5	2.0	–	–	–	0.7	2.7	0.9	61.6	6.5
IDF13-A51 in ILHC-11-9															
Outer layer	6.3	1.1	4.0	19.6	0.2	0.2	2.0	–	–	1.8	1.6	1.8	-	61.3	4.9
Inner layer	4.7	1.6	3.1	21.6	–	0.4	1.1	–	–	1.0	1.7	2.3	0.4	62.2	7.1
IDF13-A51 in ILHD-11-3															
Inner layer	6.3	1.1	4.0	19.6	0.2	0.2	2.0	–	–	1.8	1.6	1.8	-	61.3	4.9
Middle layer	4.2	1.5	3.2	21.1	–	0.4	1.9	–	–	1.3	1.6	2.3	0.4	62.2	6.6
Outer layer	4.7	1.6	3.1	21.6	–	0.4	1.1	–	–	1.0	1.7	2.3	0.4	62.2	7.1
IDF17-A60 in ILHD-11-6															
Inner layer	7.1	0.6	4.1	20.9	–	0.4	1.8	–	–	–	0.1	0.1	0.8	2.2	5.1
Middle layer	7.2	2.3	3.9	20.3	–	0.4	1.2	–	–	–	0.1	0.1	1.3	1.9	5.2
Outer layer	6.0	2.6	3.5	18.7	–	0.3	5.0	–	–	–	0.1	0.2	1.5	1.7	5.4
IDF17-A60 in ILHD-11-6															
Inner layer	7.9	0.5	3.1	21.0	–	–	2.4	–	–	–	0.8	3.0	0.5	61.0	6.8
Outer layer	5.7	3.2	3.0	19.1	0.8	–	1.1	–	–	–	3.9	1.5	0.3	60.8	6.3
IDF8-A125 in ILHD-18-17 (40°C)															
Inner layer	7.6	1.0	4.8	26.5	0.3	3.1	1.5	–	4.3	1.5	2.7	3.7	–	43.1	5.5
Outer layer	7.3	1.7	3.5	23.3	0.4	3.5	1.6	–	7.5	1.6	5.2	2.4	–	40.6	6.7
IDF3-F7in ILHA-18-11															
Ca-Si-Gel	0.8	–	2.4	21.7	–	–	13.9	–	–	–	–	–	–	61.3	0.1
IDF18-A161 in ILHD-11-9															
Ca-Si-Gel	1.43	–	0.6	20.2	–	–	18.0	–	–	–	–	–	–	59.9	0
IDF19-C100 in ILHD-11-12															
Ca-Si-Gel	1.02	–	–	24.7	0.3	–	10.2	–	–	–	0.50	–	–	62.8	0

*"Inner layer" is close to the unaltered glass; "Outer layer" is close to the solution; in between is named "Middle Layer"

Table 4.4. EDS Analyses of Zeolites and $CaSnO_3$ Crystals Observed on Altered Glasses.

Elemental at%	Na	Al	Si	K	Ca	Ti	Zn	Zr	Sn	O	Si/Al
IDF1-B2 in ILHA-18-5											
zeolite	9.0	9.6	20.5	–	–	–	0.2	0.1	–	60.5	2.1
IDF5-A20 in ILHB-18-8											
Analcime	10.3	9.4	20.3	–	–	–	–	–	–	59.9	2.2
Cross-section zeolite	7.6	9.6	21.5	–	–	–	0.1	–	–	61.2	2.2
IDF13-A51 in ILHC-11-9											
Analcime	6.6	9.9	21.6	–	–	–	0.4	–	–	61.6	2.2
IDF14-A59 in ILHC-11-12	–	–	–	–	–	–	–	–	–		
Analcime	7.5	10.3	20.4	–	–	–	0.5	0.2	–	61.0	2.0
IDF15-A57 in ILHC-11-15											
Analcime	5.3	9.2	22.0	0.2	0.6	0.2	0.5	–	–	62.0	2.4
IDF16-A58 in ILHC-11-18											
Analcime	5.6	9.2	21.1	0.6	–	–	–	–	–	62.6	2.3
IDF17-A60 in ILHD-11-6											
Analcime	6.0	9.6	22.2	0.2	–	–	–	–	–	62.0	2.3
IDF18-A60 in ILHD-11-9											
Analcime	6.9	10.9	19.9	–	1.1	–	0.3	–	–	60.9	1.8
Cubic Calcium Stannate											
IDF4-A15 in ILHB-18-5											
$CaSnO_3$ Cubic no Al	–	–	0.6	–	19.2	–	–	–	19.9	60.3	0
IDF5-A20 in ILHB-18-8											
$CaSnO_3$ Cubic, with Al	–	1.2	0.9	–	17.7	–	–	–	19.6	60.7	0

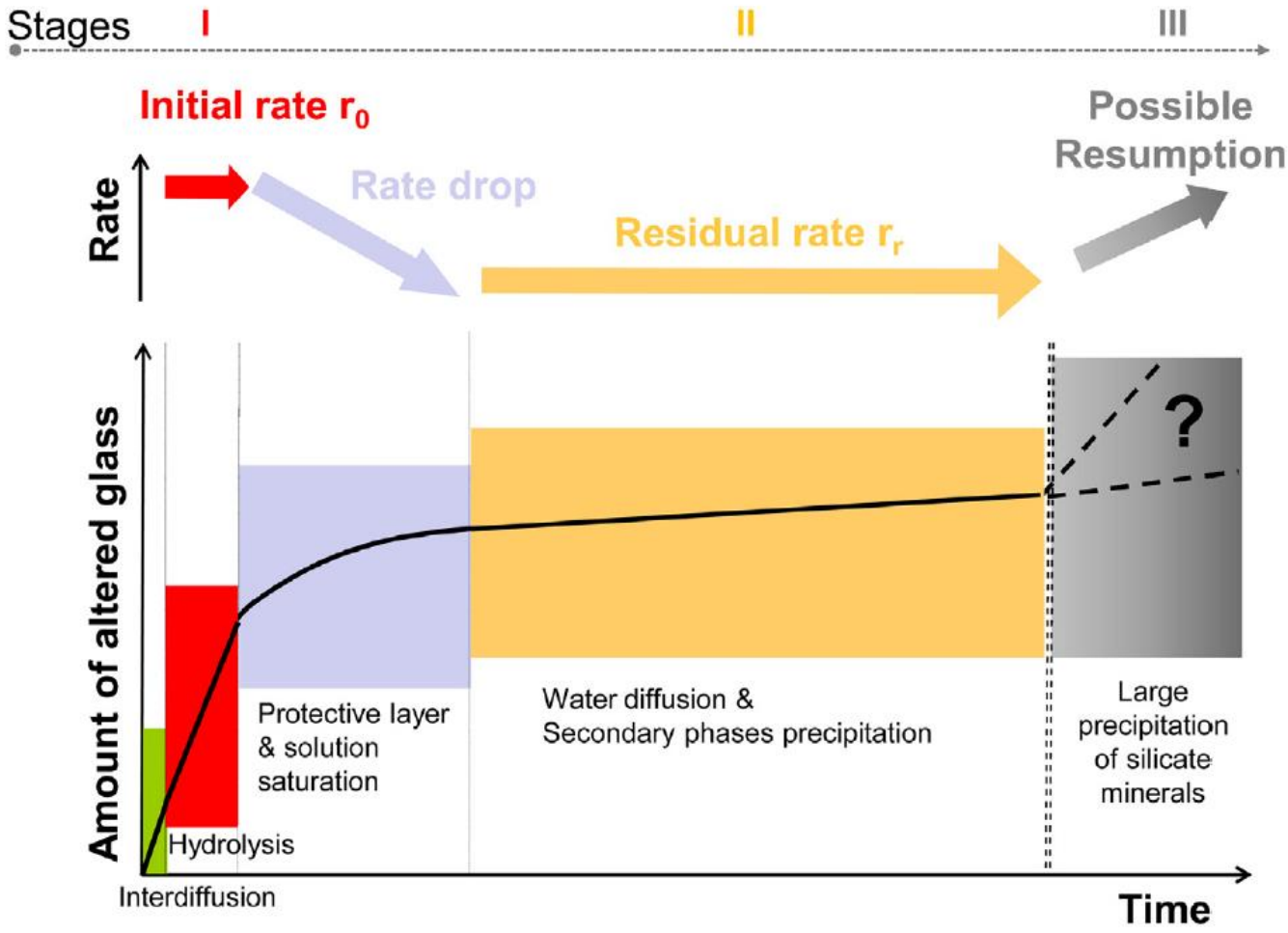

Figure 1.1. "Stages of nuclear glass corrosion and related potential rate-limiting mechanism", ***after Gin. et al. [8].***

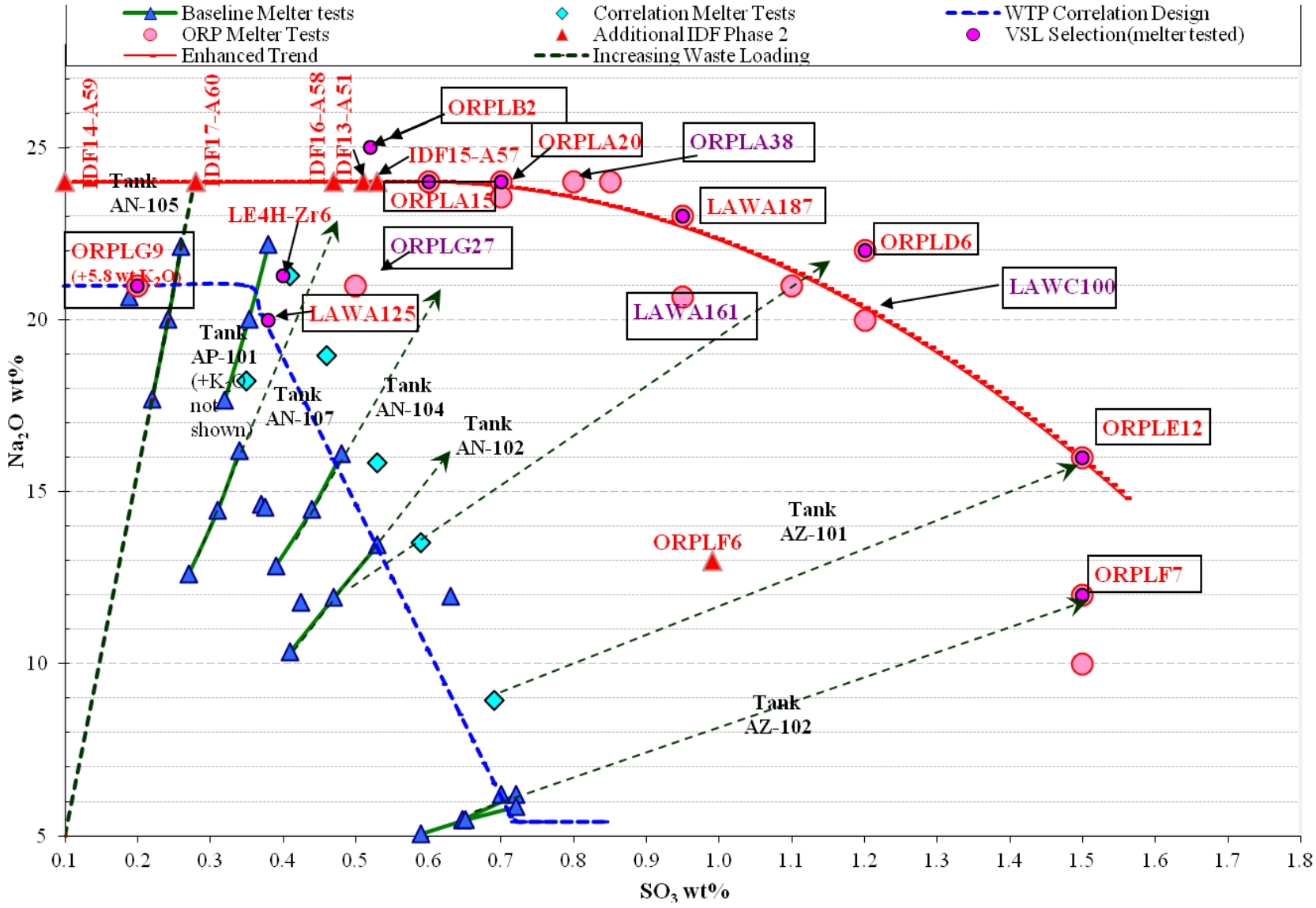

Figure 1.2. Overview of Na_2O and SO_3 loadings for WTP, ORP and selected IDF glasses.

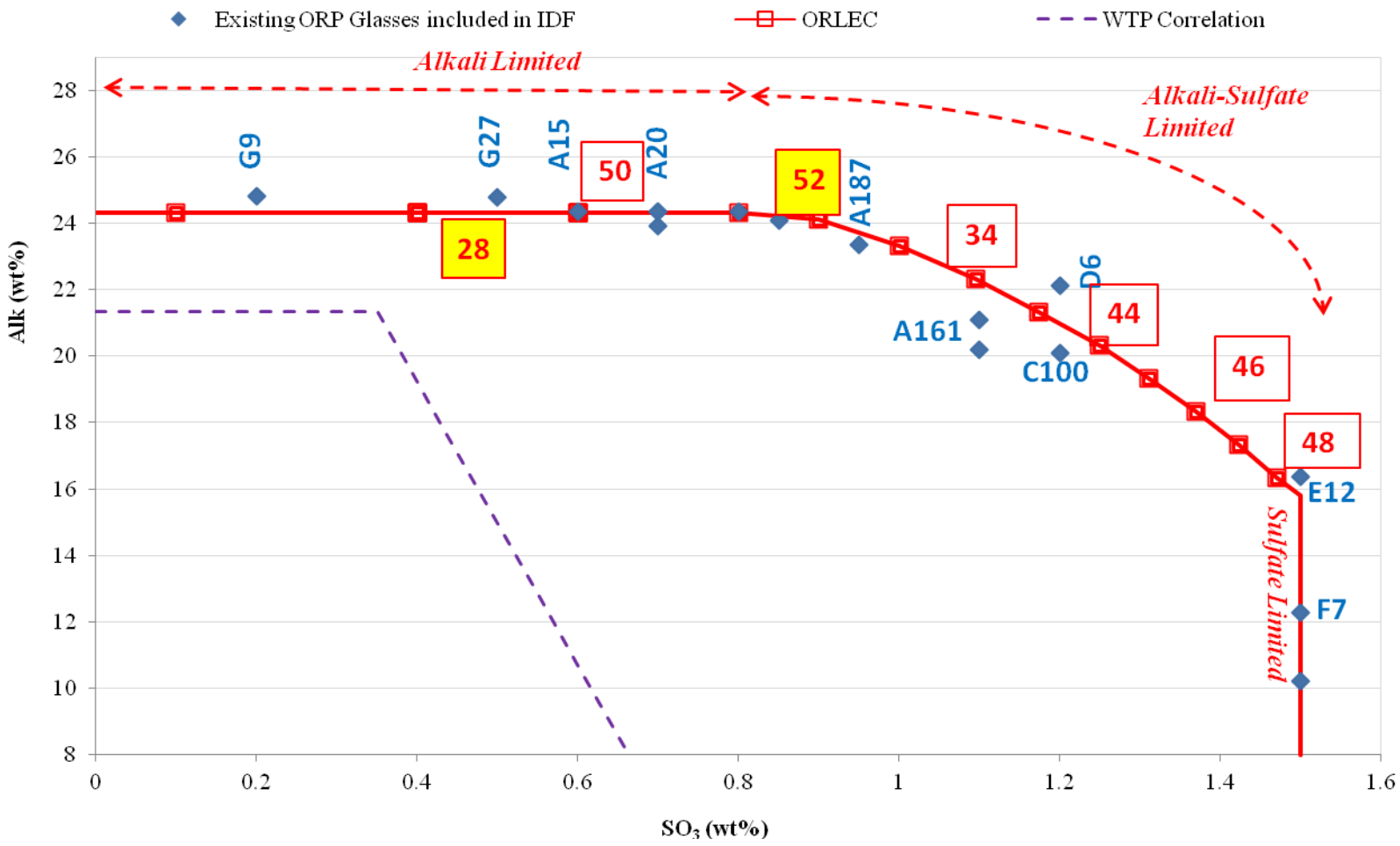

Figure 2.1. ALK ($Na_2O + 0.66 \times K_2O$) and SO_3 concentrations for the IDF glasses (blue diamonds) and the new Enhanced LAW Correlation glasses (red squares); glasses selected for long-term PCT are labeled in red squares and the two glasses tested at various S/V ratios are highlighted in yellow.

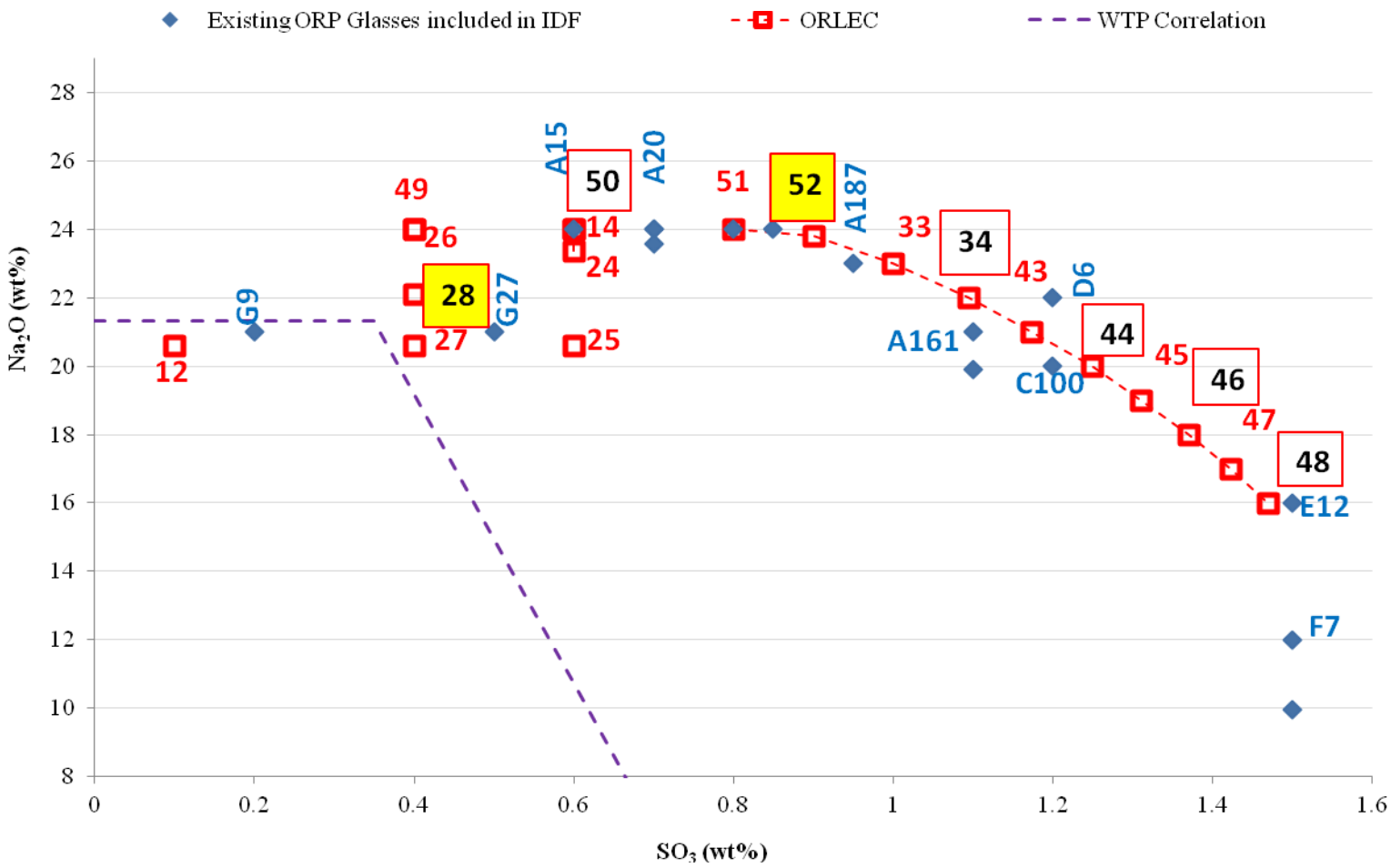

Figure 2.2. Na_2O and SO_3 concentrations for the IDF glasses (blue diamonds) and the new ORLEC glasses (red squares); glasses tested in long-term PCT are labeled in red squares and the two glasses tested at various S/V ratios are highlighted in yellow.

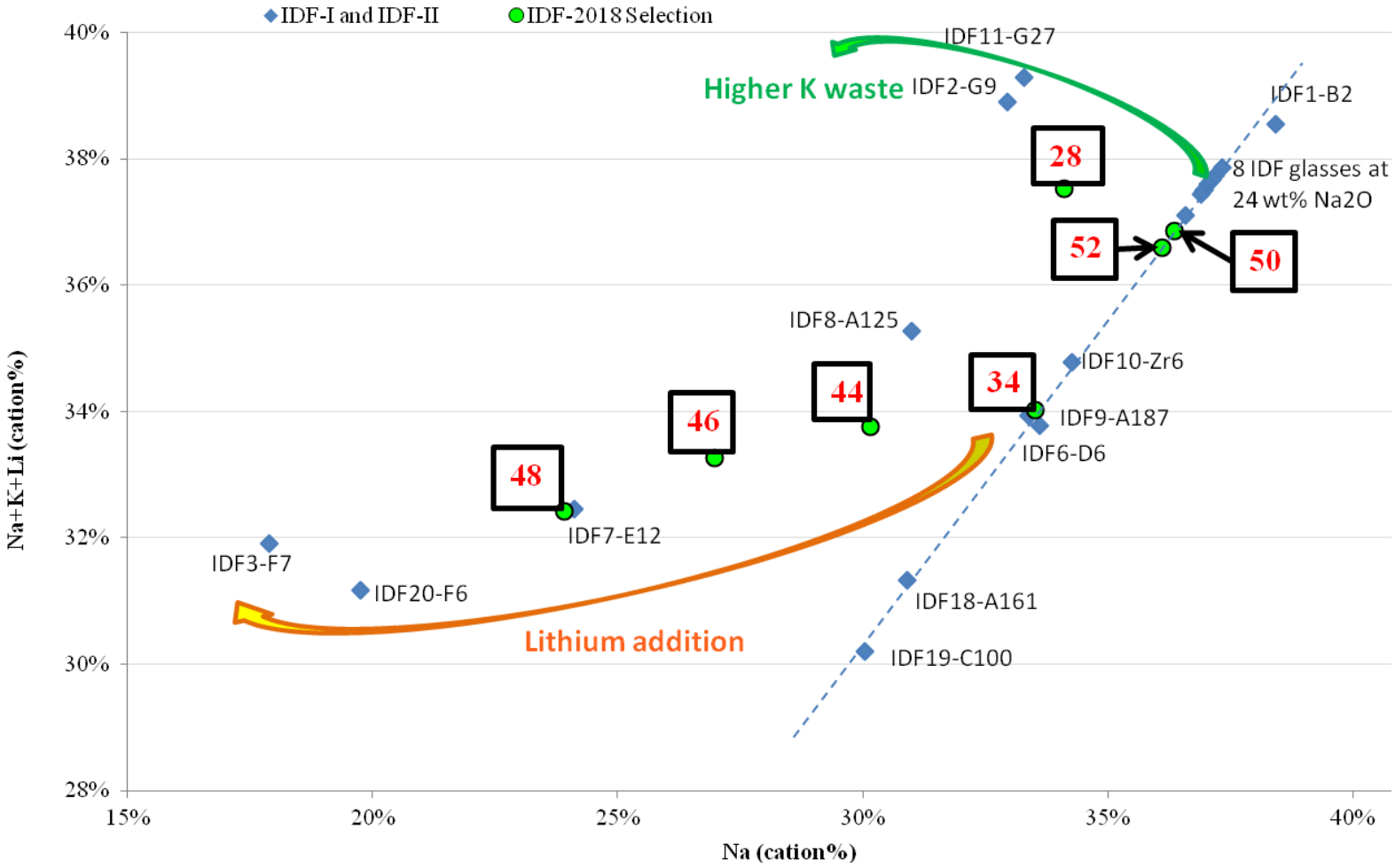

Figure 2.3. Sum of alkalis (Na, K, Li, in cation%) versus Na in the 20 IDF Phase 1 and Phase 2 glasses and the seven FY-18 IDF glasses selected for long-term PCT.

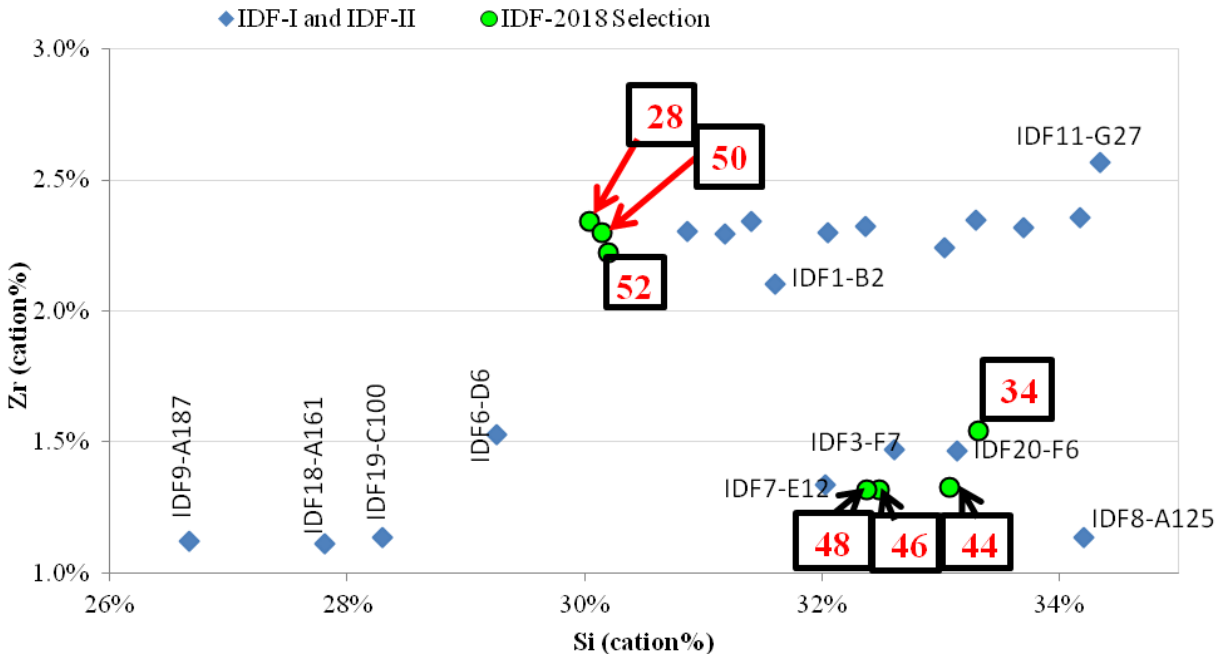

Figure 2.4. Zirconium versus silicon in the 27 IDF glasses (cation%).

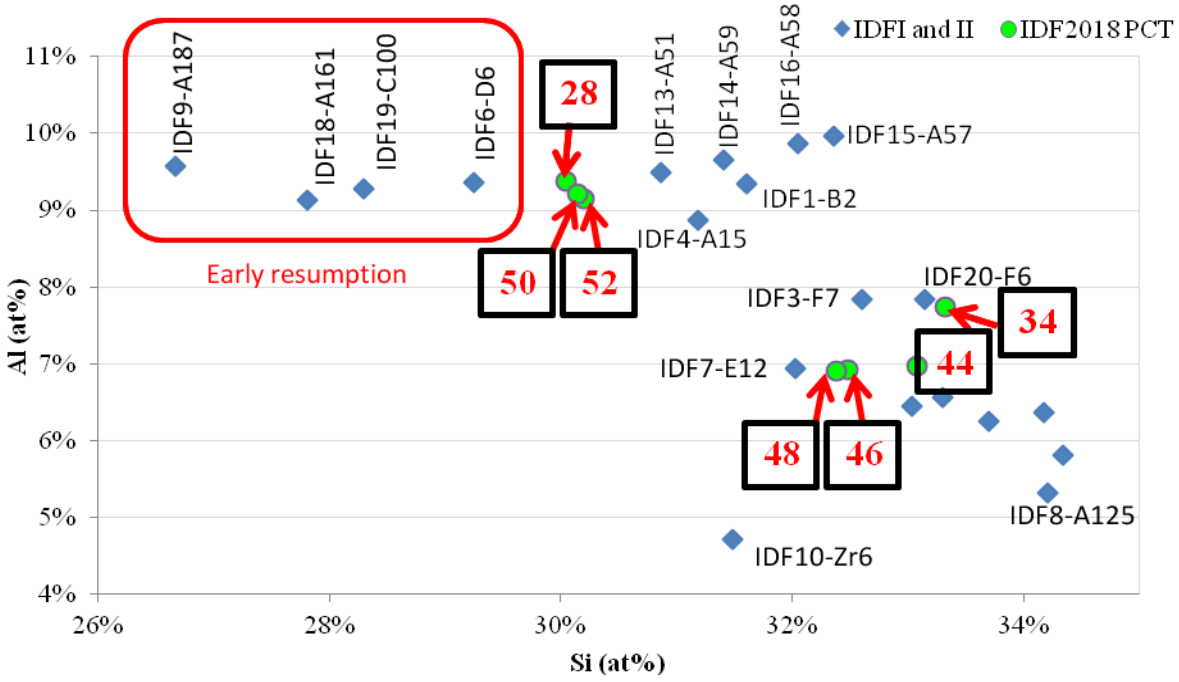

Figure 2.5. Aluminum versus silicon in the 27 IDF glasses (cation%).

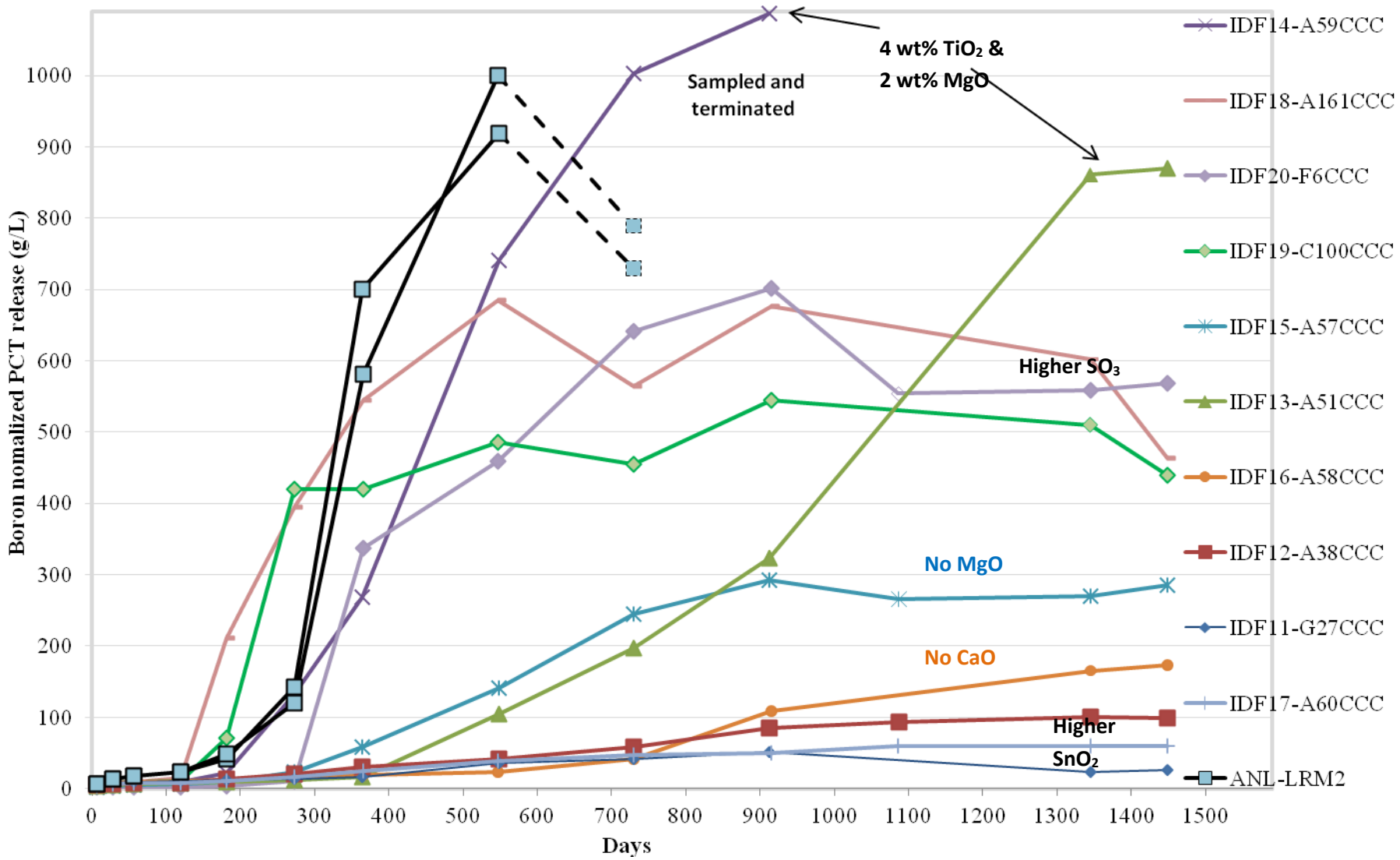

Figure 3.1. PCT-B results (90 °C and S/V 20,000 m^{-1}) for the ten IDF Phase 2 glasses and the ANL-LRM2 reference glass.

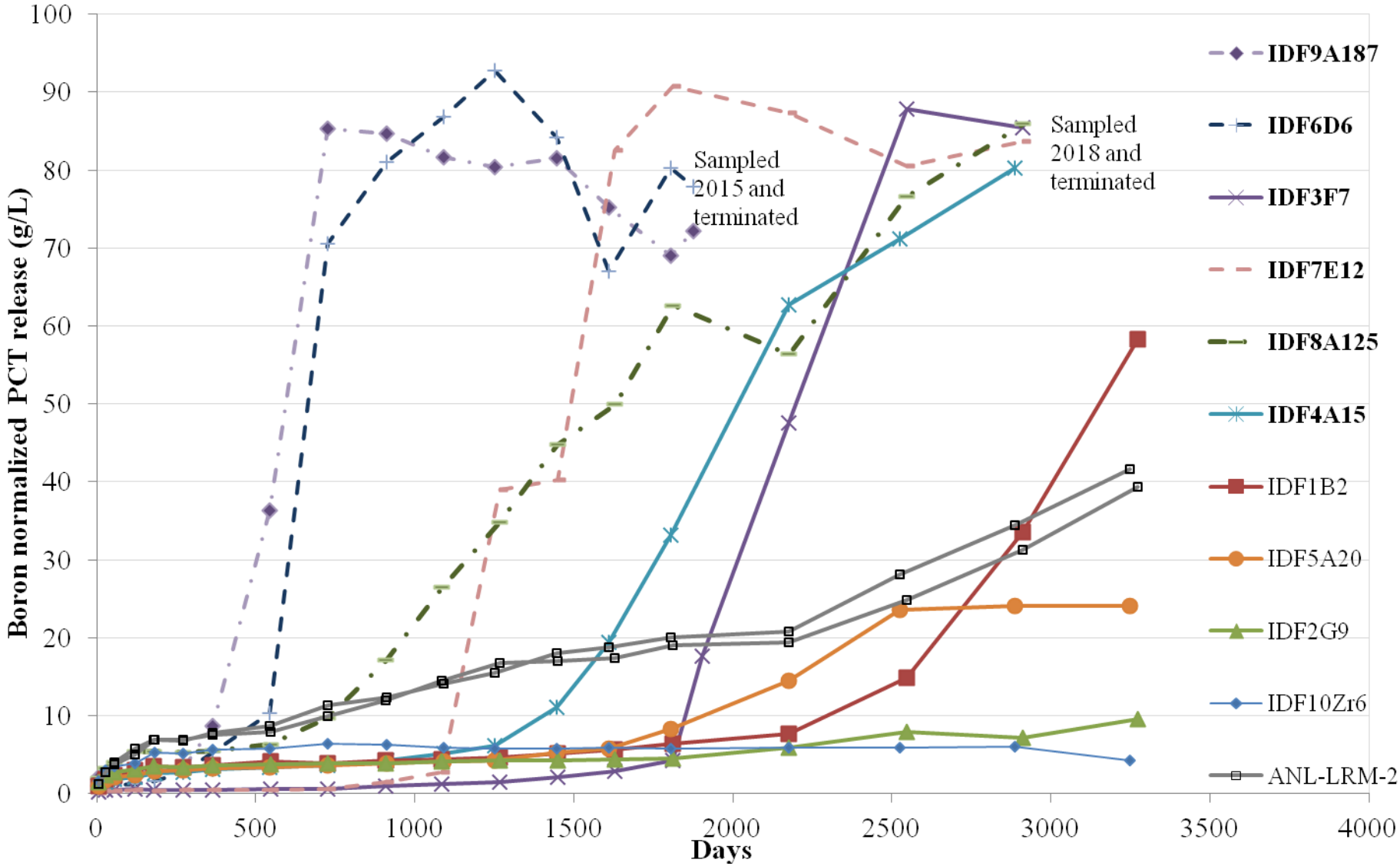

Figure 3.2. PCT-B results (90 °C and S/V 2,000 m^{-1}) for the ten IDF Phase 1 glasses.

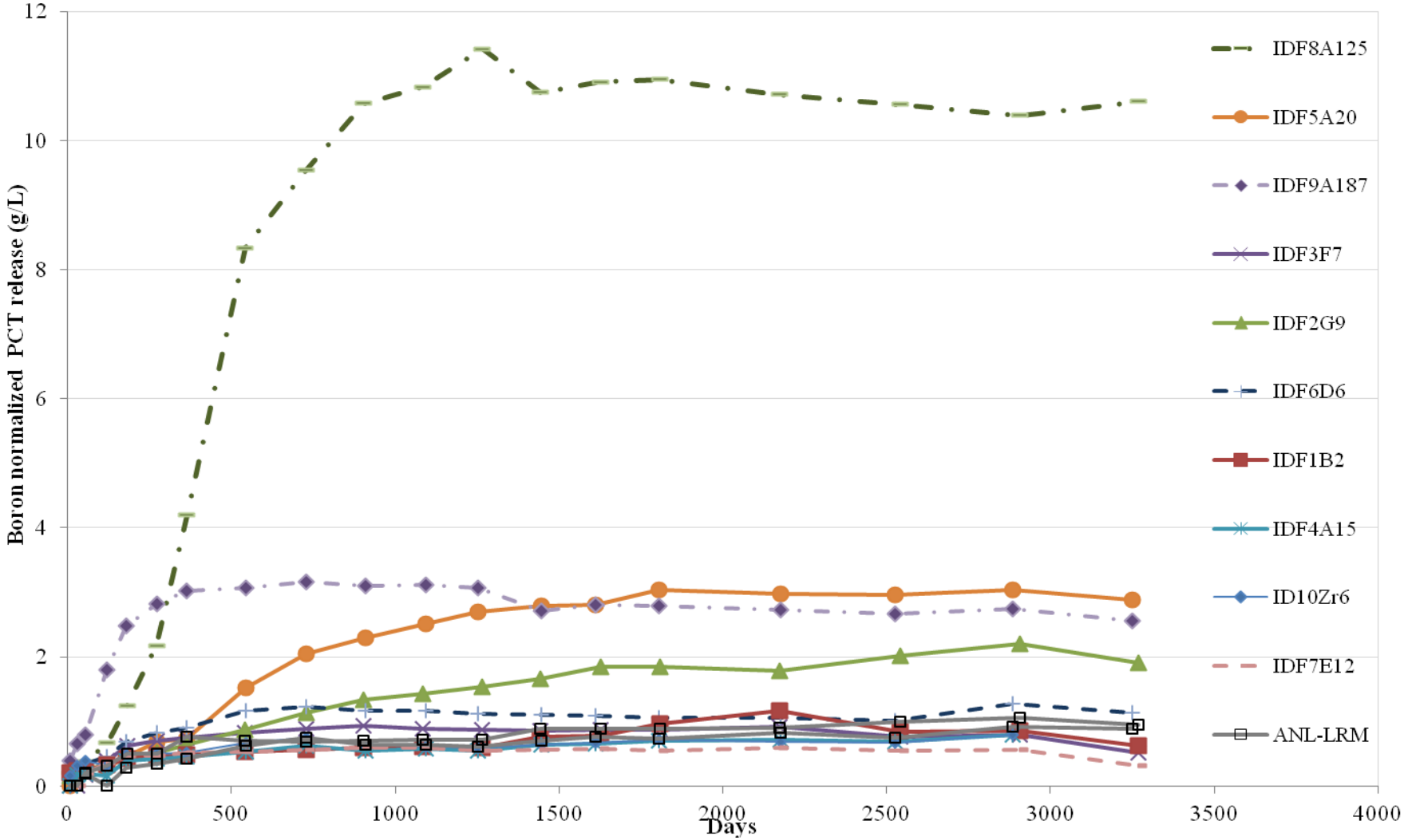

Figure 3.3. PCT-B results (40 °C and S/V 2,000 m^{-1}) for the ten IDF Phase 1 glasses.

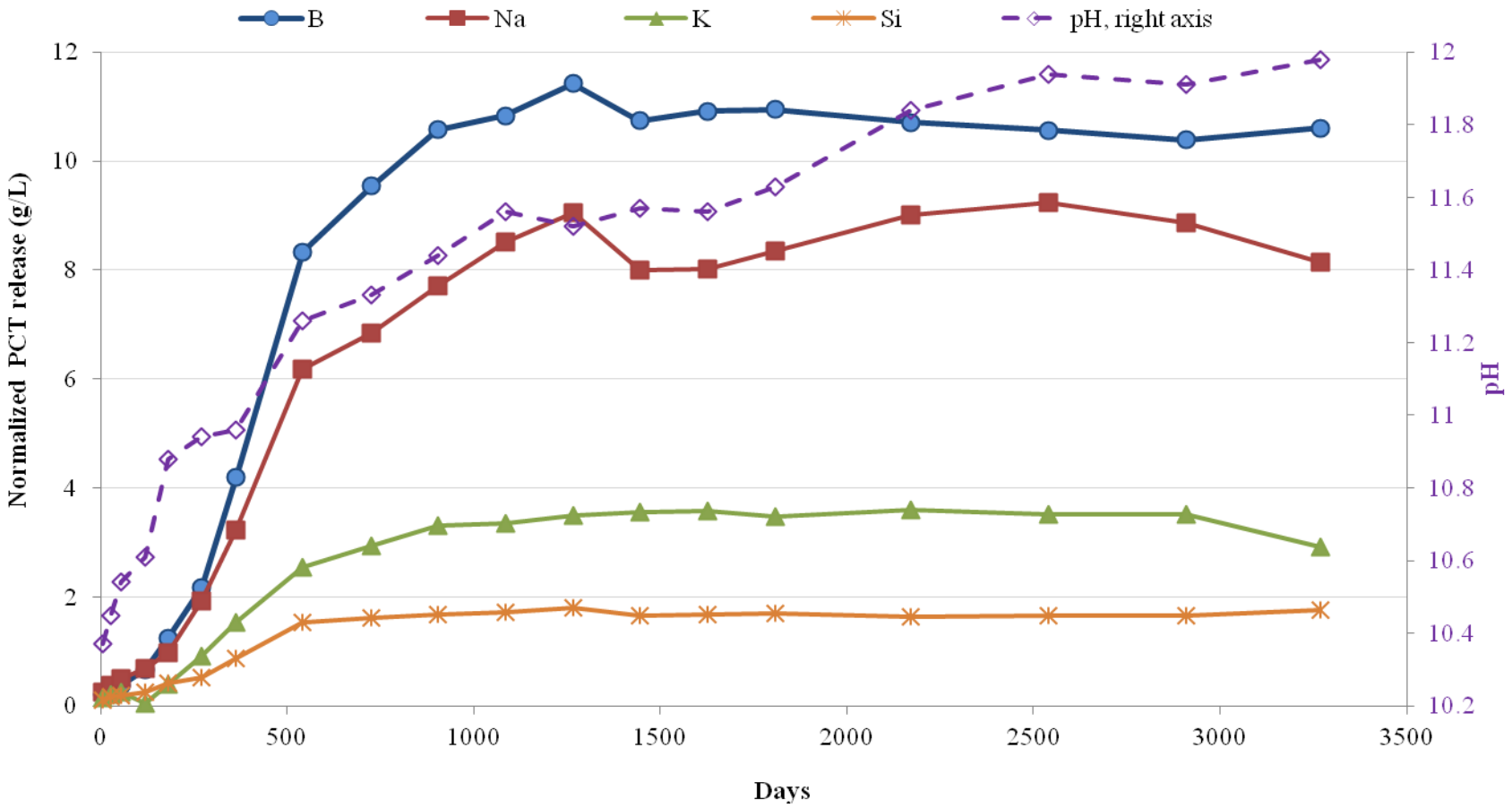

Figure 3.4. PCT-B results (40 °C and S/V 2,000 m^{-1}) for glass IDF8-A125CCC.

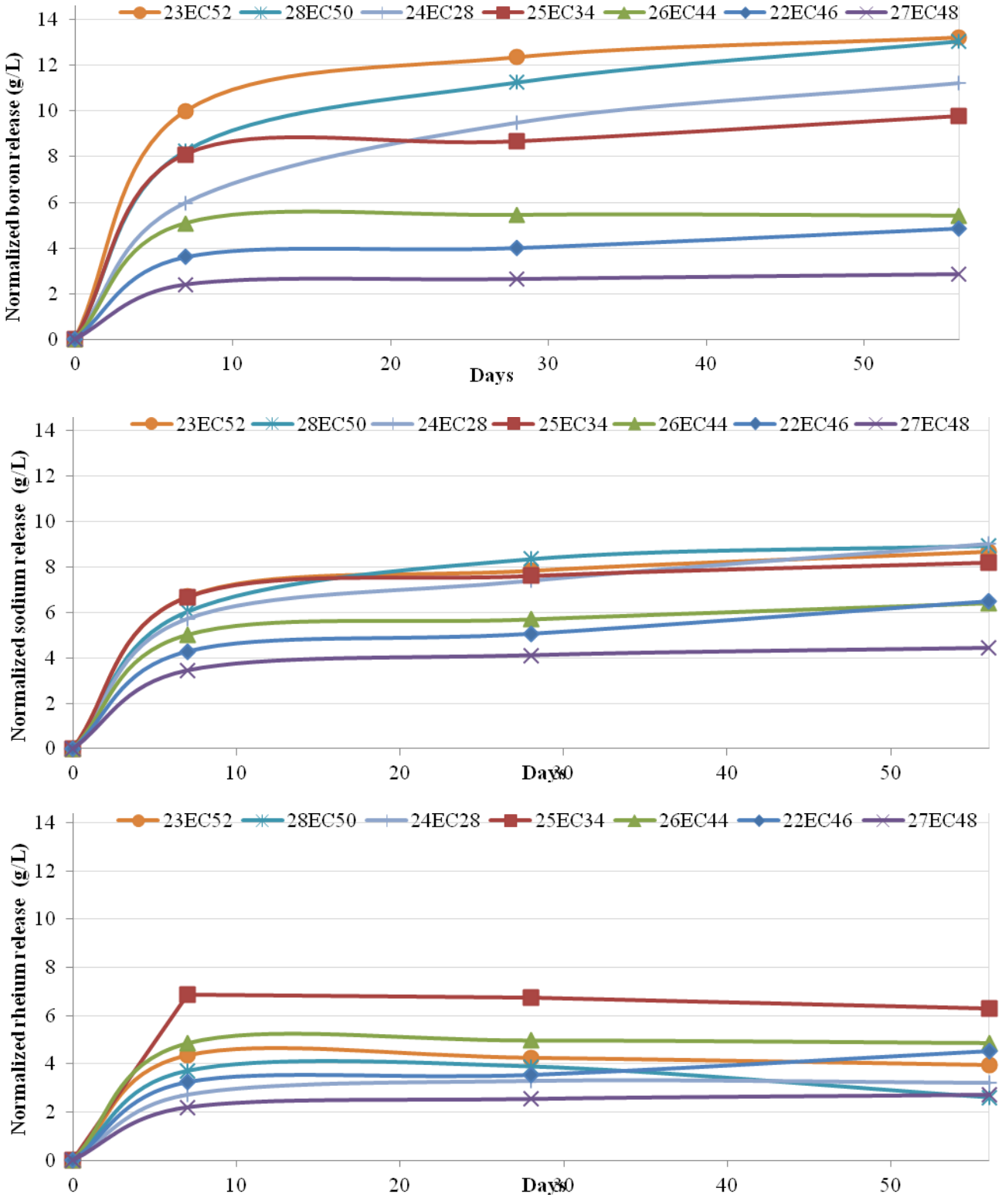

Figure 3.5. PCT normalized releases for boron, sodium, and rhenium as a function of time during the first 56 days of PCT-B for the seven ORLEC glasses in tests ILHE, ILHF, and ILHG at 90 °C and S/V 20,000 m^{-1}.

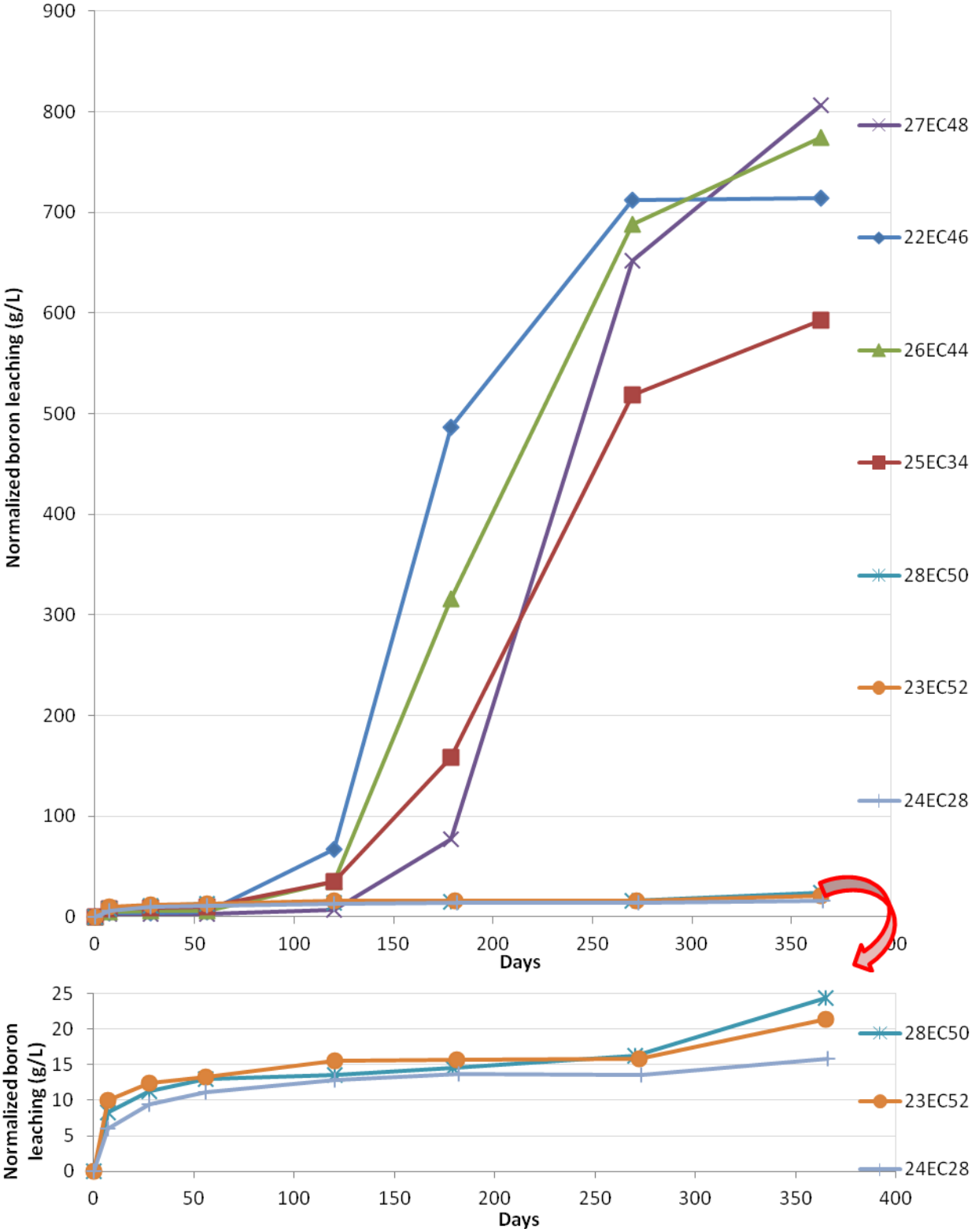

Figure 3.6. PCT boron normalized release as a function of time during the first 365 days of PCT-B for the seven ORLEC glasses in tests ILHE, ILHF, and ILHG at 90 °C and S/V 20,000 m^{-1}.

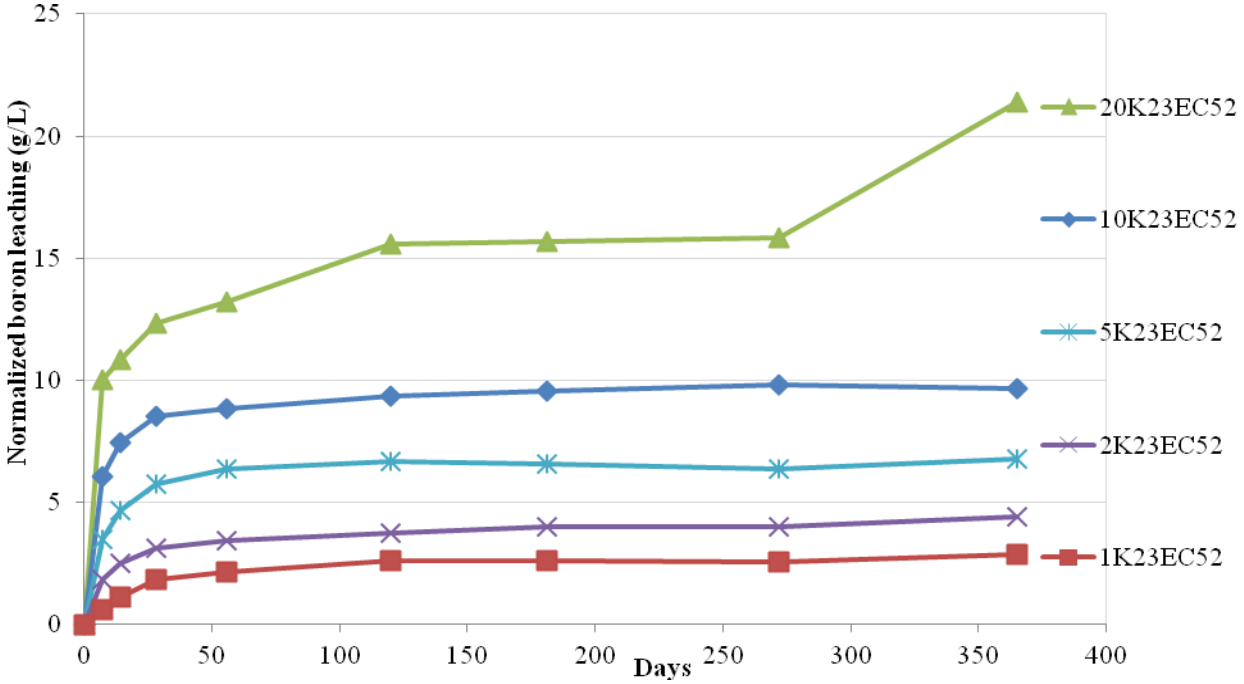

Figure 3.7. Boron normalized release from glass IDF23-EC52CCC in 90 °C PCT-B for one year at five S/V ratios from 1000 m^{-1} to 20,000 m^{-1} (denoted as 1K to 20K).

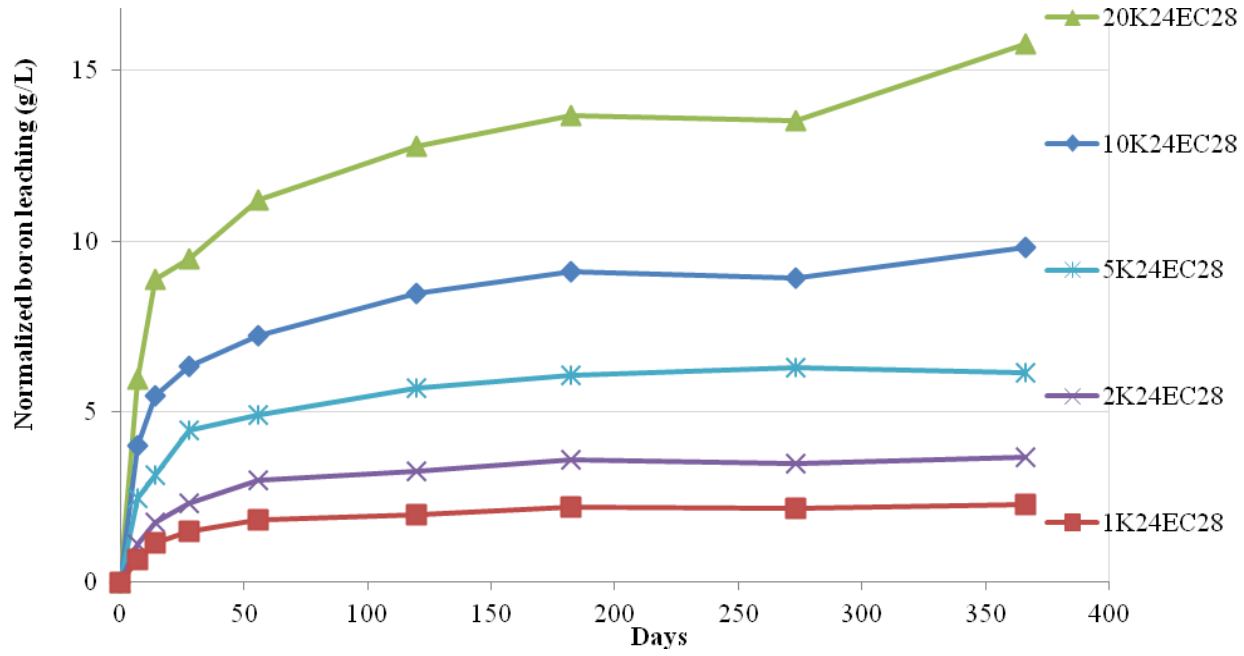

Figure 3.8. Boron normalized release from glass IDF24-EC28CCC in 90 °C PCT-B for one year at five S/V ratios from 1000 m^{-1} to 20,000 m^{-1} (denoted as 1K to 20K).

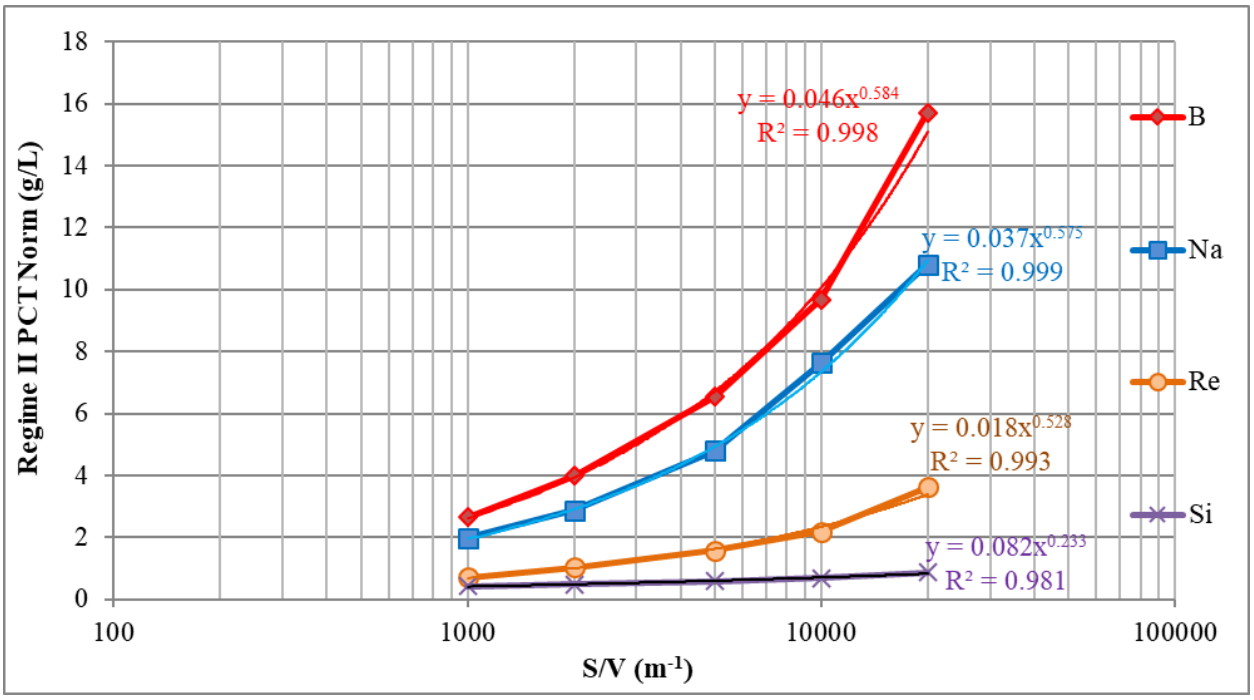

Figure 3.9. Effect of S/V ratio on the region II release of B, Na, Re, and Si from glass IDF23-EC52CCC in 90°C PCT-B between 7-day and 365-day samplings.

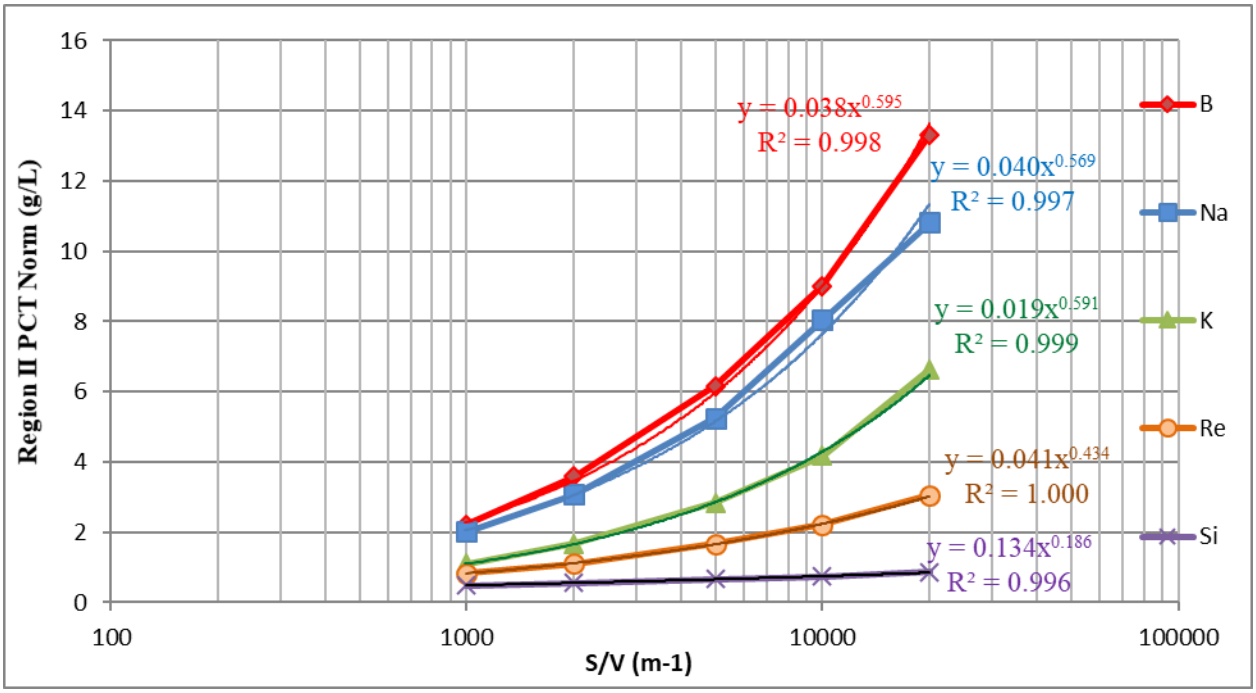

Figure 3.10. Effect of S/V ratio on the region II release of B, Na, K, Re, and Si from glass IDF24-EC28CCC in 90 °C PCT-B between 7-day and 365-day samplings.

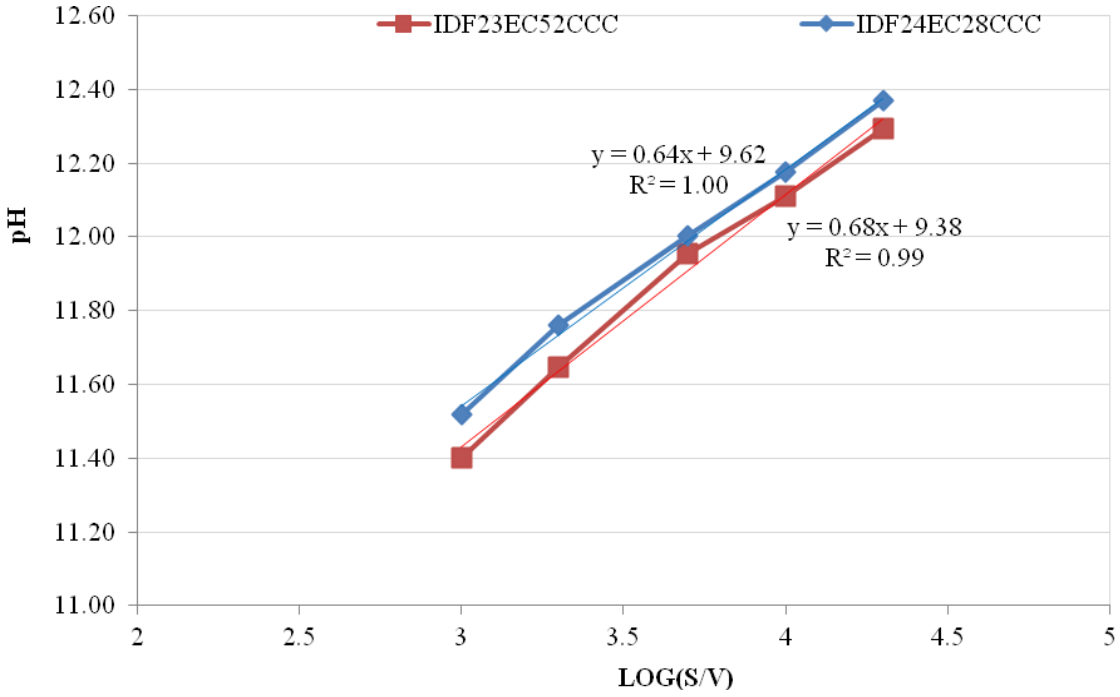

Figure 3.11. Effect of S/V ratio on leachate solution pH from glass IDF24-EC28CCC in 90 °C PCT-B (between 120 and 365-day samplings).

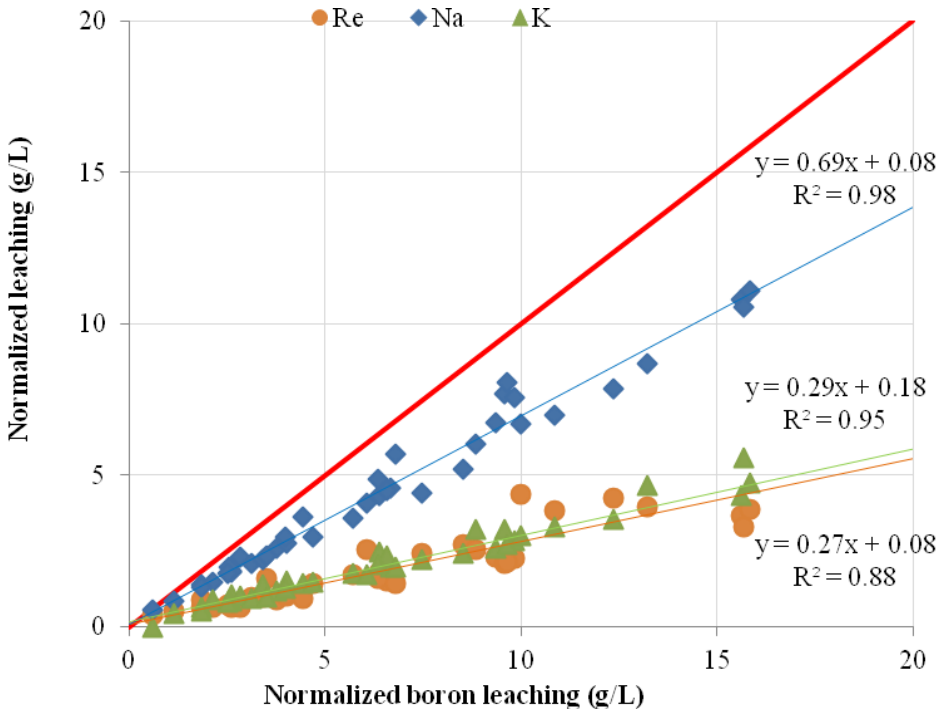

Figure 3.12. Display of deviation from congruence to boron (the red diagonal would be full congruence) for Re, K, and Na in IDF23EC52CCC over 365 days of PCT-B tests.

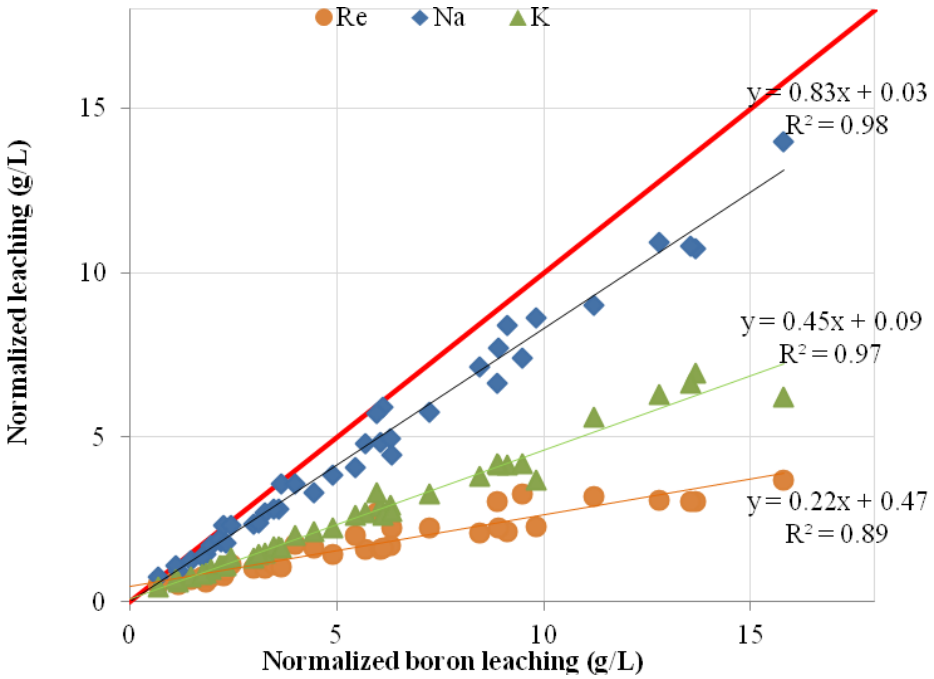

Figure 3.13. Display of deviation from congruence to boron (the red diagonal would be full congruence) for Re, K, and Na in IDF24EC28CCC over 365 days of PCT-B tests.

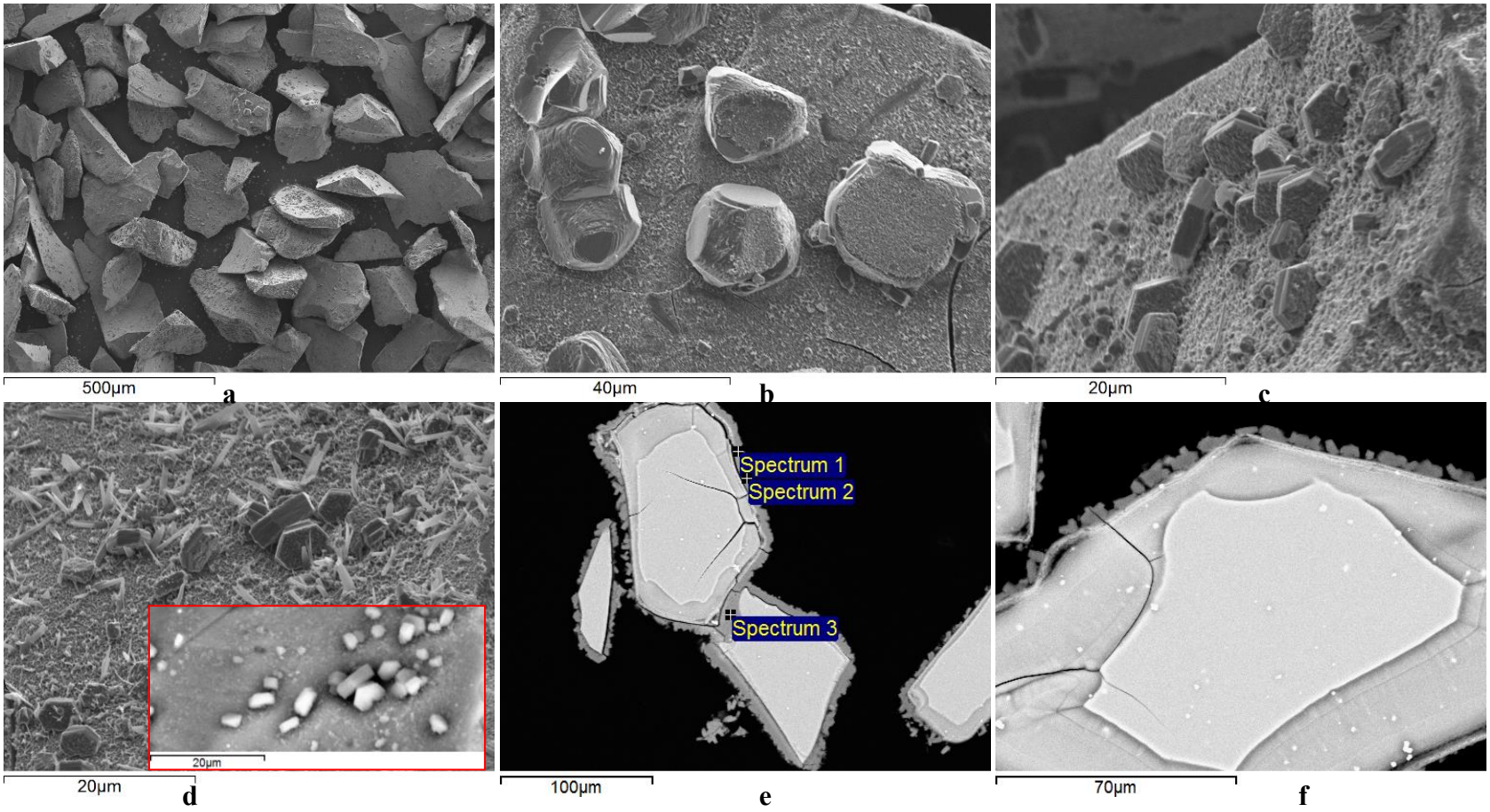

Figure 4.1. SEM micrographs from the surface (a-d) and in cross-section (e-f) of altered IDF Phase 1 glass IDF1-B2CCC subjected to PCT for 2912 days at 90 °C and S/V of 2,000 m^{-1}. Resumption was starting at 2912 days and normalized boron release was at 34 g/L.

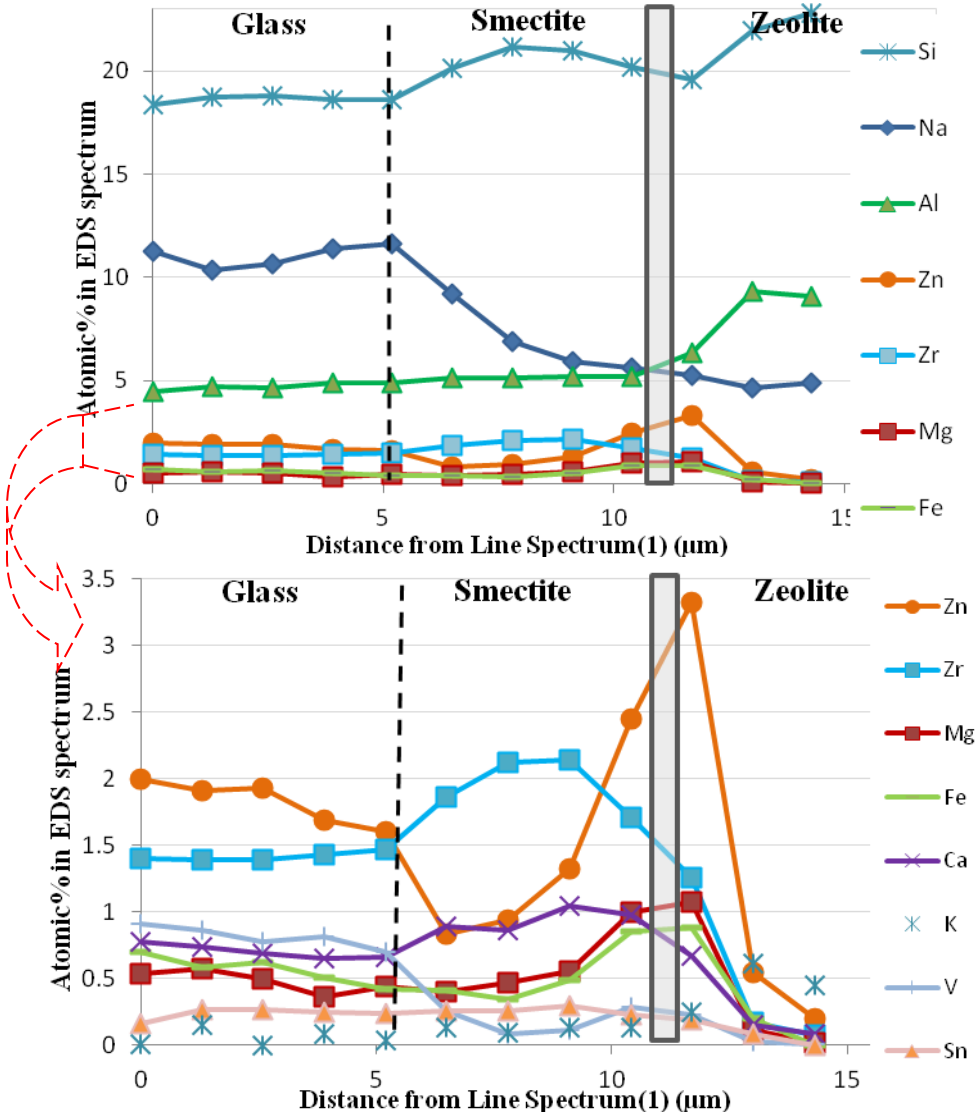

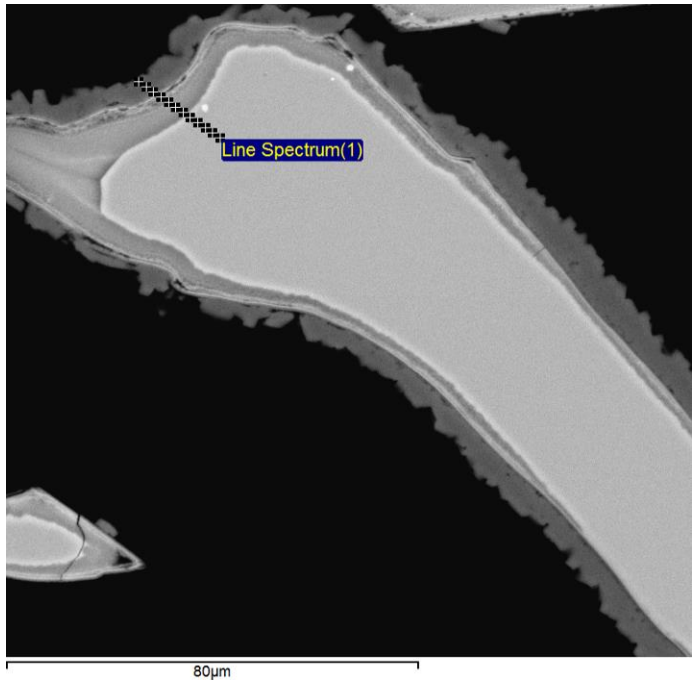

Figure 4.2. SEM micrographs and EDS analyses from the surface of altered IDF Phase 1 glass IDF1-B2CCC subjected to PCT for 2912 days at 90 °C and S/V of 2,000 m^{-1}. The red arrow on the left indicates the part enlarged in the figure below. The gray boxes indicate the demarcation zone between zeolite and smectite.

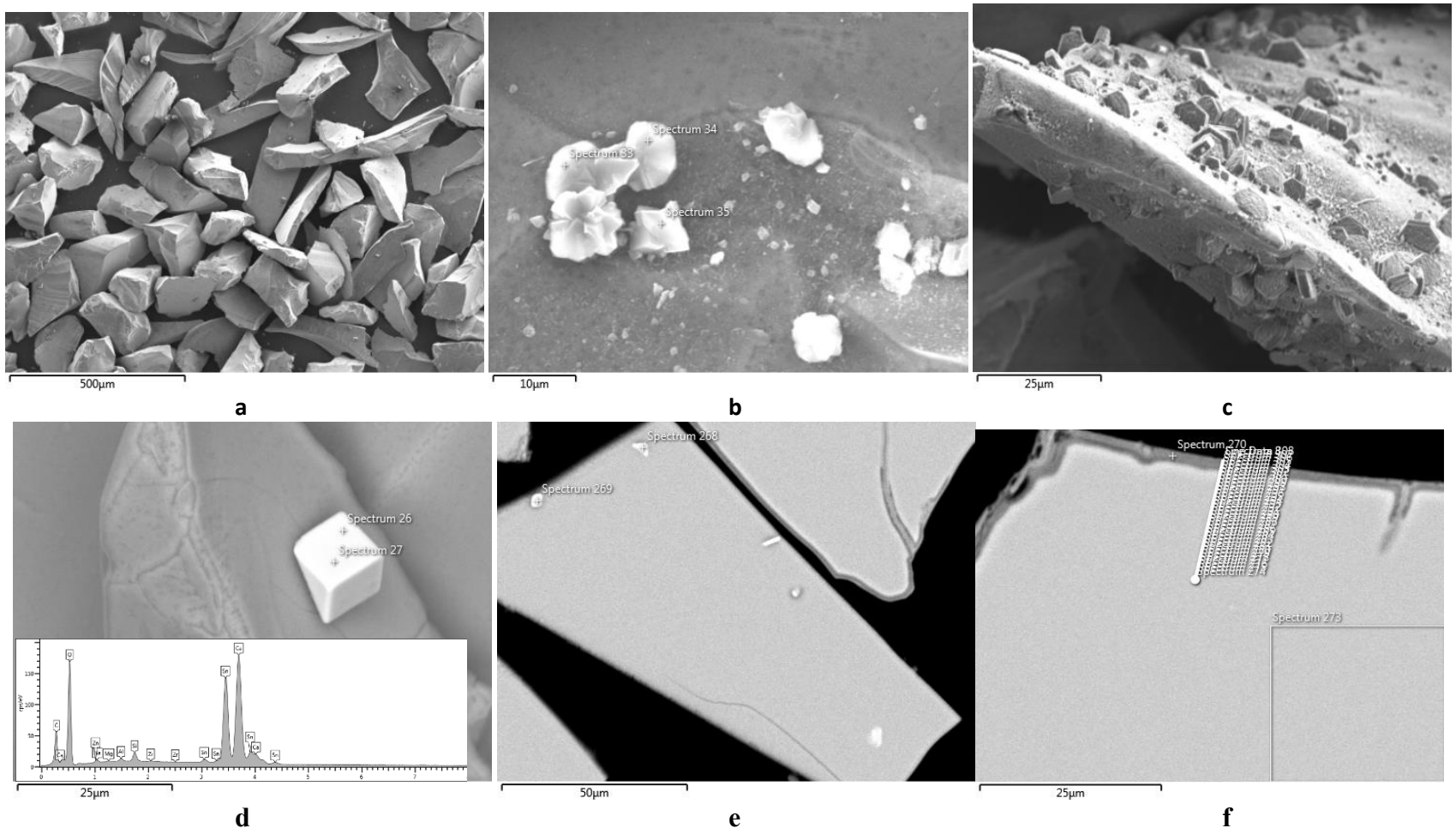

Figure 4.3. SEM Micrographs from the surface (a-d), EDS spectrum insert (d), and cross-section (e-f) of altered IDF Phase 1 glass IDF2-G9CCC at 2912 days. No resumption was observed and normalized boron release is at 6 to 7 g/L.

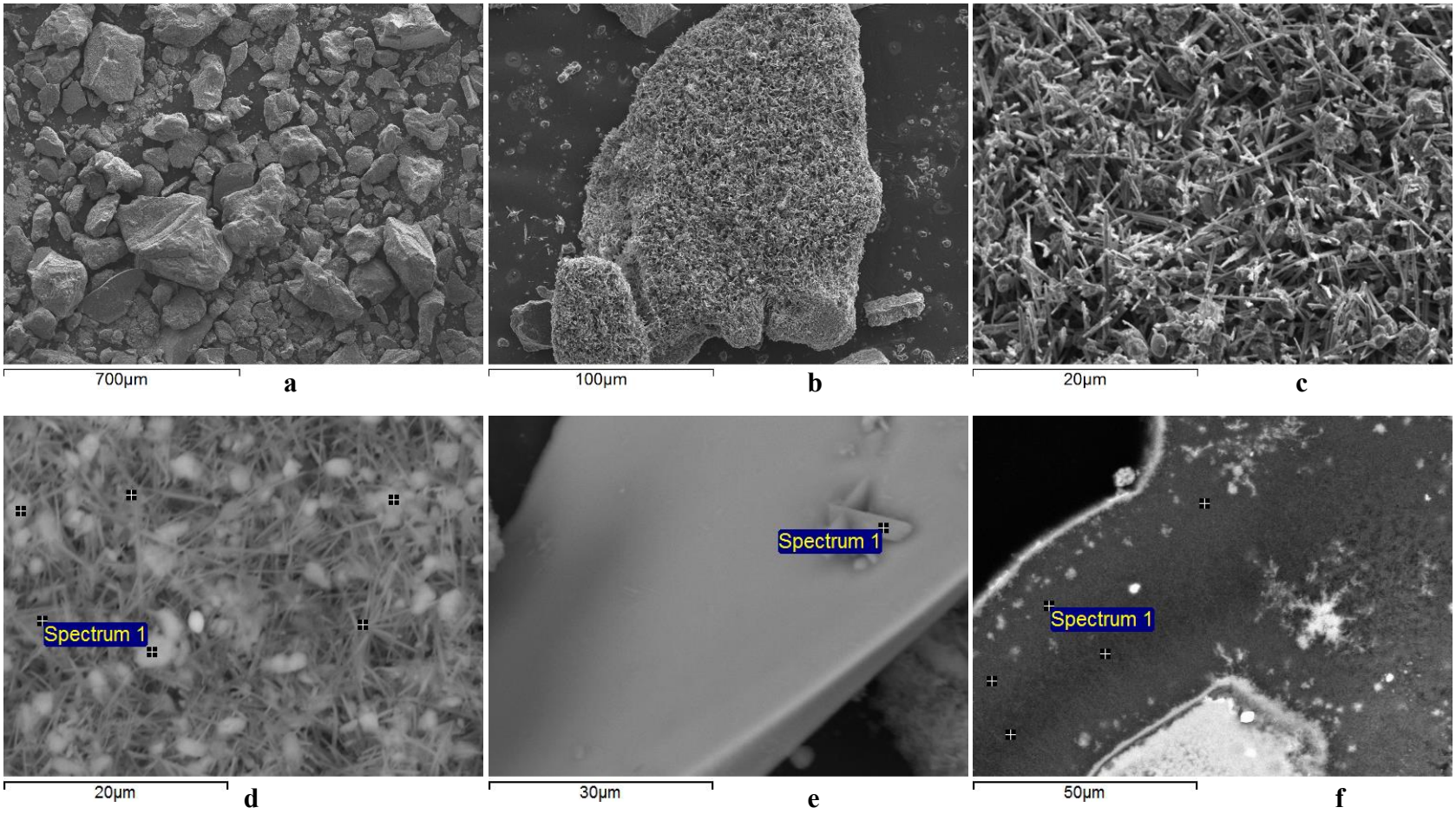

Figure 4.4. SEM micrographs from the surface (a-d) and cross-section (e-f) of altered IDF Phase 1 glass IDF3-F7CCC subjected to PCT for 2912 days at 90 °C and S/V of 2,000 m^{-1}. Resumption was at 2177 days and normalized boron release rose sharply to 88 g/L.

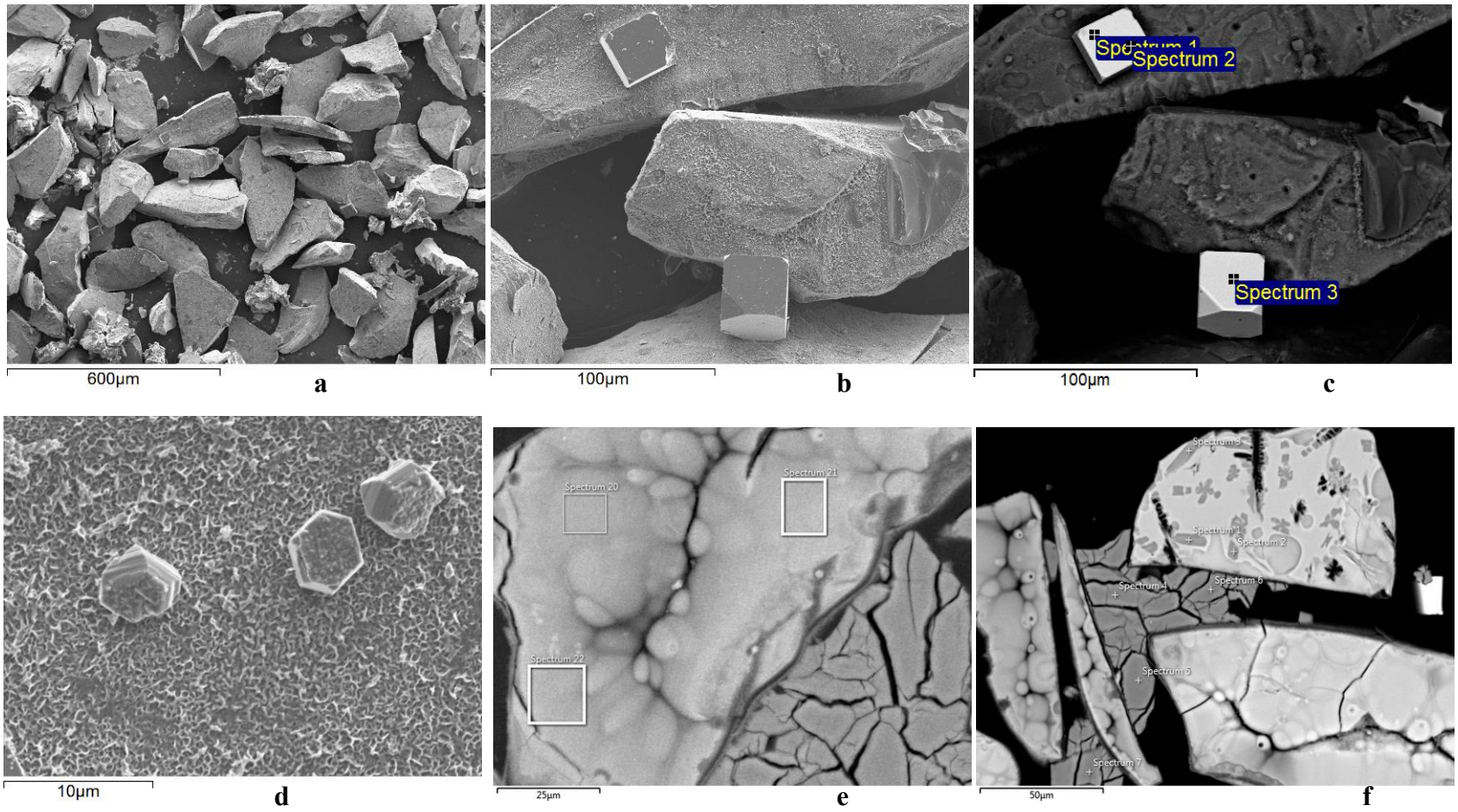

Figure 4.5. SEM micrographs from the surface (a-d) and cross-section (e-f) of altered IDF Phase 1 glass IDF4-A15CCC subjected to PCT for 2886 days at 90 °C and S/V of 2,000 m^{-1}. Resumption was at 1805 days and normalized boron release rose slowly to 80 g/L.

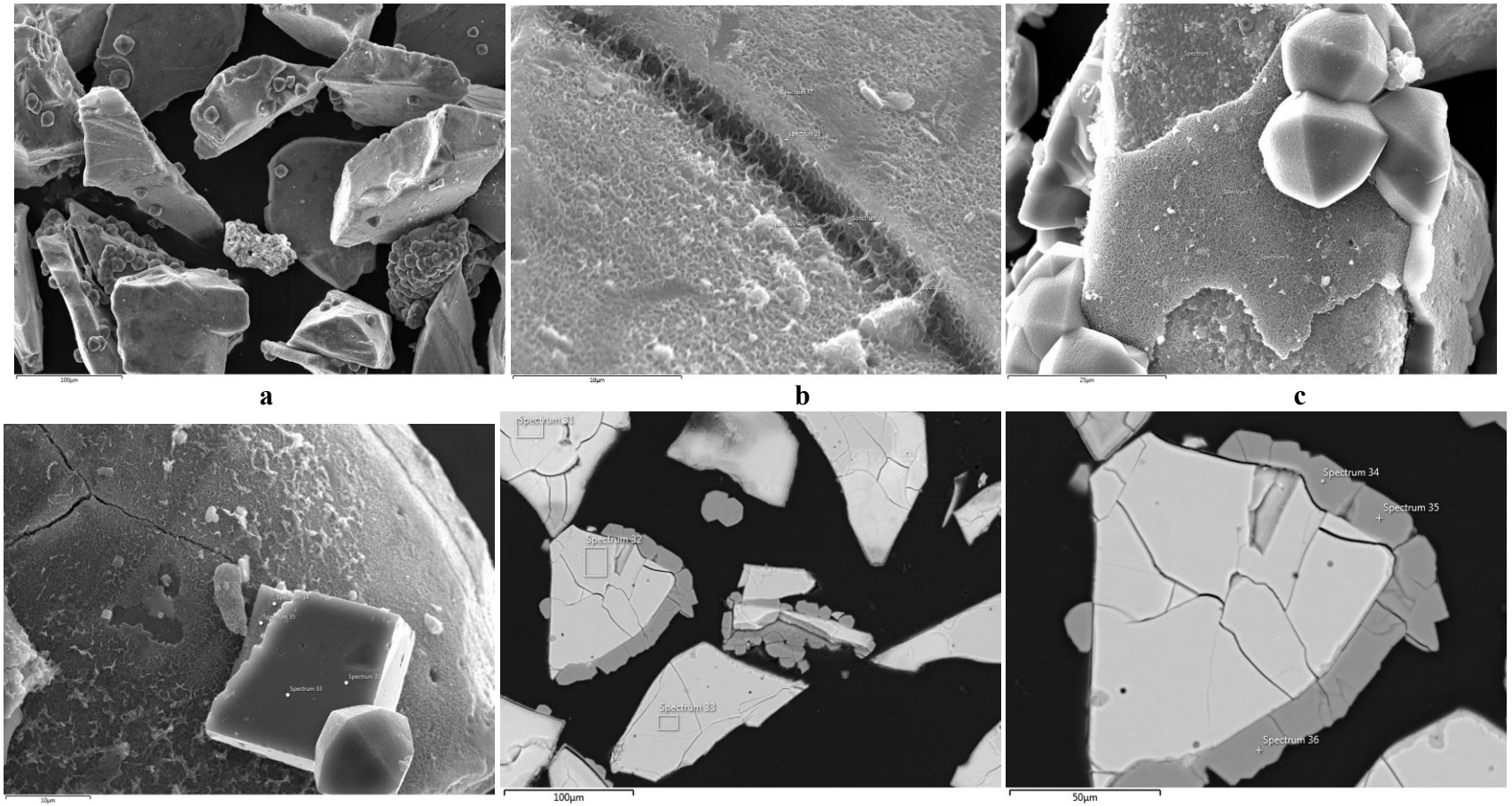

Figure 4.6. SEM micrographs from the surface (a-d) and cross-section (e-f) of altered IDF Phase 1 glass IDF5-A20CCC subjected to PCT for 2886 days at 90 °C and S/V of 2,000 m^{-1}. Resumption appears on-going and normalized boron release is at 24 g/L.

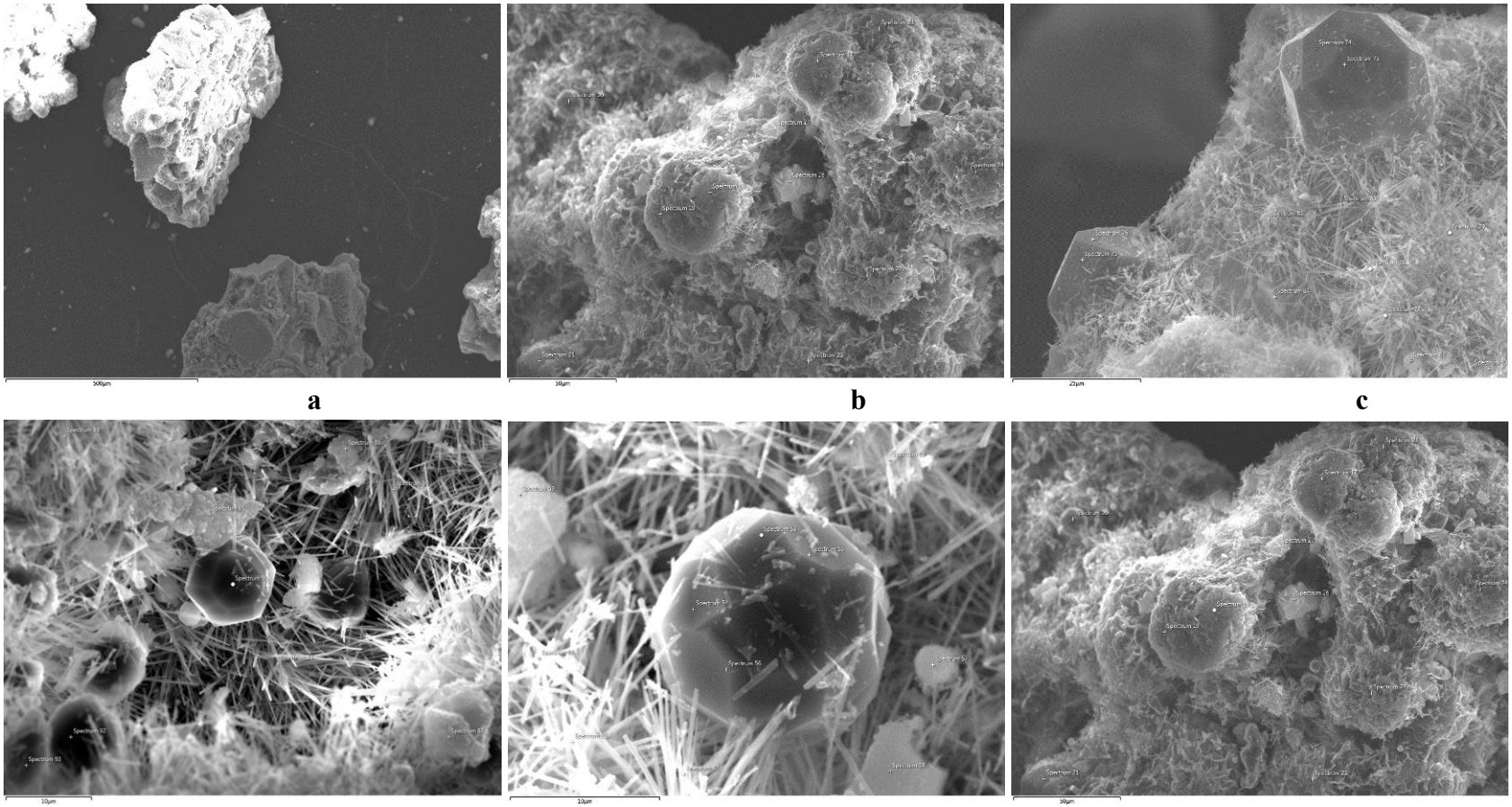

a **b** **c**

d **e** **f**

Figure 4.7. SEM micrographs from the surface of altered IDF Phase 1 glass IDF7-E12CCC subjected to PCT for 2912 days at 90 °C and S/V of 2,000 m^{-1}. Resumption was at 1266 days and normalized boron release rose sharply to 91 g/L. This glass reached full resumption (fully altered based on normalized boron release) over 3 years prior to sampling.

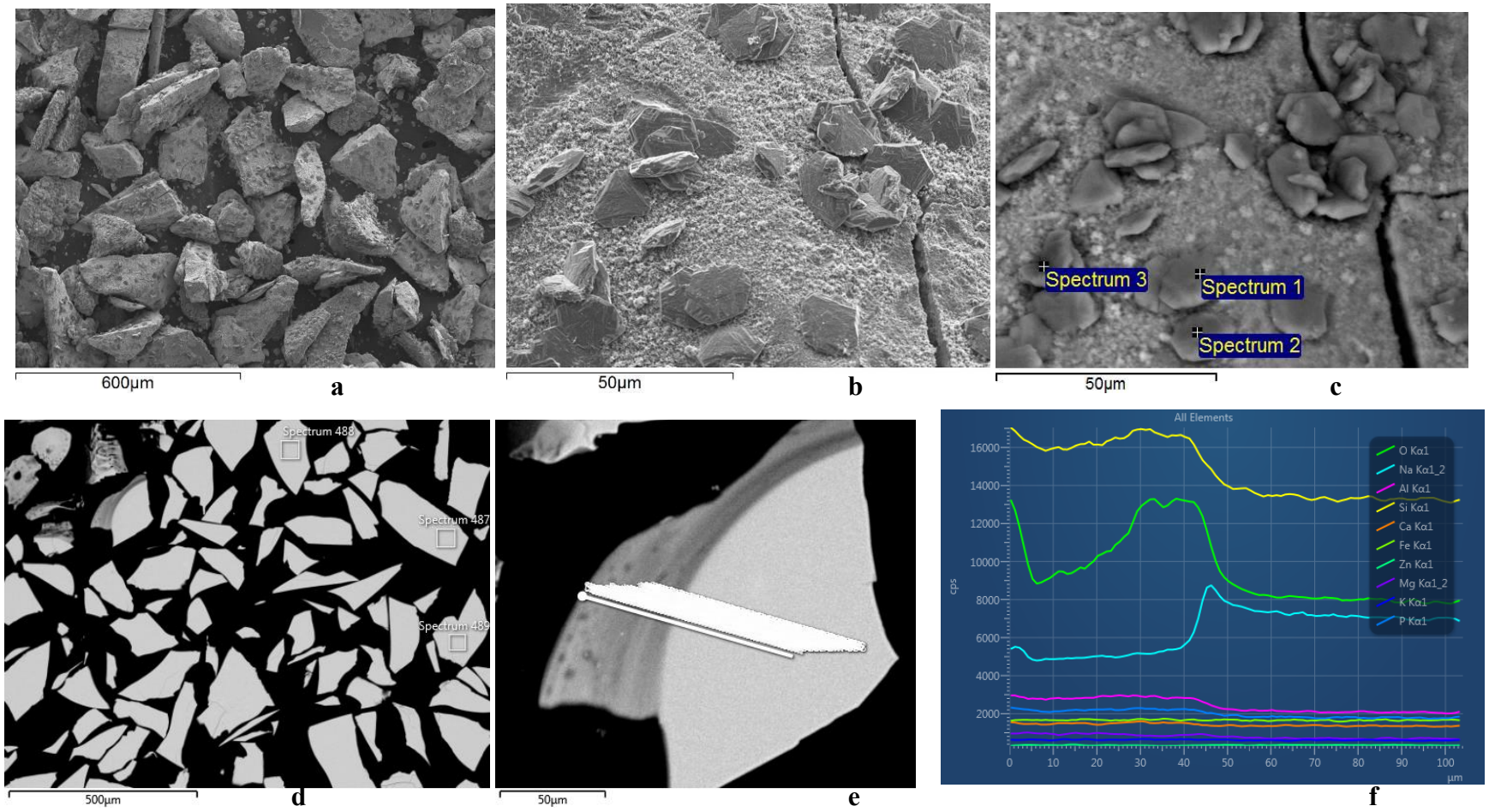

Figure 4.8. SEM micrographs from the surface (a-d) and cross-section (e) of altered IDF Phase 1 glass IDF8-A125CCC subjected to PCT for 2912 days at 90 °C and S/V of 2,000 m^{-1}; (f) shows EDS line scans of the region indicated in (e). Resumption was at 905 days and normalized boron release rose slowly to 86 g/L.

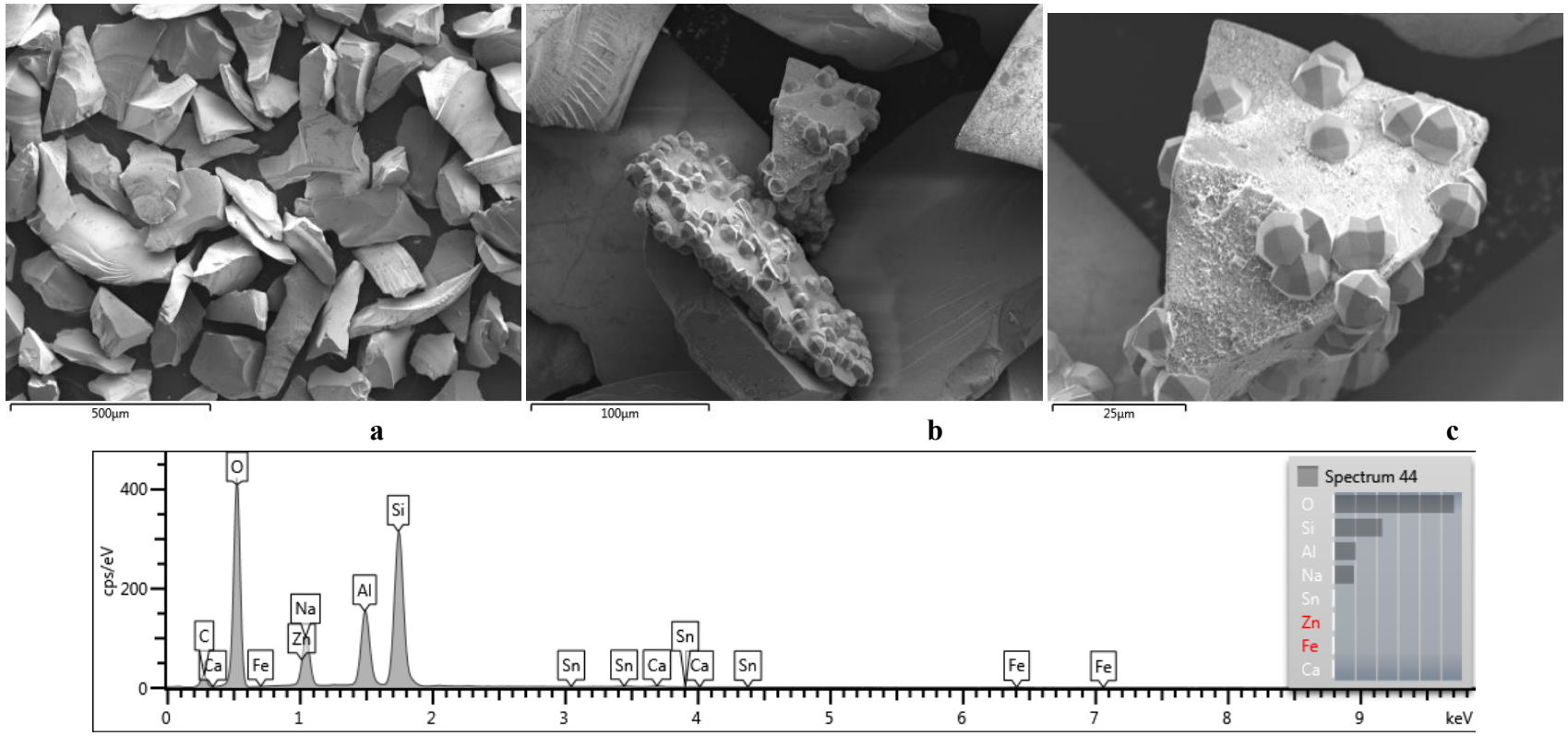

Figure 4.9. SEM micrographs (a-c) and EDS spectra of icositetrahedral analcime from the surface of altered IDF Phase 1 glass IDF10-Zr6CCC days subjected to PCT at 90 °C and S/V of 2,000 m^{-1} at 2886 days. No resumption was observed, and normalized boron release was at 6 to 7 g/L.

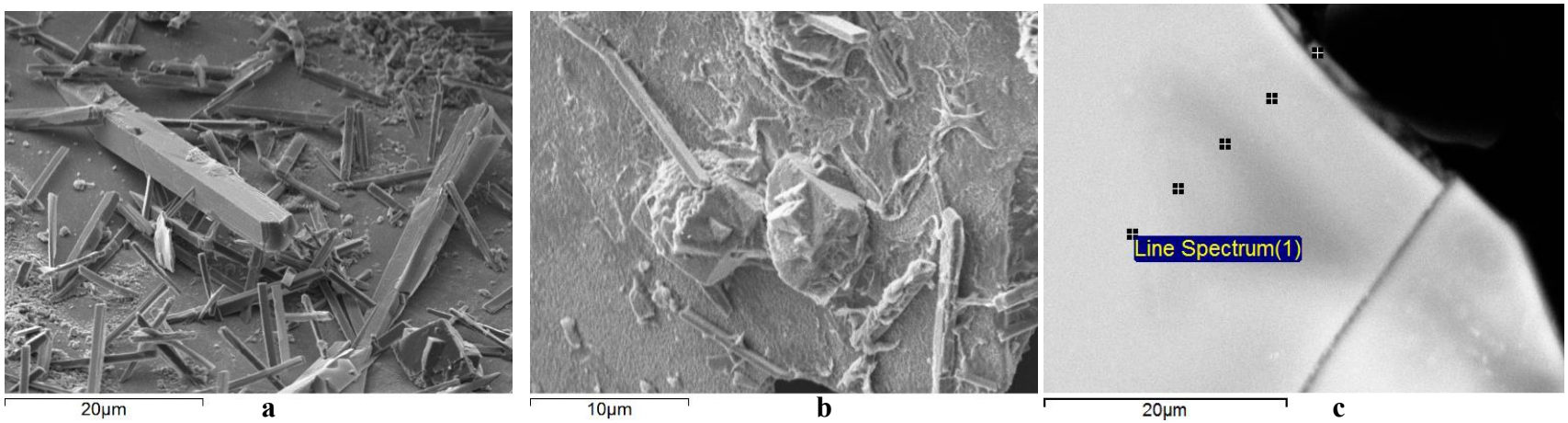

Figure 4.10. SEM micrographs from the surface (a-b) and cross-section (c) of altered IDF Phase 2 glass IDF11-G27CCC subjected to PCT at 90 °C and S/V of 20,000 m^{-1} at 1087 days.

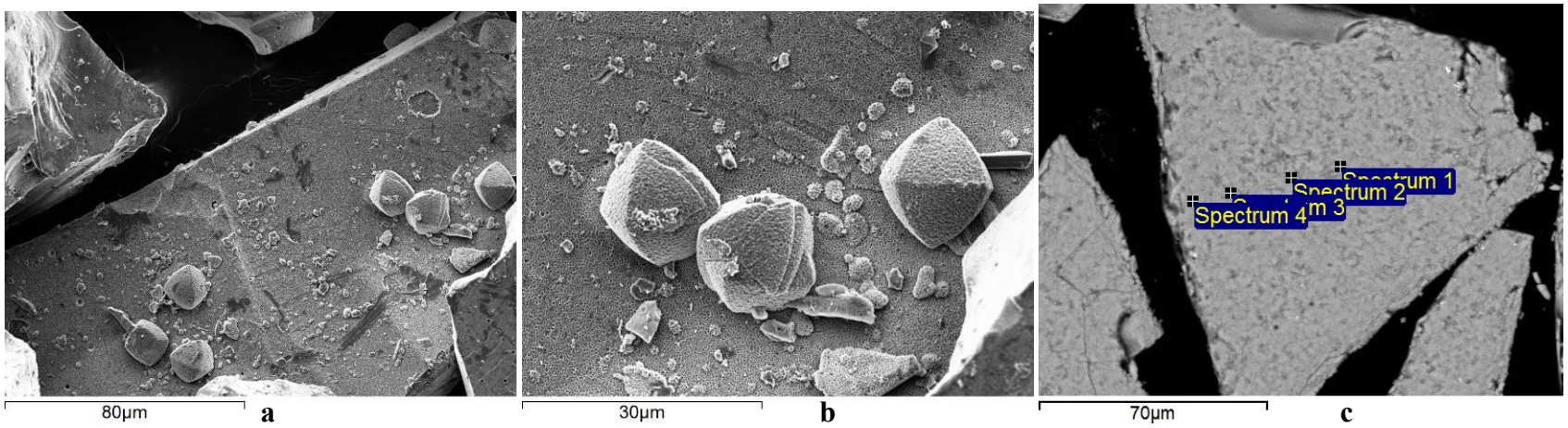

Figure 4.11. SEM micrographs from the surface (a-b) and cross-section (c) of altered IDF Phase 2 glass IDF12-A38CCC subjected to PCT at 90 °C and S/V of 20,000 m^{-1} at 1087 days.

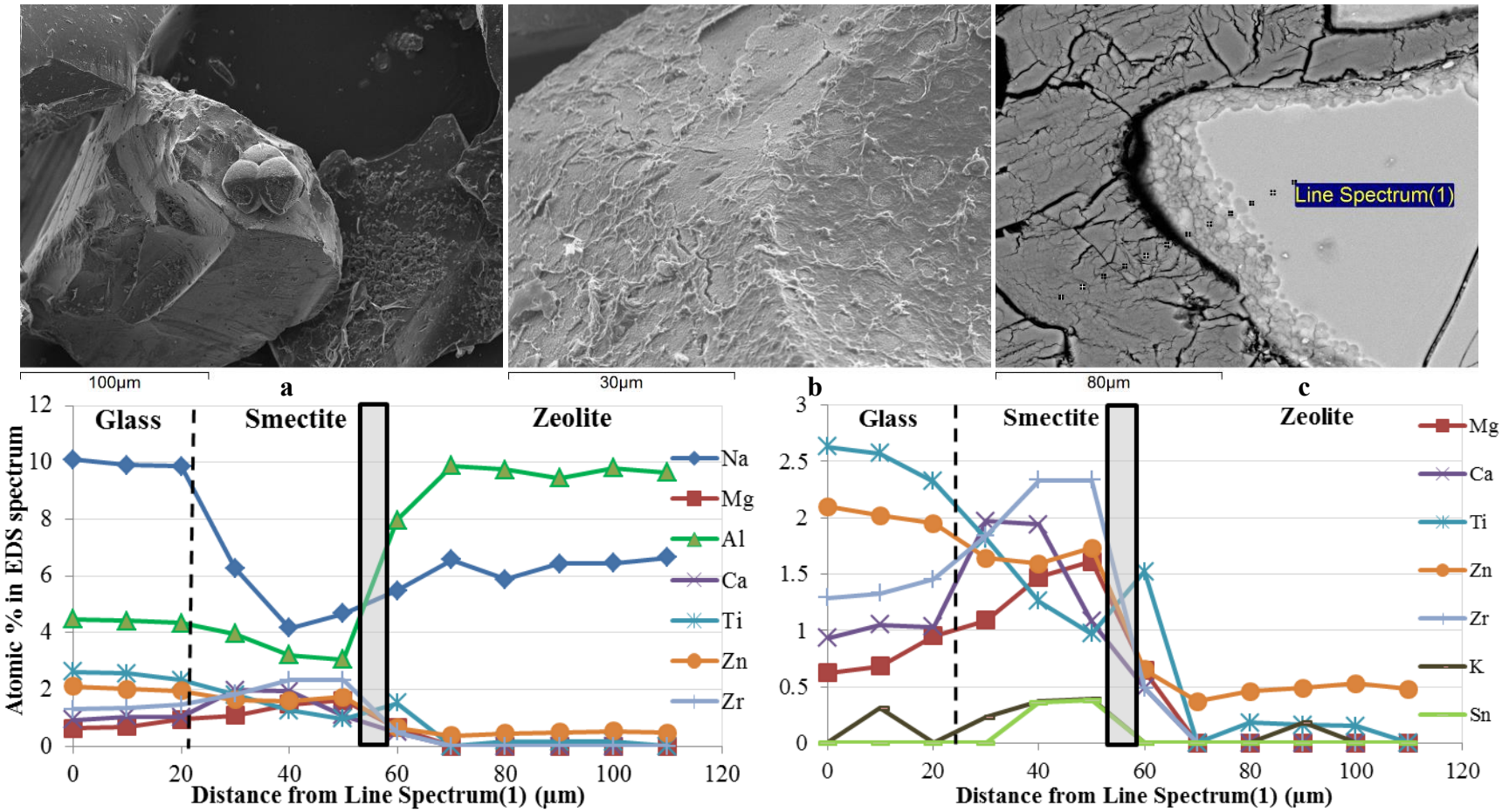

Figure 4.12. SEM micrographs from the surface (a-b) and cross-section (c) and EDS analyses of altered IDF Phase 2 glass IDF13-A51CCC subjected to PCT at 90 °C and S/V of 20,000 m^{-1} at 1087 days. The plot at right is an enlargement of the plot at left to show the lower concentration constituents, and the grey box is positioned where a gap is seen in the SEM image.

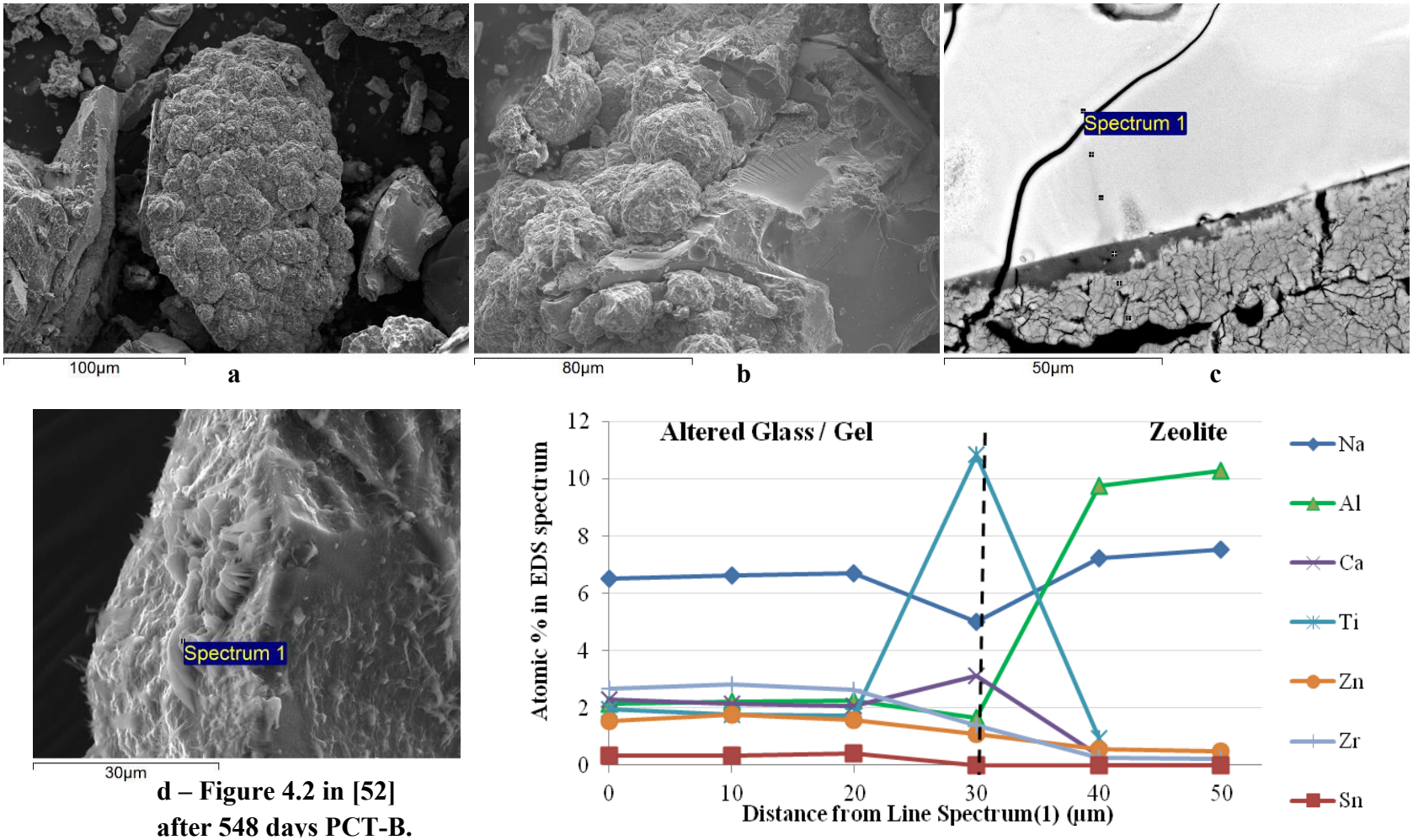

Figure 4.13. SEM micrographs from the surface (a-b) and cross-section (c), and EDS analyses of altered IDF Phase 2 glass IDF14-A59CCC subjected to PCT at 90 °C and S/V of 20,000 m^{-1} at 1087 days. It is compared to (d) from [52] at an earlier sampling, when phillipsite was in early stage of crystallization.

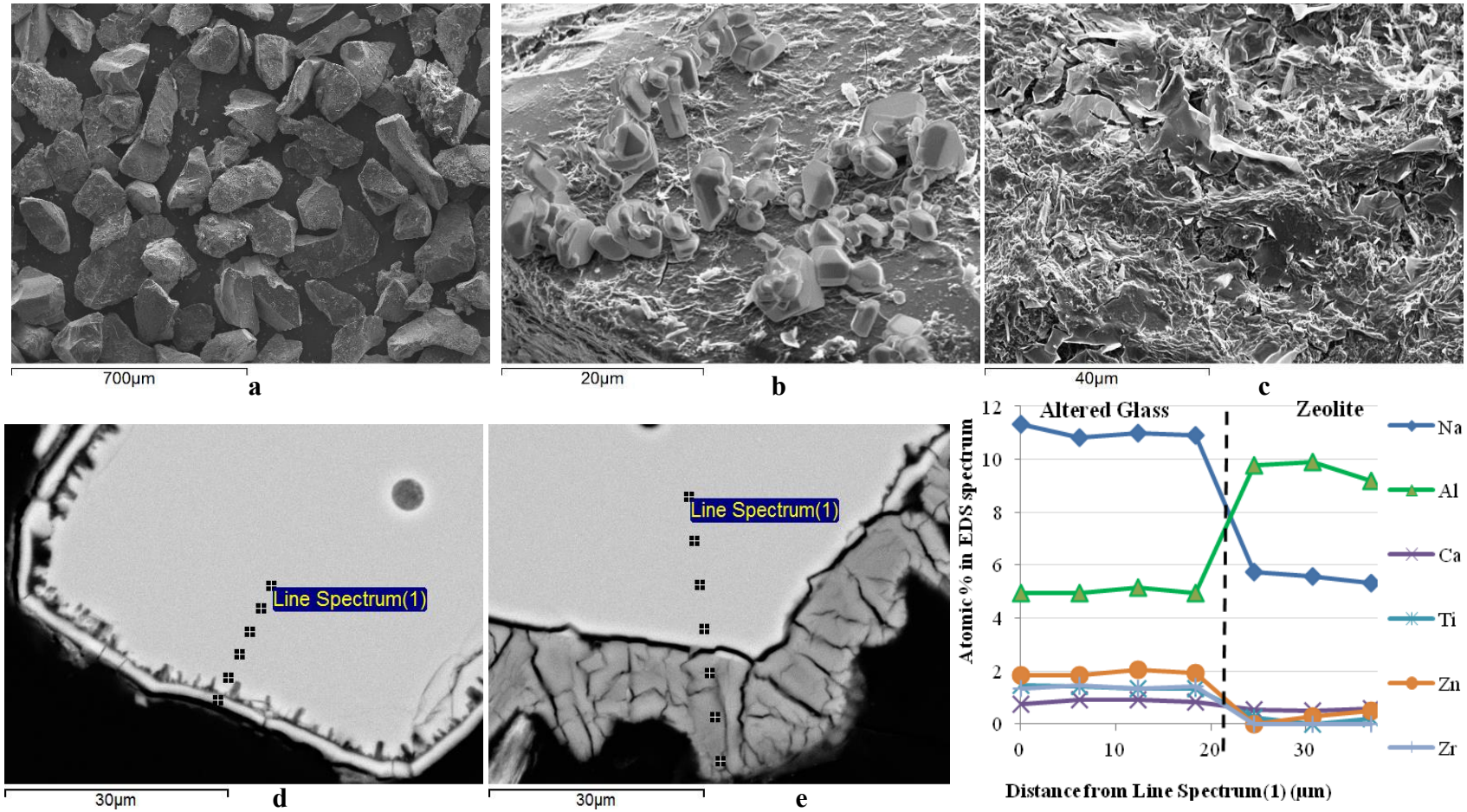

Figure 4.14. SEM micrographs from the surface (a-c), cross-section (d-e) and of EDS analyses (e) for altered Phase 2 glass IDF15-A57CCC subjected to PCT at 90 °C and S/V of 20,000 m^{-1} at 1087 days.

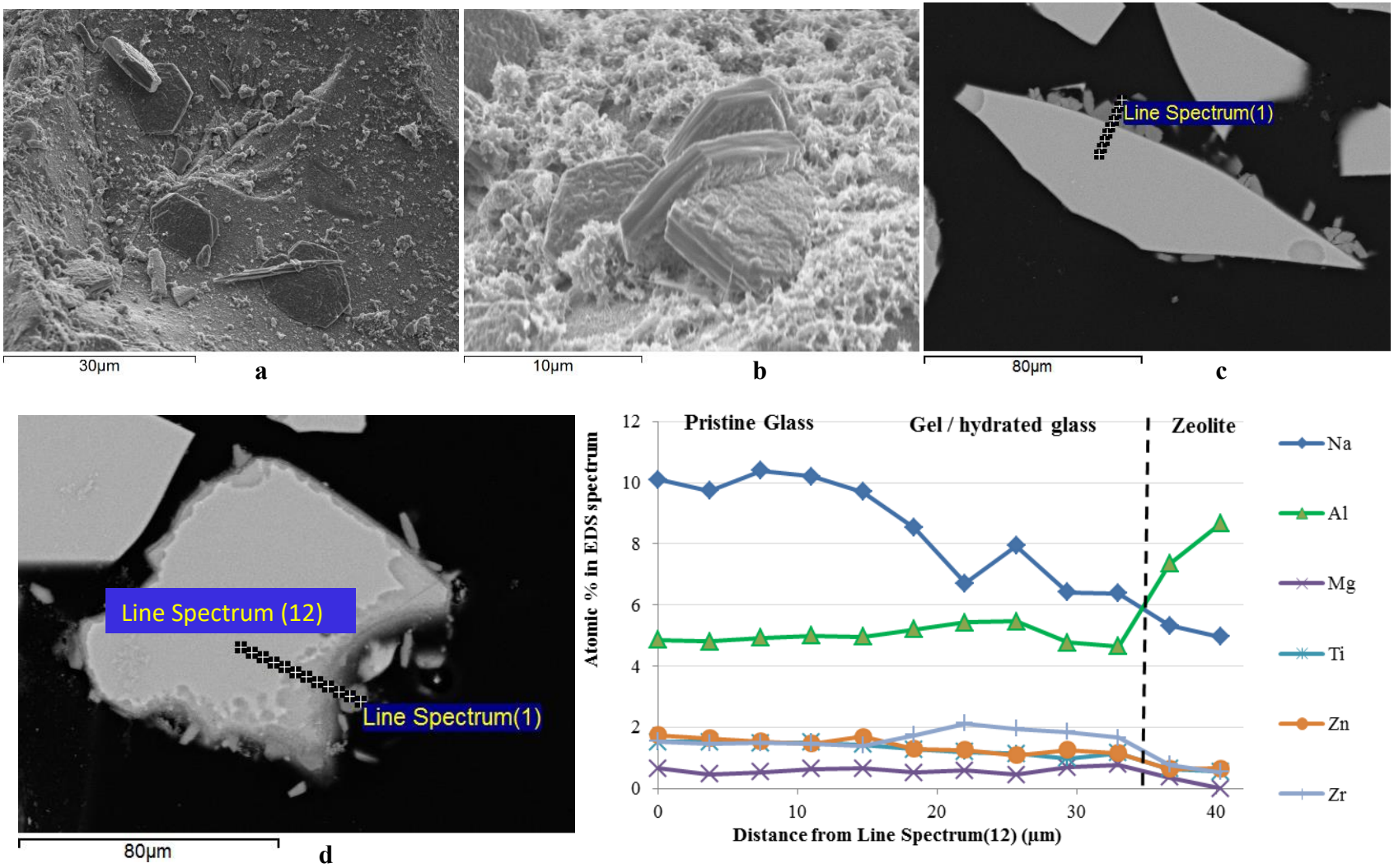

Figure 4.15. SEM micrographs from the surface (a-b), cross-section (c-d) and of EDS analyses of altered IDF Phase 2 glass IDF16-A58CCC subjected to PCT at 90 °C and S/V of 20,000 m^{-1} at 1087 days.

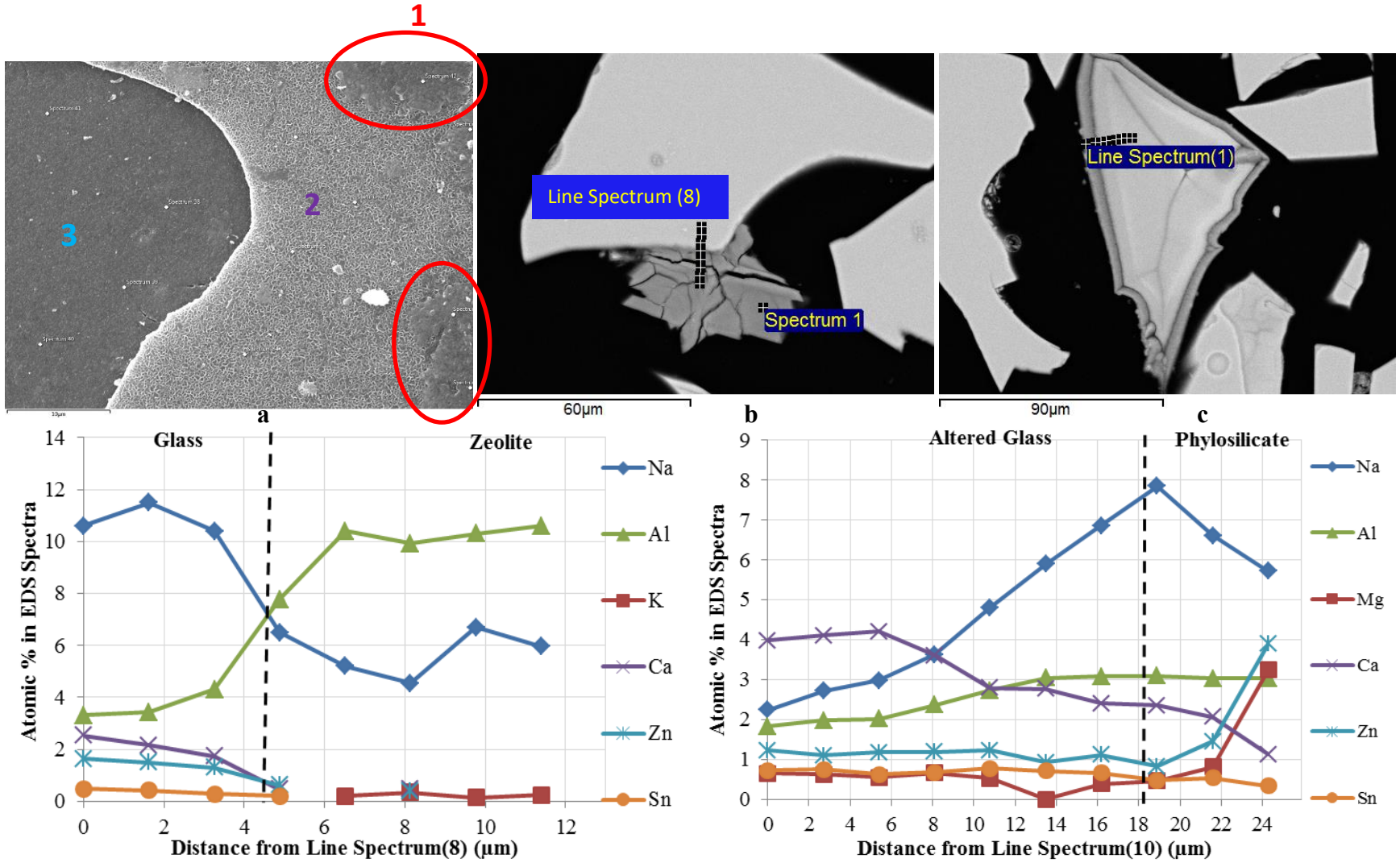

Figure 4.16. SEM micrographs from the surface (a), cross-section (b-c) and EDS analyses of altered IDF Phase 2 glass IDF17-A60CCC subjected to PCT at 90 °C and S/V of 20,000 m^{-1} at 1087 days. Three layers are identified in (a): 1- the outer most layer in the red circles, 2- the middle layer and 3- the inner layer closest to the glass.

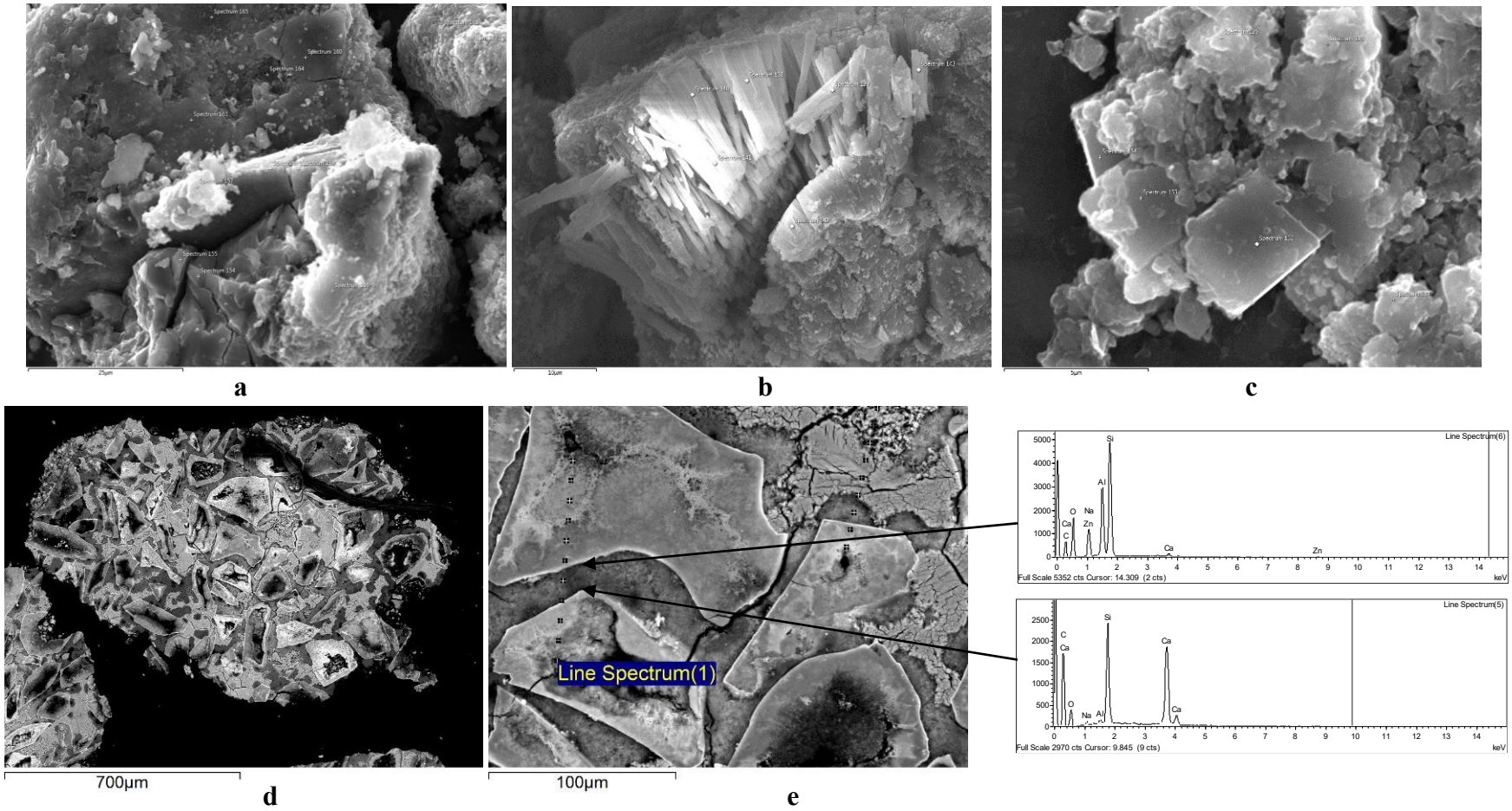

Figure 4.17. SEM micrographs from the surface (a-b) and cross-section (d-e) of altered IDF Phase 2 glass IDF18-A161CCC subjected to PCT for 3 years at 90 °C and S/V of 20,000 m^{-1}, about two years after it reached resumption.

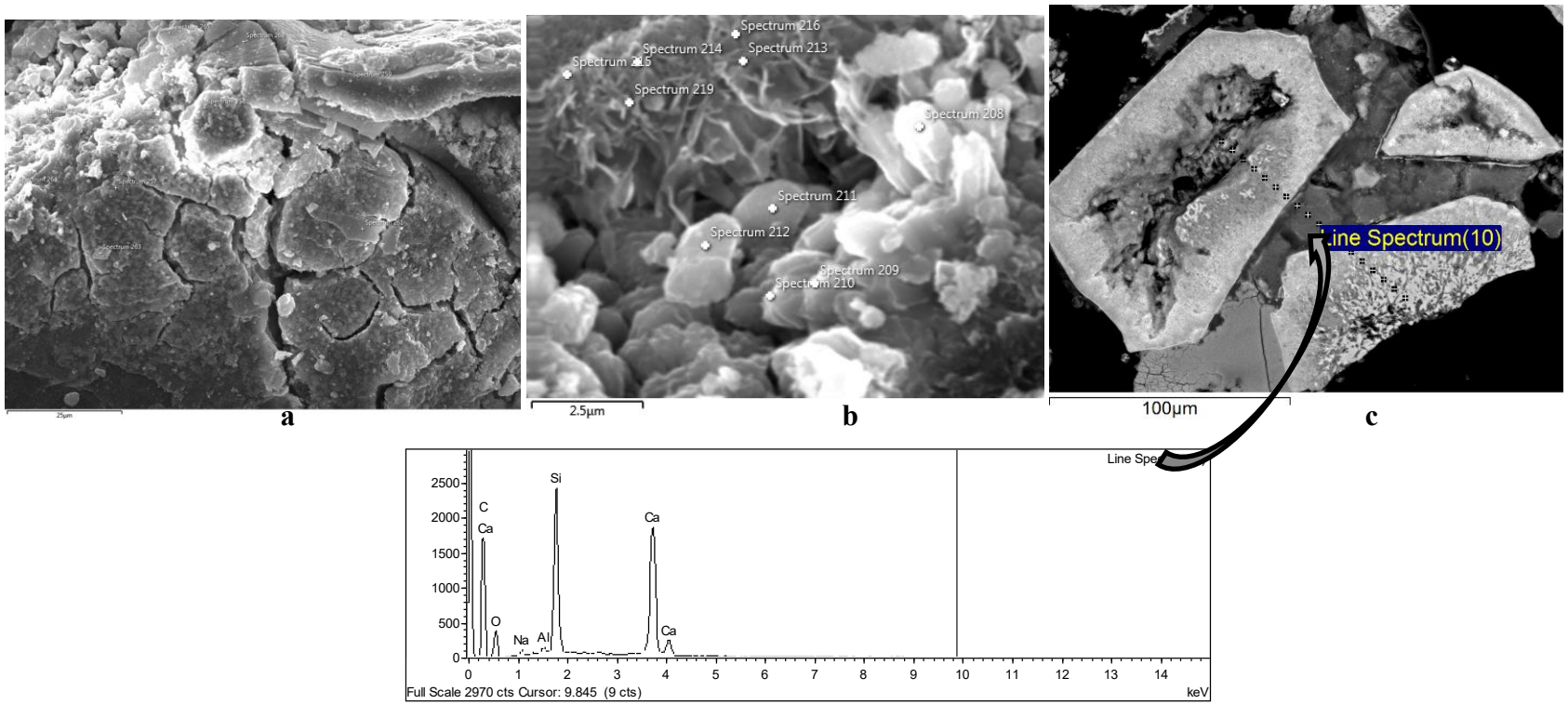

Figure 4.18. SEM micrographs from the surface (a-b) and cross-section (c) of IDF Phase 2 glass IDF19-C100CCC subjected to PCT for 3 years at 90 °C and S/V of 20,000 m^{-1}, about two years after it reached resumption.

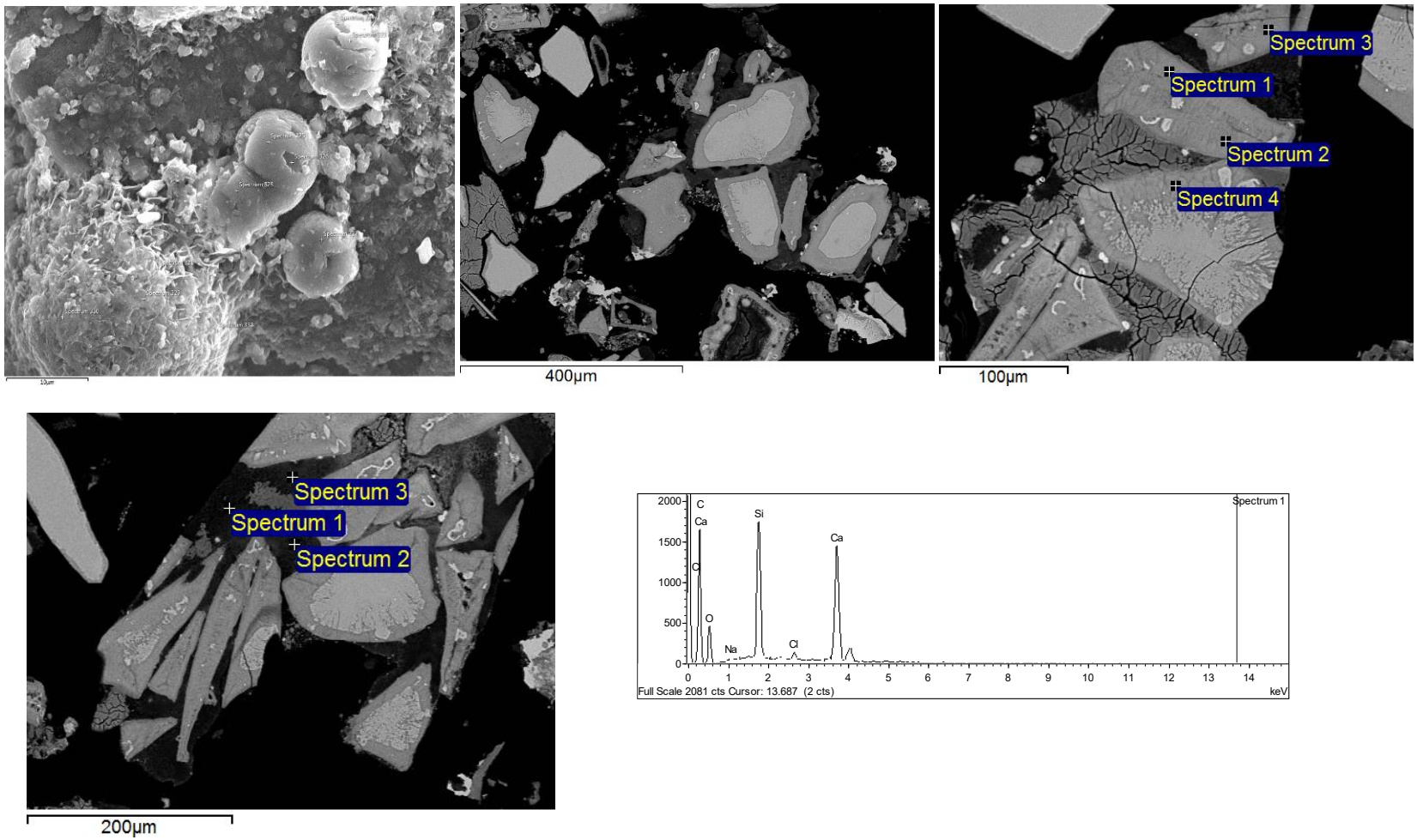

Figure 4.19. SEM micrographs from the surface (a) and cross-section (b-c) of IDF Phase 2 glass IDF20-F6CCC subjected to PCT for 3 years at 90 °C and S/V of 20,000 m^{-1}, about two years after it reached resumption.

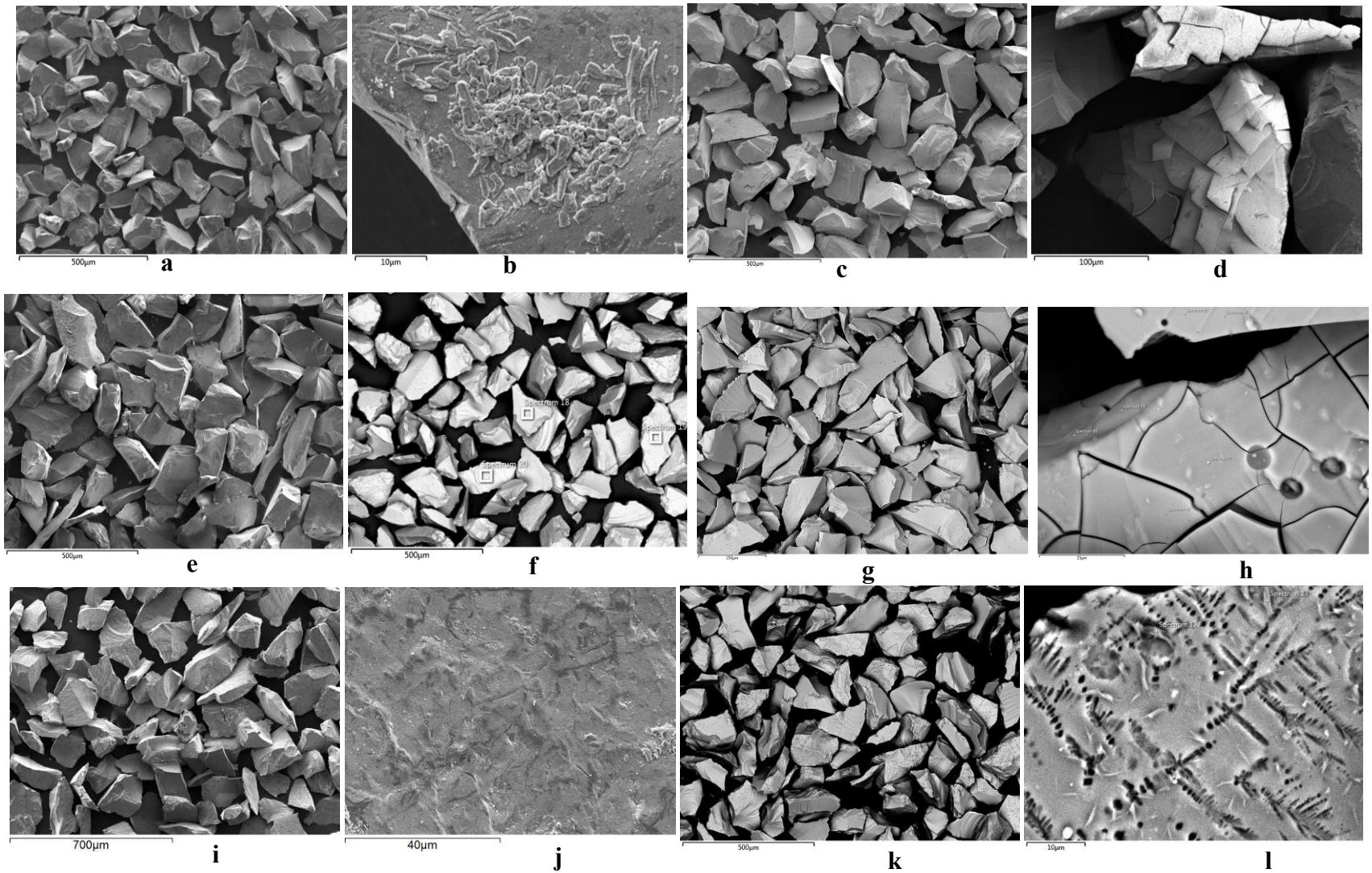

Figure 4.20. SEM micrographs from the surface of IDF Phase 2 glasses IDF1-B2CCC (a,b), IDF2G9CCC (c, d), IDF3F7CCC (e), IDF4A15CCC (f), IDF5A20CCC (g, h), IDF6D6CCC (i, j), IDF7E12CCC (k, l), subjected to PCT for 8 years at 40 °C and S/V of 2,000 m^{-1}.

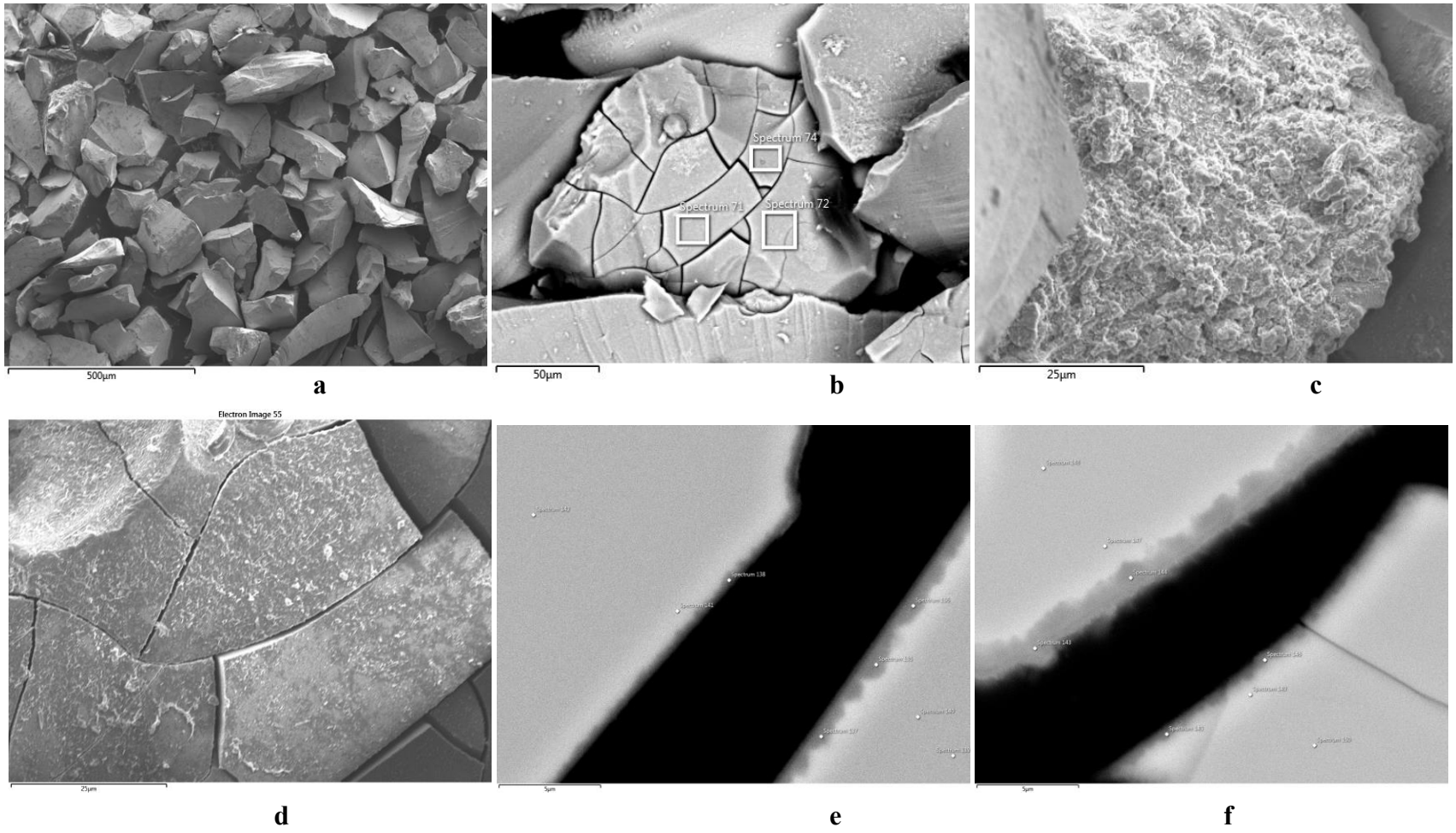

Figure 4.21. SEM micrographs from the surface (a-d) and cross-section (e-f) of IDF Phase 2 glass IDF8-A125CCC subjected to PCT for 8 years at 40 °C and S/V of 2,000 m^{-1}.

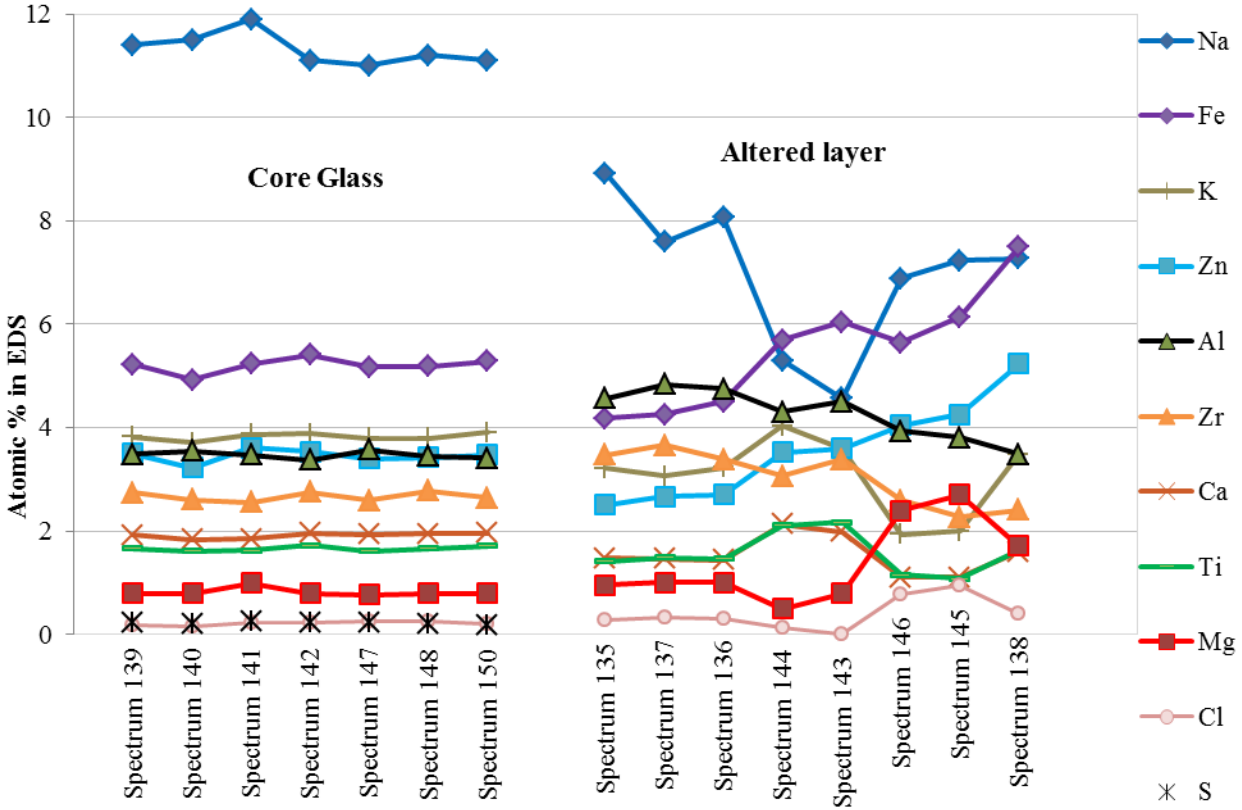

Figure 4.22. EDS analyses from the cross-section shown in Figure 4.21 e-f of IDF Phase 2 glass IDF8-A125CCC subjected to PCT for 8 years at 40 °C and S/V of 2,000 m^{-1} (spectrum numbers can be seen in Figures 4.21 e, f at high magnification)

Appendix A1. Percent Relative Standard Deviation of Triplicates in Long-Term PCT-B Results at 90 °C and S/V of 20,000 m^{-1} (Tests ILHC and ILHD).

Glass ID	Test	Immersion Date	Sampling Date	Period	%RSD measured on triplicate PCT results					
					pH	B	K	Li	Na	Si
IDF11-G27CCC	ILHC	6/9/2015	6/16/2015	7	0.1%	0.7%	1.2%	-	1.9%	0.9%
			7/7/2015	28	0.1%	0.4%	0.2%	-	2.4%	0.1%
			8/4/2015	56	0.1%	0.9%	0.6%	-	0.4%	0.6%
			10/6/2015	119	0.1%	0.9%	0.5%	-	0.8%	0.4%
			12/8/2015	182	0.1%	0.8%	0.2%	-	1.2%	0.1%
			3/8/2016	273	0.1%	0.9%	0.7%	-	1.3%	0.4%
			6/7/2016	364	0.1%	1.0%	0.6%	-	3.2%	0.6%
			12/8/2016	548	0.2%	2.2%	2.3%	-	0.7%	1.4%
			6/8/2017	730	0.1%	1.4%	0.4%	-	1.0%	2.1%
			12/8/2017	913	0.2%	2.1%	2.1%	-	0.7%	1.0%
			2/13/2019	1345	0.1%	2.5%	2.2%	-	2.8%	1.0%
			5/28/2019	1449	0.1%	0.5%	0.3%	-	5.1%	1.2%
IDF12-A38CCC	ILHC	6/9/2015	6/16/2015	7	0.1%	0.2%	0.4%	-	0.8%	0.3%
			7/7/2015	28	0.1%	0.4%	1.3%	-	0.9%	0.4%
			8/4/2015	56	0.1%	0.3%	1.2%	-	0.6%	0.3%
			10/6/2015	119	0.1%	0.6%	1.2%	-	0.4%	0.7%
			12/8/2015	182	0.1%	0.3%	2.3%	-	0.5%	0.2%
			3/8/2016	273	0.1%	0.5%	1.0%	-	1.3%	0.5%
			6/7/2016	364	0.1%	2.9%	2.2%	-	4.5%	2.3%
			12/8/2016	548	0.2%	1.4%	0.4%	-	0.7%	2.0%
			6/8/2017	730	0.2%	4.4%	0.8%	-	0.3%	1.7%
			12/8/2017	913	0.2%	1.0%	0.2%	-	4.1%	1.4%
			5/31/2018	1087	0.1%	0.3%	0.1%	-	3.6%	0.6%
			2/13/2019	1345	0.1%	1.7%	1.4%	-	3.7%	1.5%
			5/28/2019	1449	0.1%	2.3%	16.5%	-	1.0%	1.4%
IDF13-A51CCC	ILHC	6/9/2015	6/16/2015	7	0.1%	0.4%	0.4%	-	0.7%	0.8%
			7/7/2015	28	0.2%	0.3%	1.7%	-	0.4%	0.4%
			8/4/2015	56	0.2%	0.9%	1.5%	-	1.5%	0.3%
			10/6/2015	119	0.1%	0.6%	0.4%	-	1.6%	0.5%
			12/8/2015	182	0.2%	0.5%	0.9%	-	0.7%	0.6%
			3/8/2016	273	0.1%	0.5%	1.1%	-	1.3%	0.4%
			6/7/2016	364	0.2%	2.1%	2.3%	-	4.1%	1.1%
			12/8/2016	548	0.2%	2.7%	1.3%	-	1.4%	4.0%
			6/8/2017	730	0.1%	0.8%	0.4%	-	2.5%	1.2%
			12/8/2017	913	0.1%	0.5%	0.3%	-	0.6%	1.4%
			2/13/2019	1345	0.1%	2.0%	1.4%	-	2.1%	2.0%
			5/28/2019	1449	0.1%	2.3%	1.2%	-	1.0%	3.3%
IDF14-A59CCC	ILHC	6/9/2015	6/16/2015	7	0.1%	1.1%	1.2%	-	0.3%	0.5%
			7/7/2015	28	0.1%	0.6%	0.7%	-	0.3%	0.6%
			8/4/2015	56	0.1%	0.6%	1.7%	-	1.3%	0.7%
			10/6/2015	119	0.1%	0.4%	1.9%	-	1.5%	0.6%
			12/8/2015	182	0.2%	0.6%	1.1%	-	0.9%	0.9%
			3/8/2016	273	0.1%	5.1%	2.6%	-	4.7%	2.2%
			6/7/2016	364	0.1%	2.7%	2.2%	-	1.6%	2.3%
			12/8/2016[$]	548[$]	0.2%	0.2%	1.2%	-	0.8%	2.0%
			6/8/2017	730	0.1%	0.7%	1.6%	-	0.1%	0.8%
			12/8/2017	913	0.1%	1.7%	0.7%	-	1.3%	0.9%
			5/31/2018	Solid sampling and terminated						

- Release below detection limit as glass does not contain lithium.

Appendix A1. Percent Relative Standard Deviation of Triplicates in Long-Term PCT-B Results at 90 °C and S/V of 20,000 m^{-1} (Tests ILHC and ILHD) (continued).

Glass ID	Test	Immersion Date	Sampling Date	Period	%RSD measured on triplicate PCT results					
					pH	B	K	Li	Na	Si
IDF15-A57CCC	ILHC	6/9/2015	6/16/2015	7	0.1%	0.3%	0.3%	-	0.6%	0.7%
			7/7/2015	28	0.1%	0.6%	2.3%	-	1.7%	0.4%
			8/4/2015	56	0.1%	0.8%	0.8%	-	1.0%	0.4%
			10/6/2015	119	0.1%	1.4%	0.4%	-	0.3%	0.7%
			12/8/2015	182	0.2%	0.5%	0.4%	-	1.3%	0.7%
			3/8/2016	273	0.1%	0.8%	2.8%	-	2.9%	2.0%
			6/7/2016	364	0.1%	2.5%	3.4%	-	0.5%	3.2%
			12/8/2016	548	0.2%	2.2%	0.4%	-	3.2%	2.1%
			6/8/2017	730	0.1%	1.2%	0.9%	-	0.6%	0.6%
			12/8/2017	913	0.1%	0.7%	0.8%	-	1.6%	2.4%
			5/31/2018	1087	0.1%	0.6%	1.7%	-	1.6%	0.9%
			2/13/2019	1345	0.1%	0.4%	0.5%	-	1.1%	0.3%
			5/28/2019	1449	0.1%	1.1%	3.3%	-	2.1%	0.7%
IDF16-A58CCC	ILHD	6/10/2015	6/17/2015	7	0.1%	0.7%	1.2%	-	0.2%	0.2%
			7/8/2015	28	0.1%	0.4%	0.5%	-	1.6%	0.1%
			8/5/2015	56	0.1%	0.7%	0.8%	-	1.3%	0.5%
			10/7/2015	119	0.1%	0.5%	0.4%	-	1.1%	0.2%
			12/9/2015	182	0.1%	1.1%	1.3%	-	1.2%	1.1%
			3/9/2016	273	0.1%	0.8%	1.6%	-	1.7%	1.1%
			6/9/2016	365	0.2%	1.1%	3.5%	-	2.1%	1.7%
			12/8/2016	547	0.2%	0.3%	4.6%	-	1.3%	0.4%
			6/9/2017	730	0.1%	0.7%	2.0%	-	1.0%	0.2%
			12/11/2017	915	0.2%	0.7%	0.7%	-	2.1%	0.7%
			2/14/2019	1345	0.1%	2.3%	2.3%	-	2.2%	3.6%
			5/29/2019	1449	0.1%	1.1%	0.7%	-	9.3%	2.3%
IDF17-A60CCC	ILHD	6/10/2015	6/17/2015	7	0.1%	0.5%	0.9%	-	0.5%	0.1%
			7/8/2015	28	0.1%	0.4%	0.7%	-	0.5%	0.1%
			8/5/2015	56	0.1%	0.4%	1.1%	-	0.5%	0.3%
			10/7/2015	119	0.1%	0.1%	0.6%	-	0.3%	0.1%
			12/9/2015	182	0.2%	1.3%	1.0%	-	1.3%	0.5%
			3/9/2016	273	0.1%	0.2%	0.8%	-	1.5%	0.8%
			6/9/2016	365	0.2%	0.7%	1.2%	-	1.8%	1.9%
			12/8/2016	547	0.1%	1.2%	0.5%	-	0.9%	0.7%
			6/9/2017	730	0.1%	0.4%	0.9%	-	0.3%	1.0%
			12/11/2017	915	0.1%	0.8%	0.3%	-	0.6%	2.5%
			5/31/2018	1086	0.1%	1.9%	1.0%	-	0.4%	1.3%
			2/14/2019	1345	0.1%	0.2%	1.0%	-	0.7%	1.5%
			5/29/2019	1449	0.1%	1.4%	1.2%	-	6.0%	1.4%
IDF18-A161CCC	ILHD	6/10/2015	6/17/2015	7	0.1%	0.4%	0.9%	-	0.5%	0.3%
			7/8/2015	28	0.1%	0.3%	1.7%	-	1.6%	0.3%
			8/5/2015	56	0.1%	0.3%	1.0%	-	0.2%	0.3%
			10/7/2015	119	0.1%	0.0%	0.7%	-	1.4%	1.9%
			12/9/2015	182	0.2%	0.8%	0.2%	-	5.8%	0.6%
			3/9/2016	273	0.1%	1.4%	0.1%	-	1.0%	0.3%
			6/9/2016	365	0.2%	3.7%	0.9%	-	2.9%	0.2%
			12/8/2016	547	0.2%	2.8%	3.6%	-	1.5%	0.5%
			6/9/2017	730	0.1%	1.0%	1.8%	-	1.0%	0.4%
			12/11/2017	915	0.2%	1.9%	0.5%	-	1.8%	0.1%
			2/14/2019	1345	0.1%	0.8%	4.7%	-	0.2%	1.8%
			5/29/2019	1449	0.1%	1.9%	1.0%	-	3.0%	1.6%

- Release below detection limit as glass does not contain lithium.

Appendix A1. Percent Relative Standard Deviation of Triplicates in Long-Term PCT-B Results at 90 °C and S/V of 20,000 m^{-1} (Tests ILHC and ILHD) (continued).

Glass ID	Test	Immersion Date	Sampling Date	Period	%RSD measured on triplicate PCT results					
					pH	B	K	Li	Na	Si
IDF19-C100CCC	ILHD	6/10/2015	6/17/2015	7	0.1%	0.3%	0.8%	-	0.4%	0.5%
			7/8/2015	28	0.1%	0.0%	1.6%	-	0.6%	0.1%
			8/5/2015	56	0.2%	0.2%	1.4%	-	1.1%	0.8%
			10/7/2015	119	0.1%	0.2%	1.2%	-	0.4%	0.4%
			12/9/2015	182	0.2%	0.8%	0.4%	-	0.6%	0.7%
			3/9/2016	273	0.1%	0.6%	1.3%	-	0.4%	0.1%
			6/9/2016	365	0.2%	0.8%	0.3%	-	0.5%	0.9%
			12/8/2016	547	0.1%	2.1%	0.8%	-	1.4%	0.7%
			6/9/2017	730	0.1%	1.3%	0.5%	-	2.1%	0.3%
			12/11/2017	915	0.2%	2.7%	0.4%	-	1.4%	0.3%
			2/14/2019	1345	0.1%	1.4%	0.7%	-	1.3%	0.8%
			5/29/2019	1449	0.1%	1.1%	1.9%	-	7.0%	0.4%
IDF20-F6CCC	ILHD	6/10/2015	6/17/2015	7	0.1%	0.5%	1.0%	0.6%	0.5%	0.3%
			7/8/2015	28	0.2%	0.5%	1.0%	0.7%	0.5%	0.5%
			8/5/2015	56	0.2%	0.7%	0.7%	0.5%	0.2%	0.4%
			10/7/2015	119	0.1%	0.6%	2.0%	1.0%	0.5%	0.5%
			12/9/2015	182	0.1%	1.2%	2.6%	0.8%	0.3%	0.9%
			3/9/2016	273	0.1%	2.6%	2.0%	1.3%	4.2%	1.6%
			6/9/2016	365	0.2%	1.7%	2.9%	3.5%	1.7%	1.2%
			12/8/2016	547	0.1%	3.4%	0.9%	1.1%	2.9%	0.2%
			6/9/2017	730	0.1%	0.8%	0.6%	0.5%	1.7%	1.8%
			12/11/2017	915	0.1%	2.4%	1.0%	0.8%	1.1%	0.9%
			5/31/2018	1086	0.1%	0.7%	1.7%	0.8%	1.5%	0.1%
			2/14/2019	1345	0.1%	0.7%	0.8%	0.8%	0.9%	0.5%
			5/29/2019	1449	0.1%	1.6%	0.8%	0.5%	4.2%	0.1%
ANL-LRM-2	ILHC	6/9/2015	6/16/2015	7	0.1%	0.5%	0.3%	-	0.8%	0.4%
			7/7/2015	28	0.1%	0.3%	0.5%	-	1.4%	0.2%
			8/4/2015	56	0.1%	0.6%	1.6%	-	0.5%	0.2%
			10/6/2015	119	0.1%	1.2%	0.7%	2.8%	0.6%	1.4%
			12/8/2015	182	0.2%	1.6%	0.5%	1.5%	0.8%	0.9%
			3/8/2016	273	0.1%	1.2%	0.4%	1.4%	2.6%	0.7%
			6/7/2016	364	0.1%	3.0%	2.3%	4.8%	2.9%	2.4%
			12/8/2016[$]	548	0.2%	2.6%	1.9%	0.4%	4.1%	1.7%
			6/8/2017	730	0.1%	0.4%	1.0%	0.3%	0.3%	1.0%
			Test terminated							
ANL-LRM-2	ILHD	6/10/2015	6/17/2015	7	0.1%	0.2%	1.1%	-	0.3%	0.1%
			7/8/2015	28	0.2%	0.4%	1.4%	-	0.8%	0.2%
			8/5/2015	56	0.1%	0.5%	0.6%	-	0.5%	0.1%
			10/7/2015	119	0.1%	0.5%	0.5%	1.7%	1.2%	0.1%
			12/9/2015	182	0.1%	0.6%	0.2%	0.8%	0.5%	0.1%
			3/9/2016	273	0.1%	0.8%	0.3%	1.4%	1.5%	0.1%
			6/9/2016	365	0.2%	2.2%	2.9%	2.3%	1.8%	0.2%
			12/8/2016[$]	547	0.2%	0.8%	0.5%	0.8%	4.1%	0.2%
			6/9/2017	730	0.1%	1.9%	1.7%	2.2%	2.0%	0.1%
			Test terminated							

- Below detection limit; *Normalized release calculated from average of triplicate tests with less than 10% RSD (median 0.6%RSD); [#] Measured at room temperature; [$]Altered glass removed from one of the triplicate vessels

Appendix A2. Percent Relative Standard Deviation of Triplicates in Long-Term PCT-B Results at 90 °C and Various S/V Ratios (Tests ILHE, ILHF and ILHG).

Glass ID	Sample ID	Test	S/V (m^{-1})	Immersion Date	Sampling Date	Period	%RSD measured on triplicate PCT results					
							pH	B	K	Li	Na	Si
IDF22 EC46CCC	22EC46	ILHE	20000	6/4/2018	6/11/2018	7	0.5%	1.3%	4.5%	0.0%	3.9%	1.4%
					7/2/2018	28	0.2%	2.4%	0.9%	1.5%	2.1%	3.8%
					7/30/2018	56	0.3%	1.8%	2.9%	1.4%	0.4%	1.7%
					11/30/2018	179	0.3%	16.8%	13.9%	4.3%	13.6%	9.9%
					3/1/2019	270	0.3%	3.6%	5.0%	3.4%	2.5%	6.4%
					6/4/2019	365	0.2%	0.3%	6.1%	0.0%	4.5%	7.1%
IDF25 EC34CCC	25EC34				6/11/2018	7	0.3%	3.6%	10.7%	-	3.2%	1.8%
					7/2/2018	28	0.2%	0.5%	2.3%	-	0.7%	2.2%
					7/30/2018	56	0.1%	1.5%	2.7%	-	2.6%	0.7%
					11/30/2018	179	0.0%	7.6%	10.9%	21.1%	7.5%	2.3%
					3/1/2019	270	0.2%	10.9%	8.8%	6.7%	7.8%	13.2%
					6/4/2019	365	0.1%	2.6%	9.2%	0.0%	13.2%	6.5%
IDF26 EC44CCC	26EC44				6/11/2018	7	0.3%	2.3%	3.2%	2.5%	1.7%	3.1%
					7/2/2018	28	0.3%	2.7%	2.3%	2.9%	0.8%	1.2%
					7/30/2018	56	0.0%	1.8%	2.8%	3.6%	1.0%	2.5%
					3/1/2019	270	0.1%	1.5%	1.0%	2.9%	2.0%	2.5%
					6/4/2019	365	0.2%	3.3%	4.2%	0.0%	5.1%	1.5%
IDF27 EC48CCC	27EC48				6/11/2018	7	0.2%	1.1%	0.6%	1.1%	1.2%	1.1%
					7/2/2018	28	0.3%	0.5%	3.2%	1.1%	2.7%	1.7%
					7/30/2018	56	0.1%	0.4%	1.3%	0.4%	0.5%	0.1%
					10/2/2018	120	0.2%	11.8%	5.1%	7.4%	5.2%	5.4%
					11/30/2018	179	0.0%	0.0%	0.0%	4.7%	0.0%	5.4%
					3/1/2019	270	0.1%	6.4%	7.1%	5.1%	6.5%	4.6%
					6/4/2019	365	0.2%	2.0%	1.2%	0.0%	9.3%	2.1%
IDF28 EC50CCC	28EC50				6/11/2018	7	0.2%	11.7%	13.6%	-	12.3%	6.4%
					7/2/2018	28	0.2%	1.5%	5.0%	-	5.0%	3.6%
					7/30/2018	56	0.3%	3.4%	3.4%	-	2.8%	1.0%
					10/2/2018	120	0.1%	1.7%	1.7%	-	1.9%	0.4%
					11/30/2018	179	0.1%	1.7%	0.1%	-	0.5%	11.6%
					3/1/2019	270	0.1%	1.4%	1.5%	-	1.1%	0.2%
					6/4/2019	365	0.2%	3.1%	7.1%	-	6.2%	0.8%

- Release below detection limit as glass does not contain lithium.

Appendix A2. Percent Relative Standard Deviation of Triplicates in Long-Term PCT-B Results at 90 °C and Various S/V Ratios (Tests ILHE, ILHF and ILHG) (cont'd).

Glass ID	Sample ID	Test	S/V (m^{-1})	Immersion Date	Sampling Date	Period	%RSD measured on triplicate PCT results				
							pH	B	K	Na	Si
IDF23 EC52CCC	1K23 EC52	ILHF	1000	6/5/2018	6/12/2018	7	0.6%	6.3%	-	5.4%	1.3%
					7/3/2018	28	1.0%	4.2%	2.3%	2.8%	1.7%
					7/31/2018	56	4.0%	0.8%	2.9%	0.3%	0.6%
					10/3/2018	120	0.5%	0.6%	2.0%	2.1%	1.3%
					12/3/2018	181	0.4%	1.1%	0.9%	0.8%	1.2%
					3/4/2019	272	0.3%	1.1%	1.6%	0.6%	0.1%
					6/5/2019	365	0.8%	1.8%	2.6%	2.7%	2.5%
	2K23 EC52		2000		6/12/2018	7	0.4%	6.3%	15.7%	3.9%	4.4%
					7/3/2018	28	0.2%	2.1%	2.8%	1.1%	1.5%
					7/31/2018	56	0.5%	1.3%	4.1%	1.0%	1.5%
					10/3/2018	120	0.2%	0.5%	1.8%	0.3%	0.7%
					12/3/2018	181	0.2%	0.9%	1.4%	0.4%	0.7%
					3/4/2019	272	0.1%	0.1%	1.3%	1.2%	0.7%
					6/5/2019	365	0.3%	2.2%	2.0%	3.5%	1.4%
	5K23 EC52		5000		6/12/2018	7	0.6%	5.7%	3.9%	4.6%	3.1%
					7/3/2018	28	0.2%	1.3%	4.1%	1.3%	0.2%
					7/31/2018	56	0.2%	0.8%	2.2%	1.9%	0.7%
					10/3/2018	120	0.1%	1.8%	1.1%	1.0%	1.0%
					12/3/2018	181	0.1%	0.8%	1.1%	0.2%	1.1%
					3/4/2019	272	0.3%	1.1%	1.1%	0.3%	1.4%
					6/5/2019	365	0.2%	1.6%	4.0%	4.2%	2.2%
	10K23 EC52		10000		6/12/2018	7	0.4%	6.6%	4.9%	7.2%	3.4%
					7/3/2018	28	0.1%	1.9%	2.6%	0.9%	1.8%
					7/31/2018	56	0.2%	0.5%	1.1%	2.2%	2.5%
					10/3/2018	120	0.1%	2.7%	6.4%	3.2%	1.4%
					12/3/2018	181	0.1%	1.7%	2.0%	2.3%	1.4%
					3/4/2019	272	0.2%	1.7%	1.8%	3.5%	2.7%
					6/5/2019	365	0.6%	9.5%	0.6%	4.1%	0.9%
	20K23 EC52		20000		6/12/2018	7	0.3%	0.5%	2.7%	1.6%	0.6%
					7/3/2018	28	0.1%	1.5%	2.0%	4.5%	2.2%
					7/31/2018	56	0.2%	2.4%	2.4%	3.3%	2.5%
					10/3/2018	120	0.2%	4.5%	6.5%	4.5%	0.9%
					12/3/2018	181	0.2%	2.7%	5.2%	2.3%	1.3%
					3/4/2019	272	0.1%	3.4%	1.9%	2.6%	7.4%
					6/5/2019	365	0.1%	8.3%	5.5%	9.1%	5.7%

- Empty data field; *Normalized release calculated from average of triplicate tests with less than 10% RSD
[#] Measured at room temperature

Appendix A2. Percent Relative Standard Deviation of Triplicates in Long-Term PCT-B Results at 90 °C and Various S/V Ratios (Tests ILHE, ILHF and ILHG) (cont'd).

Glass ID	Sample ID	Test	S/V (m^{-1})	Immersion Date	Sampling Date	Period	%RSD measured on triplicate PCT results				
							pH	B	K	Na	Si
IDF24 EC28CCC	1K24 EC28	ILHG	1000	6/5/2018	6/12/2018	7	1.1%	4.2%	7.1%	4.6%	1.1%
					7/3/2018	28	0.2%	2.0%	3.8%	1.8%	2.4%
					7/31/2018	56	1.2%	1.8%	2.7%	0.4%	1.0%
					10/3/2018	120	0.4%	0.8%	1.7%	1.5%	1.2%
					12/4/2018	182	1.5%	1.1%	1.0%	0.6%	1.6%
					3/5/2019	273	0.2%	2.4%	4.1%	1.9%	2.6%
					6/6/2019	366	0.8%	3.1%	3.8%	3.1%	3.8%
	2K24 EC28		2000		6/12/2018	7	0.1%	1.2%	2.9%	2.9%	1.2%
					7/3/2018	28	0.1%	0.9%	1.2%	0.7%	0.7%
					7/31/2018	56	0.3%	0.9%	1.9%	0.2%	1.2%
					10/3/2018	120	0.3%	1.2%	2.2%	1.6%	1.9%
					12/4/2018	182	0.2%	0.8%	1.0%	4.8%	0.8%
					3/5/2019	273	0.3%	2.1%	0.8%	0.8%	0.4%
					6/6/2019	366	0.2%	1.9%	2.8%	2.2%	2.0%
	5K24 EC28		5000		6/12/2018	7	0.2%	0.5%	2.1%	2.5%	0.5%
					7/3/2018	28	0.2%	1.0%	0.8%	4.0%	0.9%
					7/31/2018	56	0.1%	0.4%	0.4%	0.5%	0.7%
					10/3/2018	120	0.2%	1.3%	2.6%	0.7%	1.2%
					12/4/2018	182	0.1%	1.0%	1.9%	0.6%	1.5%
					3/5/2019	273	0.4%	0.7%	1.0%	0.4%	0.8%
					6/6/2019	366	0.3%	2.5%	3.3%	2.3%	1.9%
	10K24 EC28		10000		6/12/2018	7	0.2%	1.6%	2.0%	0.4%	2.7%
					7/3/2018	28	0.2%	2.0%	4.0%	0.4%	2.0%
					7/31/2018	56	0.2%	0.3%	0.7%	0.5%	0.8%
					10/3/2018	120	0.1%	0.1%	1.2%	0.9%	1.0%
					12/4/2018	182	0.1%	0.9%	1.5%	1.8%	1.1%
					3/5/2019	273	0.2%	2.4%	5.1%	3.6%	1.7%
					6/6/2019	366	0.2%	1.7%	0.3%	1.4%	1.2%
	20K24 EC28		20000		6/12/2018	7	0.2%	7.1%	6.7%	8.0%	4.2%
					7/3/2018	28	0.1%	0.2%	0.6%	0.9%	0.9%
					7/31/2018	56	0.1%	0.2%	0.9%	1.4%	0.7%
					10/3/2018	120	0.2%	0.6%	4.7%	3.6%	1.8%
					12/4/2018	182	0.2%	0.9%	1.5%	2.2%	0.9%
					3/5/2019	273	0.2%	2.2%	2.6%	3.5%	1.4%
					6/6/2019	366	0.1%	4.8%	1.5%	3.8%	0.8%

- Empty data field; *Normalized release calculated from average of triplicate tests with less than 10% RSD
[#] Measured at room temperature

Appendix A3. Percent Relative Standard Deviation of Triplicates in Long-Term PCT-B Results for Reference Glass ANL-LRM at 90 °C and S/V of 2,000 m^{-1} (Tests ILHE, ILHF and ILHG).

Glass ID	Test	S/V (m^{-1})	Immersion Date	Sampling Date	Period	%RSD measured on triplicate PCT results					
						pH	B	K	Li	Na	Si
ANL-LRM-2	ILHE	2000	6/4/2018	6/11/2018	7	0.8%	2.4%	5.3%	-	3.2%	2.0%
				7/2/2018	28	0.5%	1.6%	2.9%	-	1.8%	0.9%
				7/30/2018	56	0.4%	1.9%	0.6%	1.8%	1.3%	1.1%
				10/2/2018	120	0.1%	0.7%	2.0%	2.0%	0.7%	0.7%
				11/30/2018	179	0.4%	3.3%	4.3%	3.2%	1.1%	2.2%
				3/1/2019	270	0.5%	2.0%	0.6%	3.1%	0.6%	1.0%
				6/4/2019	365	0.1%	0.5%	2.1%	0.4%	0.1%	0.4%
	ILHF		6/5/2018	6/12/2018	7	0.4%	2.9%	3.8%	-	2.0%	0.9%
				7/3/2018	28	0.4%	4.0%	2.7%	-	3.8%	1.5%
				7/31/2018	56	0.9%	1.5%	2.5%	2.8%	1.6%	0.4%
				10/3/2018	120	1.1%	0.4%	1.4%	1.0%	1.9%	0.9%
				12/3/2018	181	0.4%	2.3%	4.4%	1.6%	1.5%	1.4%
				3/4/2019	272	0.1%	2.9%	1.5%	2.1%	0.8%	2.6%
				6/5/2019	365	0.2%	1.4%	2.9%	3.9%	0.6%	1.2%
	ILHG		6/5/2018	6/12/2018	7	3.2%	1.2%	17.3%	-	4.7%	3.8%
				7/3/2018	28	0.5%	1.9%	2.4%	-	2.4%	2.0%
				7/31/2018	56	0.4%	1.3%	0.9%	2.8%	0.9%	0.8%
				10/3/2018	120	0.3%	1.8%	1.9%	3.6%	1.0%	0.2%
				12/4/2018	182	0.2%	2.1%	2.4%	3.2%	1.6%	0.9%
				3/5/2019	273	0.3%	1.6%	2.2%	1.9%	1.6%	1.6%
				6/6/2019	366	0.3%	2.1%	4.3%	1.6%	2.6%	5.4%

- Release below detection limit.